Copper partitioning in mid-Miocene flood basalts from the Northern Great Basin (U.S.A): implications for Cu behavior in flood basalt provinces

by

Christopher Thomas Wierman

B.S., University of Oklahoma, 2015

A THESIS

submitted in partial fulfillment of the requirements for the degree

MASTER OF SCIENCE

Department of Geology
College of Arts and Sciences

KANSAS STATE UNIVERSITY
Manhattan, Kansas

2018

Approved by:

Major Professor
Matthew Brueseke

Abstract

It is generally accepted that beneath flood basalt provinces, Cu-Ni-PGE sulfide deposits may be found (Ridley, 2013). The focus of this study is the Steens Basalt, a mid-Miocene flood basalt from the northern Great Basin (USA) which contains between ~5-400 ppm copper and is characterized by large plagioclase phenocrysts, some of which can contain primary inclusions of copper despite the chalcophile nature of Cu (Hofmeister and Rossman, 1985; Johnston et al., 1991). The purpose of this project is to identify the distribution of Cu among coexisting phases in Steens Basalt, test whether plagioclase crystals in Steens lavas can host Cu, even when Cu is not visible, and test whether sulfide minerals/droplets are present in Steens Basalt samples with low Cu concentrations. Samples of Steens lavas were examined for sulfide minerals via reflected light microscopy, Raman spectroscopy, and X-ray diffraction with a molybdenum tube. Using an electron microprobe, silicate minerals, oxides, glass, and sulfides were analyzed for their Cu concentration, as well as other major and trace element chemistry. Glass did not contain detectable Cu which precluded partition coefficient (K_d) calculations. Based on average Cu concentration for the non-sulfides, magnetite contains the most Cu, followed by (forsteritic) weathered olivine, pyroxene, olivine, plagioclase, and ilmenite. Copper sulfides were discovered in samples MB97-19 and MB97-76C with additional non-copper sulfides in MB97-76B. In conclusion, these results lay the groundwork for further investigation into potential copper sulfide reserves in the magma plumbing as with other flood basalt packages linked to economically important mineral deposits.

Table of Contents

List of Figures

List of Tables

Acknowledgements

I thank everyone who has supported me in this graduate school journey, most especially my parents—Tom and Paula Wierman. I thank Dr. Brueseke for accepting me as his student and Dr. Kempton for providing financial assistance with a GTA position and stipend. I thank Mr. and Mrs. Lindley Reimer for the Ronald D. Schultz Memorial Scholarship, Mr. and Mrs. Paul Strunk for the Paul and Deanna Strunk Geology Fellowship Funds, and Mrs. Dorothy Mudge for the Mudge-Thompson Geology Scholarship. Thank you for your generous scholarships which helped fund my education. The funding meant a lot to me. I thank my committee members, Dr. Kempton and Dr. Datta for their useful comments and edits to this thesis document and Dr. Allaz, formerly of University of Colorado Boulder, for all his help with the microprobe work. I thank the faculty of the Kansas State Geology Department for furthering my education with their courses. I think I have learned a lot. This project was made possible by the generous grants from the Geological Society of America, the McKinstry Fund from the Society of Economic Geology, Brueseke's discretionary fund, and access to the facilities at the KSU Geology Department.

Chapter 1 - Introduction

Flood basalt provinces are associated with both Au-Ag epithermal ores and Ni-Cu-PGE magmatic sulfide deposits (Ridley, 2013). According to Song et al. (2011), magmatic sulfide deposits occur underneath flood basalt provinces in magma plumbing systems. This is reinforced by Starostin and Sorokhtin (2011), who documented the sill-like structures of the Talnakh deposit underneath the Siberian Traps. Au, Ag, Cu, Ni, and Pt group elements are critical for modern society and a better understanding of the origin of these deposits can help guide exploration efforts. The northern Great Basin, USA (Figure 1A) is characterized by widespread ~17-14 Ma flood basalt volcanism and coeval epithermal Au-Ag deposits. Pb and Cu isotope studies (Kamenov et al., 2007; Saunders et al., 2016; Maynard, 2016) indicate a petrogenetic link between the ores and mafic magmas. The Cu isotope work includes analyses of ore minerals (Saunders et al., 2016) as well as basaltic lavas (Maynard, 2016) and is based on using Cu as a proxy for Au-Ag in the magma-to-epithermal environment (Saunders and Brueseke, 2012; Saunders et al., 2016). It is also likely, however, that Cu concentrations in these mafic magmas are controlled by sulfide crystallization/liquid immiscibility in crustal magma bodies or vapor phase transport, which controls Au and Ag mobility in these types of systems (Heinrich et al., 1992; Doe, 1994; Heinrich et al., 2004; Williams-Jones and Heinrich, 2005; Zajacz and Halter, 2009; Ridley, 2013).

The Steens Basalt (and its local geochemical equivalents; see Brueseke et al., 2007 for details on Steens Basalt distribution) is an ~16.5 Ma flood basalt package consisting of tholeiitic to slightly alkalic basalts and basaltic andesites that erupted across the Oregon Plateau before shifting to the central location of Steens Mountain, OR (Brueseke et al. 2007; Camp et al., 2013). Steens Basalt lavas range from aphyric to coarsely plagioclase-phyric with some lavas being

composed of up to 50% (vol.) plagioclase megacrysts the size of which can reach 40 mm and is intergranular to diktytaxitic in hand sample (Johnson, 1996; Brueseke et al., 2007; Camp et al., 2013). Most lavas show pahoehoe textures, although some lavas near the top of the package at Steens Mountain are a'a type and other lavas are transitional or not easily classified into the pahoehoe-a'a classification (Brueseke et al, 2007; Bondre and Hart, 2008; Camp et al., 2013). These upper lavas tend to be more evolved, aphyric, and phenocryst-poor (Camp et al., 2013). Local eruptions of Steens Basalt are present outside the shaded area in Figure 1 in ID and NV, and include the Owyhee Mountains, Buckskin-National/National (Santa Rosa-Calico volcanic field); Midas/Ivanhoe area, Mule Canyon, and Jarbidge region where there is co-occurrence of epithermal ore deposits.

Some Steens Basalt lavas are characterized by ~2-4 cm plagioclase phenocrysts that sometimes host visible native Cu inclusions (Figure 1B) (Hofmeister and Rossman, 1985; Johnston et al., 1991). Data from melt inclusions in plagioclase from Steens lavas show that the crystals formed in mid-crustal (<2-3 kbar) magma bodies (Johnson et al., 1996).

Cu differences in Steens magmas have been suggested to reflect different magma recharge events in these crustal magma bodies (Gunn and Watkins, 1970). Thus, Cu concentrations in Steens magmas varied through time and Cu is observed to have partitioned into some labradorite crystals (Gunn and Watkins, 1970; Hofmeister and Rossman, 1985; Johnston et al., 1991). These crystals, called Oregon Sunstones, contain exsolved metallic copper which causes the labradorite to turn different colors (green, red, pink) and contain, in some high-grade gemstones, copper schiller (Hofmeister and Rossman, 1985). In this scenario, some evolved Steens magmas are associated with Cu enrichment (and partitioning into plagioclase), whereas periodic recharge of the magma chamber by Cu-poor, less-evolved magma, lowers the Cu

concentration of the melt (Hofmeister and Rossman, 1985). The other possibility is that Cu nanoparticles formed in the magma and aggregated onto the growing plagioclase crystals. Faure (1998) states that, according to an addition to Goldschmidt's rules (Goldschmidt, 1937) by Ringwood (1955), Cu^+ and Na^+ would not substitute for each other, despite their similar charge and atomic radii (Ahrens, 1952), due to differences in electronegativity (Cu^+ forms more covalent bonds than Na^+). Cu nanoparticles would circumvent these issues; however, other obstacles arise with this hypothesis. First, the crystallographic location of Cu within the plagioclase crystals seems to be within the crystal lattices instead of randomly distributed (Johnston et al., 1991; Hill, 2009; Xu et al., 2017). Second, the melting point of Cu (1084.5ºC at 1atm; Mirwald and Kennedy, 1979) is lower than the lowest solidus temperature for plagioclase (albite at 1124ºC; Greenwood and Hess, 1998).

However, a detailed study of the Steens Basalt, suggests that the stratigraphic (temporal) variations in bulk rock Cu concentrations may be due to the variable presence of sulfide phases (possibly droplets) in an evolving magma body affected by crystallization (plagioclase+olivine+clinopyroxene+magnetite±sulfide phases) and recharge (Gunn and Watkins, 1970). This mechanism of Cu enrichment in sulfide phases occurs in most Mid-Ocean Ridge Basalts (Cu in silicate melt concentration drops). Conversely, published K_d values (

Table 1) suggest that Cu behaves incompatibly with olivine fractionation in mafic magmas, thus the Cu concentration in the residual melt (if no sulfide fractionation) could rise and might lead to enriched Cu concentrations. To investigate the incompatibility of Cu with olivine fractionation, we plotted Cu data of global flood basalts and Neogene Steens and Yellowstone-Snake River Plain Volcanic Province continental flood basalts against MgO (wt. %) to see if such an enrichment exists (Figure 2, Figure 3). For the global record, in more evolved magmas (increasing wt. % MgO beyond 5-9 wt. %), Cu only slightly increases; however, there is a large range of Cu concentration (4-3008 ppm) at 3-9 wt. % MgO for the global record. The data for Steens and Yellowstone-Snake River Plain Volcanic Province continental flood basalts, however, are much more scattered. It is interesting to note that Cu in Neogene Yellowstone-Snake River Plain Volcanic Province basalts seem to increase slightly with increasing wt. % MgO as with the global pattern whereas the Steens Basalt does not exhibit this pattern. The large variation in Cu at 3-5 wt. % MgO is not readily apparent in this isolated dataset, however.

In Steens lavas, it is unclear which crystallizing phases (and matrix glass) host Cu, as well as whether any of these phases are enriched in Cu (and by proxy, Au and Ag; Saunders et al., 2016), other than the uncommon Cu-enriched plagioclase phenocrysts (e.g., “sunstones”). It is also unclear whether Steens lavas with low Cu concentrations are sulfide-bearing. If they are sulfide-bearing, the presence of sulfides has important implications, because the association between sulfides and flood basalts is what characterizes most worldwide Cu-Ni-PGE deposits (Schulz et al., 2010) and could point to undocumented, mid-Miocene Cu-Ni-PGE mineralization in the northern Great Basin (NGB), Oregon Plateau, and Columbia Plateau.

The purpose of this project is to discern whether there are any copper sulfides in Steens lavas and if so what mineral species they are, discover what mineral phases (and glass) host

copper and in what amount, discuss possible mechanisms of Cu enrichment and evaluate the consequences of our research for potential Cu-Ni-PGE ores in the Steens Mt. area, Oregon (U.S.A.).

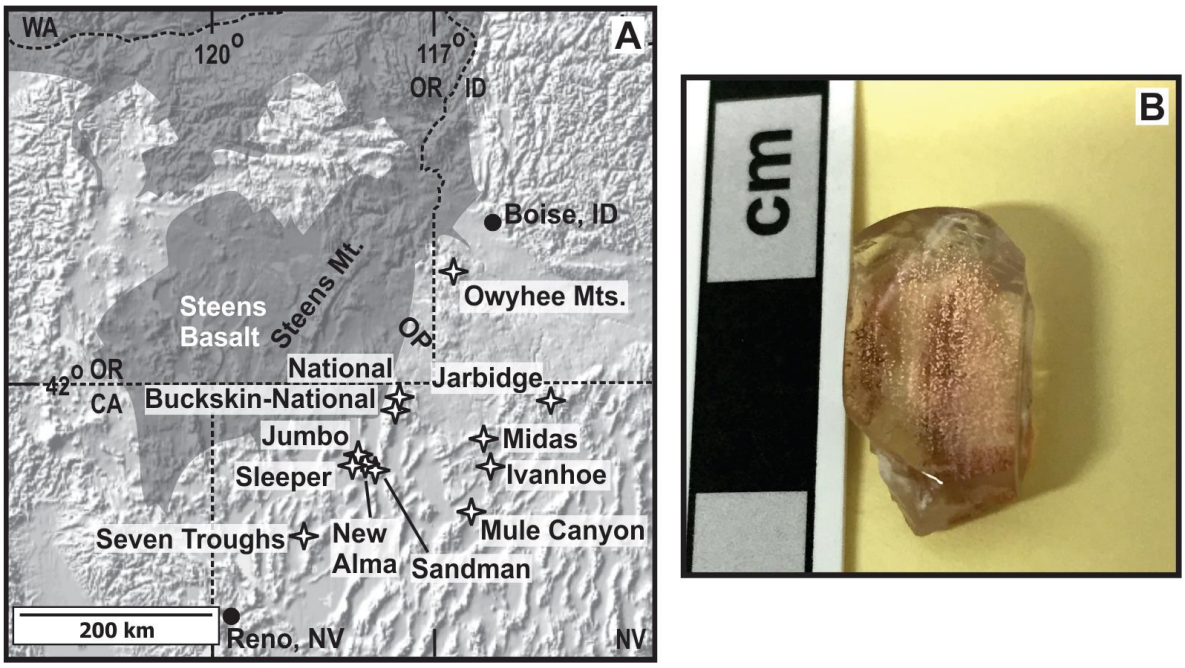

Figure 1A: Map of the northern Great Basin (NGB) United States depicting voluminous Columbia River-Steens flood basalt lavas (gray shading; Steens Basalt is all south of the latitude of Boise, ID) and ~17-14 Ma epithermal Au-Ag districts (named and marked by white stars). Local eruptions of Steens Basalt are present outside the shaded area in ID and NV, and include the Owyhee Mountains, Buckskin-National/National (Santa Rosa-Calico volcanic field); Midas/Ivanhoe area, Mule Canyon, and Jarbidge region. OP, Owyhee Plateau. Map after Saunders et al. (2016). B: Steens Basalt plagioclase phenocryst ("Oregon Sunstone") with visible native Cu inclusions. This was mined from a Steens basalt lava in Lake County, OR (located under the Steens Basalt label in Figure 1A).

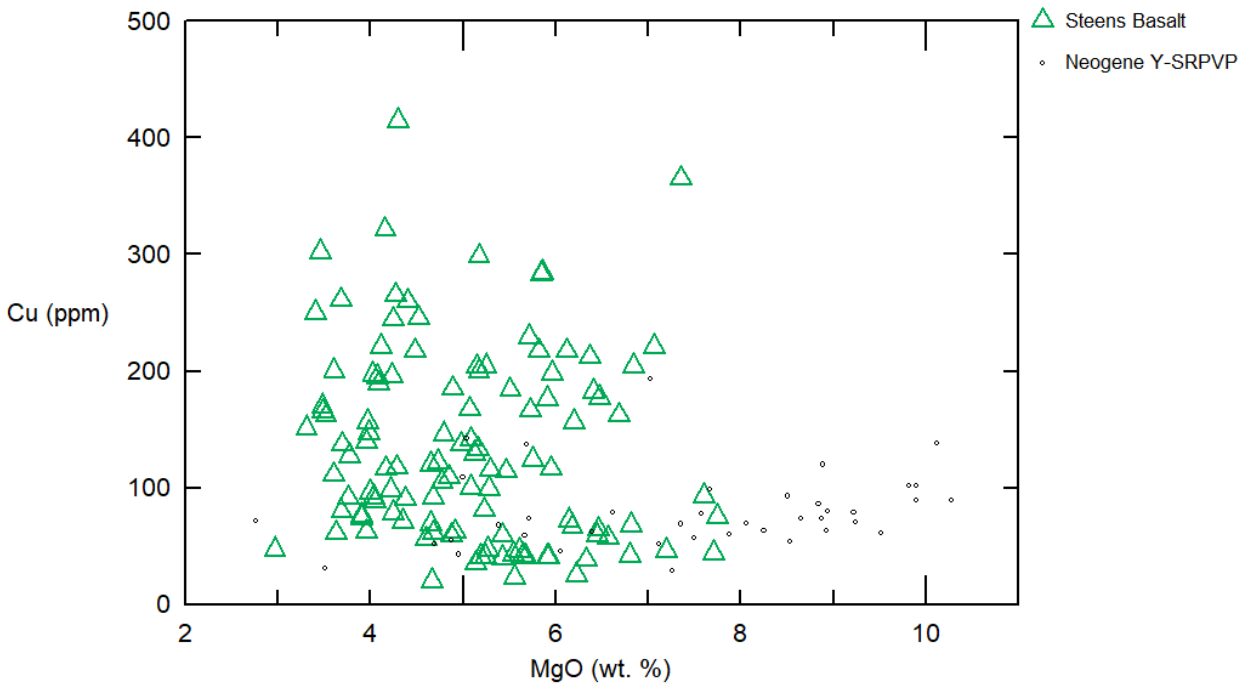

Figure 2: A plot of MgO (wt. %) vs Cu (ppm) in Steens Basalt (or its equivalent) and other Neogene continental flood basalts from the Yellowstone-Snake River Plain Volcanic Province (Y-SRPVP). Cu concentration in average mafic magmas is about 100 ppm (Ridley, 2013). Data from the GEOROC database and Brueseke et al., 2007; 154 basalts plotted.

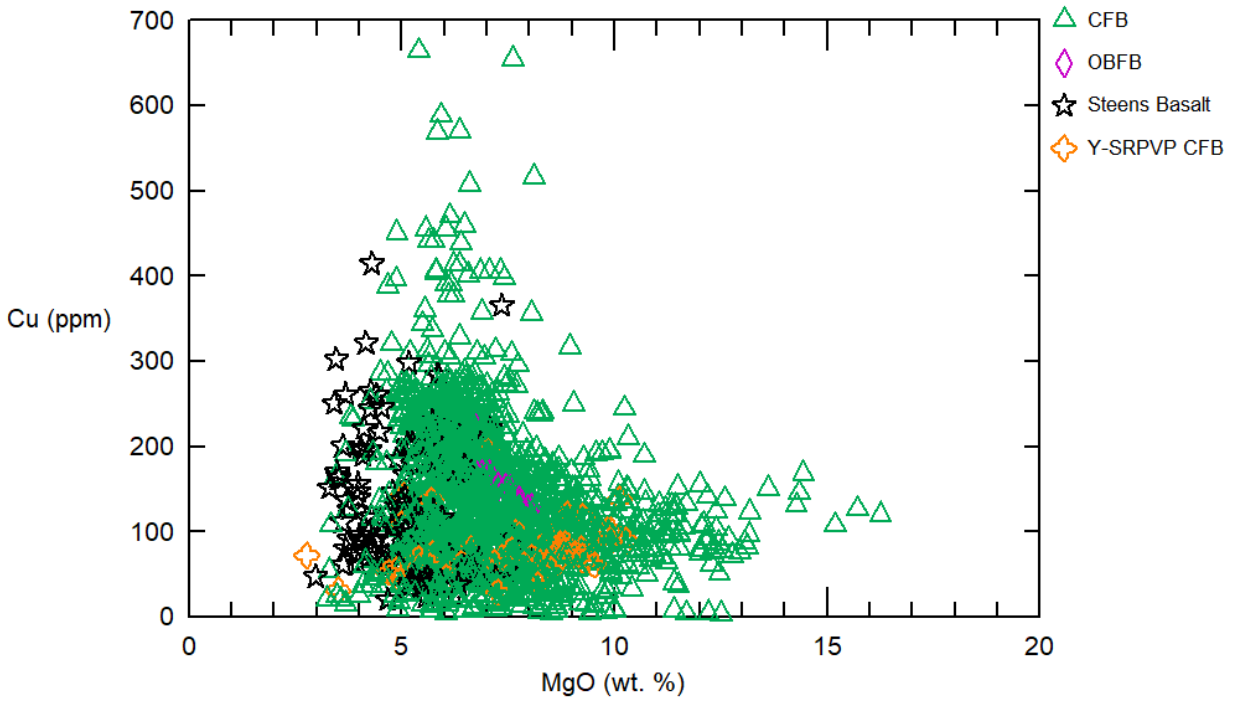

Figure 3: A plot of 1604 basalts from the GEOROC database and Brueseke et al., 2007. The full plot extends to 3008 ppm Cu (with those Cu concentrations mainly between 5-9 wt. % MgO) but these were cropped to facilitate comparison with Figure 2. CFB = continental flood basalts, OBFB = ocean basin flood basalts, Y-SRPVP CFB = Yellowstone-Snake River Plain Volcanic Province continental flood basalts.

Background

Geologic Background

From 155 Ma to 55 Ma, subduction of the Farallon plate under the North American plate produced a compressional tectonic regime. During the late Cretaceous to Eocene, this contractional deformation yielded the Nevadaplano, a high-elevation, low relief region of thickened lithosphere analogous to the Tibetan Plateau and the Andean Plateau (Henry et al., 2012). This feature was located where the modern Great Basin is located today (Brueseke et al., 2014). From about 45 Ma to 18 Ma, subduction-related magmatic activity continued coeval with topographic uplift driven by upwelling asthenosphere, further increasing its average elevation to about 4 km (Henry et al., 2012; Chamberlain et al. 2012). During the mid-Miocene the Nevadaplano collapsed, coeval with the onset of extension in the Basin and Range (Colgan and Henry, 2009). Also at ~17 Ma, large volumes of tholeiitic basalts and ferroandesites began erupting from vents positioned along the western margin of the Wyoming Craton (Carlson and Hart, 1987; Camp and Ross, 2004). These flood basalt eruptions consist of the Columbia River Basalt Group and the Oregon Plateau mafic lavas and are the manifestation of the Yellowstone hotspot (Camp and Ross, 2004). The most voluminous NGB flood basalt unit is the Steens Basalt (Brueseke et al., 2007; Camp et al., 2013) which erupted at ~16.8 Ma, centered on Steens Mountain, OR (Figure 1A). Geochemically identical lavas erupted for at least approximately two million years from locations across the NGB (Brueseke et al., 2007; Brueseke and Hart, 2008). While the Steens Basalt type section is at Steens Mountain, other temporally and geochemically similar lavas have been mapped (Hart and Carlson, 1985; Carlson and Hart, 1987; Brueseke et al., 2007). These eruptions are also spatially and temporally associated with widespread silicic volcanism and low-sulfidation, Au-Ag epithermal mineralization (John, 2001; Kamenov et al.,

2007; Saunders et al., 2008; Brueseke, 2010). Pb isotope data from Au ores in the NGB suggest that Au is derived from mid-Miocene mafic magmas and transported by low-density fluids to the epithermal environment (e.g., vapor phase; Heinrich et al, 2004; Kamenov et al., 2007; Saunders et al., 2008). Cu and Pb isotopes also indicate a mafic magma origin for epithermal Au and Ag in these NGB epithermal ores (Saunders et al., 2016).

Geochemical Background

Cu is a chalcophile element that is typically incompatible in plagioclase and olivine in basalt through andesite; that is, its concentration increases in silicate melt as a function of magma differentiation (Ridley, 2013; Liu et al., 2014). Partition coefficients (K_d) are a measurement of how compatible or incompatible an element is, commonly simplified by anthropomorphizing the element, asking which phase it prefers. A value above 1 indicates that the element prefers the solid phase whereas a value below 1 indicates it prefers the liquid. In the case of the value equaling 1, the element has no preference. K_d values for Cu in various minerals in basalt and basalt to andesite are listed in Table 1. Hofmeister and Rossman (1985) suggested that as Cu concentrations increase in a host magma, higher concentrations of Cu are incorporated into plagioclase, where native Cu later exsolves from the plagioclase. LeHuray (1989) suggested that Cu^+ can substitute for Na^+ in plagioclase. Jensen (1982) also suggested that Cu^+ can substitute for Na^+ in plagioclase whereas Cu^{2+} can substitute for Fe^{2+} in Fe-Ti-oxides and Fe-Mg-silicates. Jensen (1982) stated that a small amount of Cu will be incorporated into these minerals, likely due to pressure and temperature changes that slightly affect Cu relative compatibility in these minerals (Blundy and Wood, 2003), and that the residual magma will continue to be enriched in Cu. Xu et al. (2017) also suggests that Cu is incorporated into the feldspar crystal (spatially associated with protoenstatite) at high P-T conditions during early crystal formation before

exsolving and crystallizing during the last phases of magma chamber crystallization but prior to eruption. Complicating Cu behavior in these systems is the fact that, because it is a chalcophile element, Cu tends to complex with sulfur if it is present in the silicate melt as an immiscible liquid, a liquid that cannot physically mix with the host liquid (Doe, 1994; Ridley, 2013; Barnes and Ripley, 2016). This type of behavior in flood basalt provinces is associated with the formation of layered mafic intrusions such as the Bushveld Complex and Noril'sk-Talnakh, and Cu-Ni-Platinum Group Element (PGE) mineralization (Ridley, 2013; Barnes and Ripley, 2016). Furthermore, low density fluids (e.g., magmatic vapors) can also transport Cu, as well as Au, Ag, and other metal(loid)s (Heinrich, 1992; Zajacz and Halter, 2009) from the magmatic environment to the surface. This vapor-phase transport is linked to porphyry copper and epithermal deposits and mafic to intermediate magmatic systems (Heinrich et al., 1992; Heinrich et al., 2004; Williams-Jones and Heinrich, 2005; Saunders et al., 2008).

Table 1: K_d values for Cu in common minerals in basalt and basalt to andesite (GERM database; 1: Paster et al., 1974; 2: Hart and Dunn, 1993; 3: Bougault and Hekinian, 1974; 4: Lemarchand et al., 1987; 5: Kloeck and Palme, 1988; 6: Pedersen, 1979; 7: Rajamani and Naldrett 1978; 8: Dostal et al., 1983; 9: Ewart et al., 1973; 10: Esperança et al. 1997; 11: Gaetani & Grove 1997).

Element	Mineral	Rock	K_d value(s)
Cu	Plagioclase	Basalt	0.004-0.17[1,3]
Cu	Plagioclase	Basalt to andesite	0.08-0.24[9]
Cu	Olivine	Basalt	0.023-0.55[1,3,5]
Cu	Olivine	Basalt to andesite	0.075-0.19[11]
Cu	Clinopyroxene	Basalt	0.071-0.36[1,2,3]
Cu	Clinopyroxene	Basalt to andesite	0.05-0.69[8,9]
Cu	Magnetite	Basalt	0.42[4]
Cu	Magnetite	Basalt to andesite	0.15[10]
Cu	Ilmenite	Basalt	1.46[1]
Cu	Sulfide	Basalt	180-380[6,7]
Cu	Amphibole	Basalt to andesite	0.05[8]
Cu	Low Ca Pyroxene	Basalt to andesite	0.16-0.92[9]

Chapter 2 - Methods

Datasets

Global Basalt Dataset

Whole rock geochemical data was taken from the GEOROC database. Samples that did not match basalt chemistries (were not between 45 to 56 wt%. SiO_2) or where the rock name was not basalt were eliminated. Samples which were labeled as extensivly or moderately altered were eliminated. Samples which did not have Cu data were eliminated. Samples which did not have FeO or FeO_{total} were eliminated for consistency in Mg# comparisons and to avoid erroneous Mg# values. Following these restrictions, data from Brueseke et al. (2007) was added.

For samples where Fe was not split, Mg# was calculated with the formula $\frac{100*Mg}{(Mg+0.9*Fe)}$ following Gill (2010). Mg and Fe are atomic element values. Fe was multiplied by 0.9 based on the assumption that 90% of Fe is Fe^{2+} (as also outlined in Gill, 2010). For samples were Fe was split, the formula became $\frac{100*Mg}{(Mg+Fe^{2+})}$ (Johnson et al., 1996; Gill, 2010). Mg and Fe are atomic element values. Samples with Mg# less than 45 or greater than 71 were eliminated following Gill (2010), Casey et al. (2007) and Stolper and Walker (1980).

Steens and Yellowstone-Snake River Plain Volcanic Province Basalts

The same procedures were followed as for the global basalt dataset with the additional restriction that all samples must be from the Yellowstone-Snake River Plain Volcanic Province, be continental flood basalts, and be of Neogene age. Some data does not specify which epoch, only period; hence, no further restriction beyond Neogene was used.

Sample Selection for Detailed Study

A previous study (Brueseke et al., 2007) reported the geochemistry and physical characteristics of many samples from the Steens lavas and geochemical equivalents, in the vicinity of Steens Mountain, Oregon (see Brueseke et al., 2007 for details on Steens Basalt distribution). Samples were chosen from that database. Samples were initially evaluated for potential copper sulfides or other sulfides based on analysis of non-polished thin sections. Incorporating the results of this investigation, we selected samples that were spread over the range of Cu and MgO concentrations that characterizes Steens basalt magmas. Samples selected were MB97-15, MB97-19, MB97-37, MB97-38, MB97-39 MB97-51, MB97-74A, MB97-75, MB97-76A, MB97-76B, and MB97-76C (Brueseke et al., 2007).

Sample Chemistry

MB97-15 is aphyric, MB97-19, MB97-37, MB97-38, MB97-51, MB97-74A, MB97-75, MB97-76A, MB97-76B, and MB97-76C are mega plagioclase-phyric, and MB97-39 is intermediate between aphyric and megaplagioclase-phyric. On a total alkali vs. silica diagram (Figure 4; Le Maitre and Bateman, 1989), MB97-76A is a trachybasalt, MB97-74A and MB97-75 are on the border between basalt and trachybasalt, MB97-76B is a basaltic trachyandesite, and MB97-39 is a basaltic andesite, all other samples are basalts. On an AFM diagram (Figure 5; Irvine and Baragar, 1971) the samples plot across a range between tholeiitic to mildly calc-alkaline.

Based on the bulk rock geochemistry, SiO_2 ranges from 46.54 to 54.52 wt. %, TiO_2 ranges from 1.46 to 3.13 wt. %, Al_2O_3 ranges from 11.73 to 18.83 wt. %, Fe_2O_3 ranges from 3.74 to 6.9 wt. %, FeO ranges from 6.15 to 12.4 wt. %, MnO ranges from 0.14 to 0.28 wt. %, MgO ranges from 3.46 to 7.35 wt. %, CaO ranges from 6.64 to 9.62 wt. %, Na_2O ranges from 2.99 to

3.68 wt. %, K_2O ranges from 0.26 to 0.82 wt. %, P_2O_5 ranges from 0.26 to 0.82 wt. %, Mg# ranges from 47.4 to 60.9 and Cu ranges from 72 to 365 ppm. Harker diagrams of the selected samples are displayed in Figure 6-Figure 8.

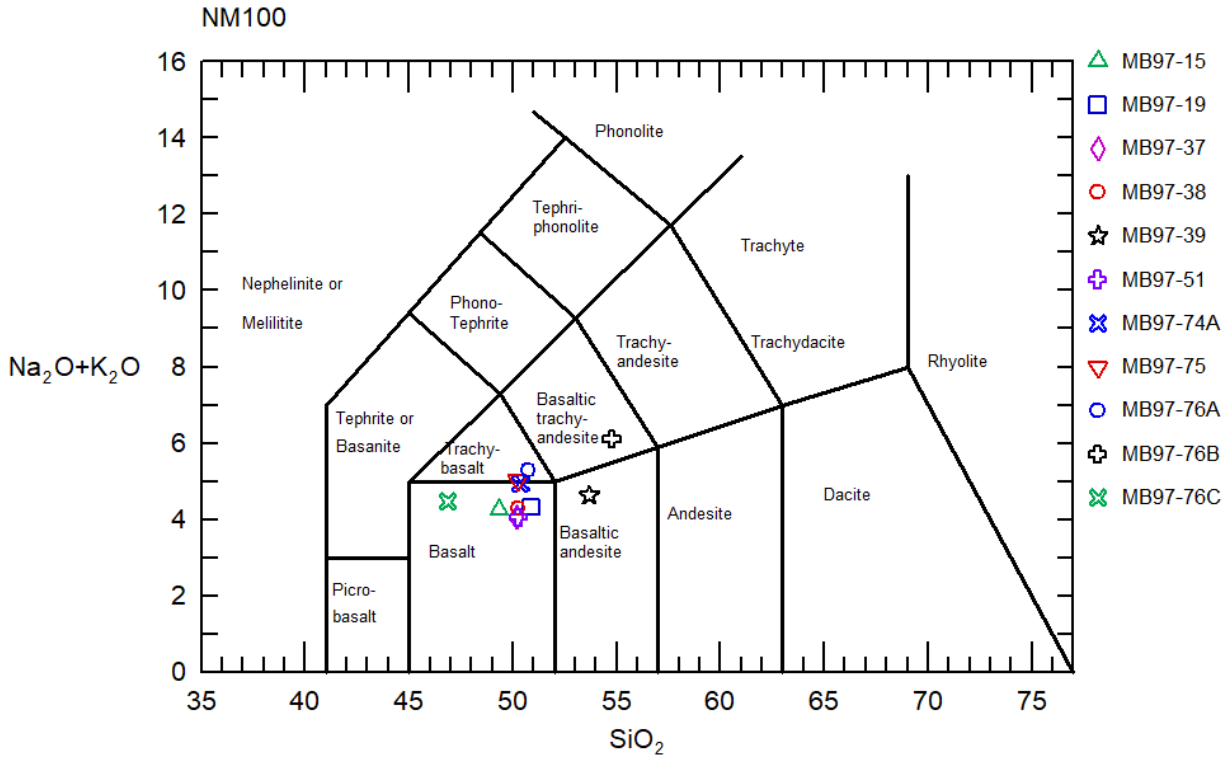

Figure 4: TAS (Total Alkali-Silica) Diagram plotting Steens Basalt samples selected for analysis (after Le Maitre and Bateman, 1989).

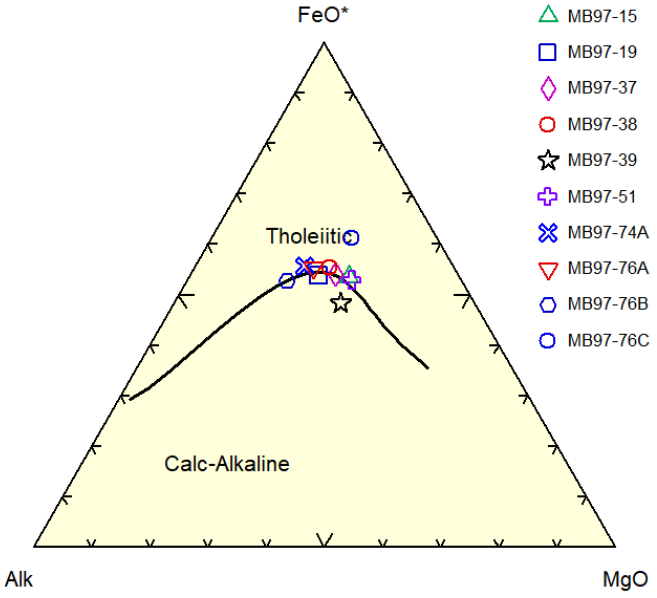

Figure 5: AFM Diagram plotting Steens Basalt samples selected for analysis (after Irvine and Baragar, 1971).

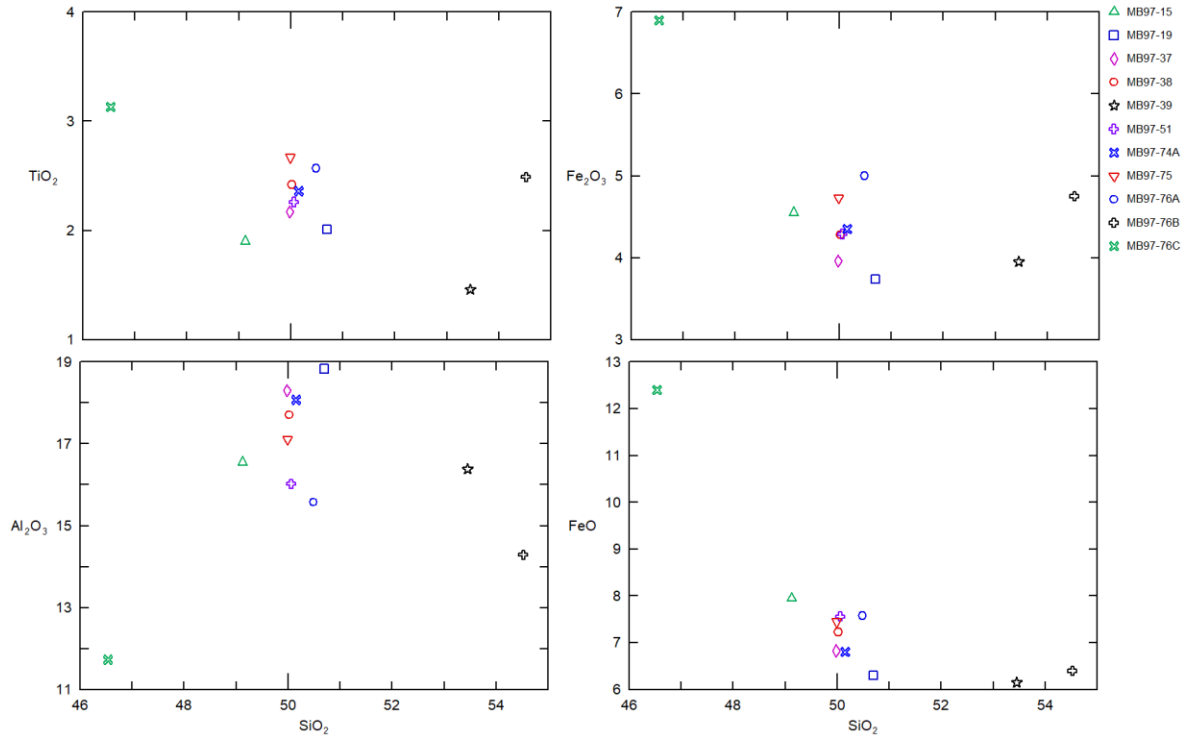

Figure 6: Harker Diagrams (TiO_2, Al_2O_3, Fe_2O_3, FeO) of Steens Basalt samples chosen for analysis.

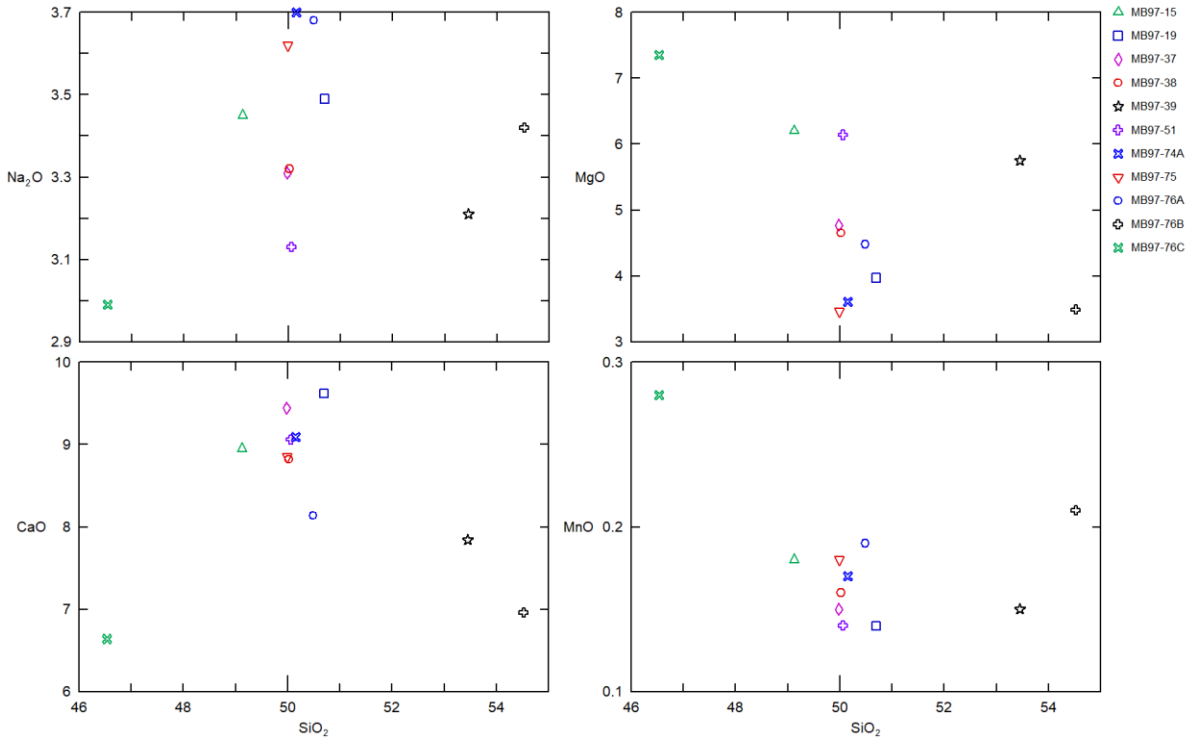

Figure 7: Harker Diagrams (Na_2O, CaO, MgO, MnO) of Steens Basalt samples chosen for analysis.

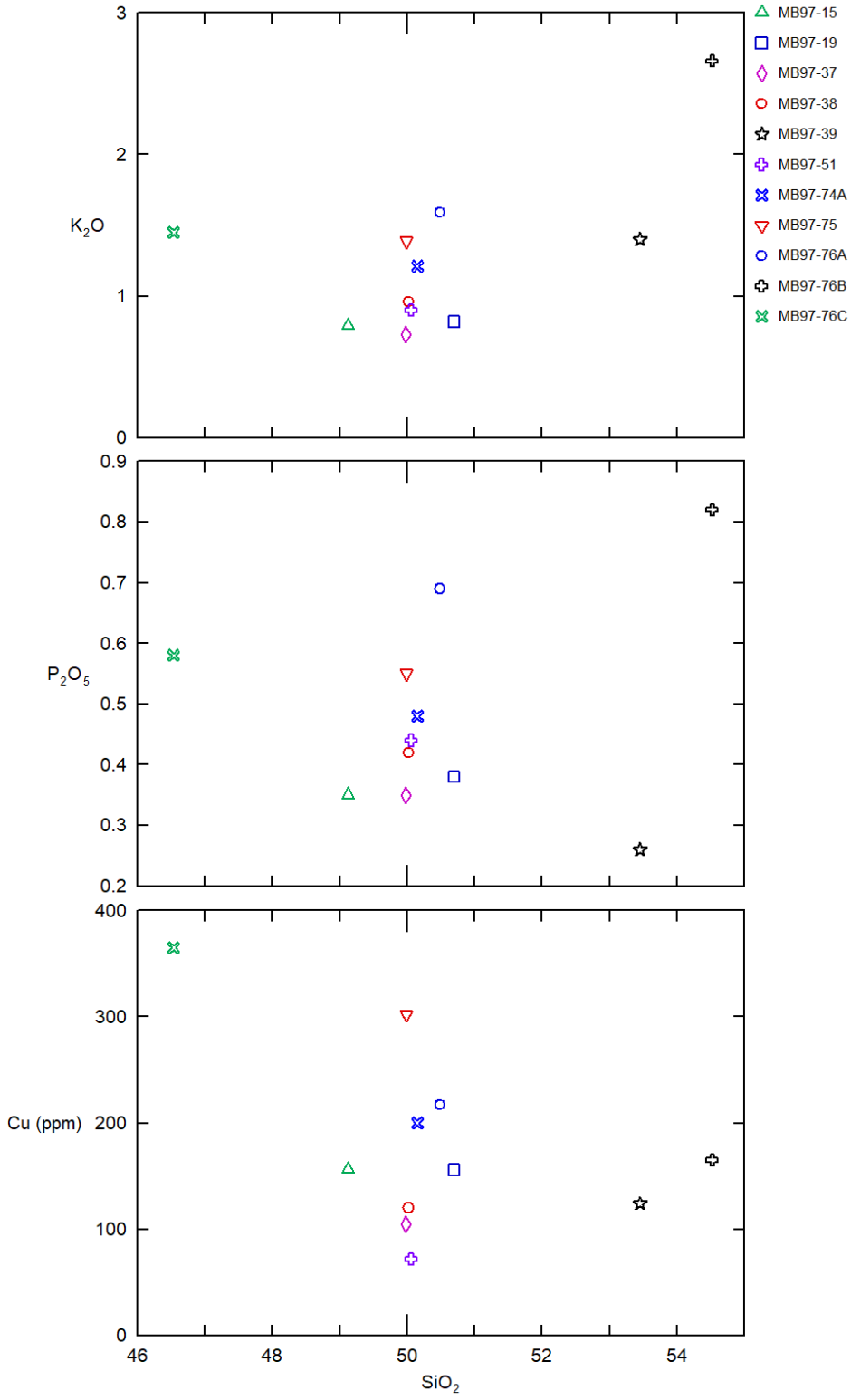

Figure 8: Harker Diagrams (K_2O, P_2O_5, Cu (ppm)) of Steens Basalt samples chosen for analysis.

Reflected Light Microscopy

Samples were prepared and made into polished thin sections by Spectrum Petrographics from rock slabs. Thin sections were examined by reflected light microscopy using a Carl Zeiss Axio Scope.A1 reflected light microscope equipped with an Axiocam 105 color camera (connected to a computer). Samples were scanned at 20x magnification in plane polarized light with increases of magnification for identification. We looked for minerals that had a yellowish tinge because copper sulfides tend to have a yellowish tinge in reflected light. We ignored yellowish phases that had a high relief as we judged them to be relict grit from polishing. Phases that met these criteria were then circled using a 0.25mm Sakura 34061 Microperm pen then analyzed under a Renishaw inVia Raman Microscope (at Kansas State University) for mineral identification.

Microprobe

The thin sections were first coated with a thin film of carbon. Thin sections were then loaded into the sample holder four at a time along with the standards. After being scanned to produce an image file, they were loaded into a JEOL-8230 electron microprobe at the University of Colorado, Boulder. The machine was then calibrated for stage movement. Samples were examined and imaged using the backscattered-electron composition mode (COMPO). Points for analysis were selected using the COMPO mode with assistance from the backscattered-electron topography mode (TOPO) in order that points selected for analysis would not be on areas that were poorly polished. This was mainly the case for the highly weathered olivine minerals. Beam setups are reported in Table 2. Samples too small for the beam conditions were qualitatively identified using an EDS (energy dispersive spectrometer) spectrum. A few copper sulfides and iron sulfides that were too small to be analyzed by the beam were identified in this way. The

microprobe standards are located in Table 31-Table 38 in Appendix C - . The analytical errors and constraints for Cu and other elements are located in Table 3-Table 9 in the results section. In this study, percent error (sigma-1) was an issue because it was both high (often 30% or greater) and highly variable (36% to 71% in plagioclase, for example). For silicates, glass, sulfides, and iron-titanium oxides analytical totals below 97% were eliminated from consideration. Based on FeO and Fe_2O_3 recalculations, iron oxides (but not iron-titanium oxides) with analytical totals below 94% were eliminated. This is because the cation charge is too high for iron recalculation for iron-titanium oxides.

Table 2: Microprobe beam parameters.

Phase	Kilovolts (kV)	Current (nA)	Beam size (μm)
Plagioclase	15	40	10
Olivine	15	50-100	5-10
Pyroxene	15	50-100	0-5
Oxides	15	100	0
Weathered olvine	15	50	10
Copper sulfides	15	50	0
Glass	15	20	10
Amphibole	15	30	2

XRD

An X-Ray Diffractometer (XRD) machine was used to investigate samples for the presence of sulfide and copper sulfide minerals. Samples were ground by hand using an agate mortar and pestle into approximately sub-100μm size. MB97-51 was not run due to lack of material. MB97-74A was machine powdered to sub-100μm size. Samples were not sieved in order to prevent a sampling bias being introduced. Samples were then backloaded into 27mm steel sample holders before being placed into a sample stage. Samples were then placed into a PANalytical Empyrean X-Ray Diffractometer (at Kansas State University) and run using a molybdenum tube for one hour per sample with generator settings of 40 mA, 60 kV. Samples were scanned from 5.0(°2θ) to 70.0(°2θ) with a step size of 0.0070(°2θ) and a divergence slit size of 0.1250°. Once samples were run, they were processed using HighScore Plus software. First, the background was determined to reduce the amount of noise. Then peaks were hand combed and picked that the peaks might be more properly identified. Once identified, the peaks were matched with International Center for Diffraction Data (ICDD) reference data cards. The matches with the highest scores were then manually evaluated for fit by comparing the 2θ of the card to the sample. If the top three peaks, by intensity, matched between the two, the mineral was then evaluated for plausibility of being in the sample before being accepted as a solution.

Raman

After the thin sections were evaluated with a reflected light microscope and the relevant areas marked, they were then loaded onto the stage for the Renishaw inVia Raman Microscope for further characterization of possible sulfide minerals. The instrument was calibrated using an internal silicon standard and an external silicon standard. Using WiRE 4.3 software, the areas of interest were located using the opticals and the camera feed. Once the laser was centered, the

target mineral was struck with a 532 nm (green light) Ar-ion laser for three seconds at 10% laser power (~2 mW) with three accumulations. The laser spot size was 5 μm. This process was repeated for all target minerals except analysis 8-3 which was run at 50% power (all other settings kept the same). Once all target areas were analyzed, the thin section was unloaded and a new thin section was loaded. Analyses 1-14 are associated with MB97-75 and analyses 15-32 are associated with MB97-19.

After acquiring 51 spectra, the spectra were then processed using WiRE 4.3 and 5.0. First, the background was determined by the software and removed and the spectra smoothed. Spectra analyses 5-1 and 8-3 were truncated for better matching. Spectra were then manually labeled as fit for analysis or unfit based on the peak counts. Of those fit for analysis, there were two ranks established. A minimum of 600 counts was required to be considered good (the maximum value was 1900 counts) and a minimum of 540 counts was required to be considered acceptable. Spectra that only showed carbon peaks were eliminated. Of the 51 spectra acquired, 10 (seven good and three acceptable) were selected for analysis. The Spectrum Search tool was used to match the acquired spectra to an internal Renishaw inorganic database by comparing spectra similarity. The top 20 scored minerals were then manually evaluated for fit and the library spectrum that was most fit was selected as the solution. A secondary evaluation was conducted using Spectragryph software (Menges, 2018) to compare identification for those spectra whose identification was less certain. WiRE software was given priority in determining the match. Spectragryph searched a RRUFF database consisting of 5185 Raman spectra from 1677 minerals at four laser wavelengths. Only minerals from 532nm wavelengths were considered. and aquired spectra were identified by spectral similarity.

Chapter 3 - Results

Microprobe

Results of the microprobe analysis are reported as wt% oxide for the major elements and ppm for the trace elements. Cu is considered a major element for sulfides or else it is considered a trace element. The full data from the microprobe is located in Appendix B - . Data that summarizes each subsection is located at the end of the microprobe section after the figures in Table 3-Table 9.

Feldspar

Plagioclase ranges from An_{22}-An_{66} with the majority being labradorite. In terms of abundance, labradorite accounts for 87.3% of all samples followed by andesine (10%) and oligoclase (2.7%). There are also six anorthoclase minerals with An_{3}-An_{18}, Kfs_{15}-Kfs_{35}. See figure 9 for a feldspar ternary diagram plotting the data. For one labradorite analysis the beam spot included an iron oxide (See Figure 10A and Figure 40) in the analysis and, thus, contains an erroneous 563 ppm Cu. This analysis is eliminated from consideration in the results. Based on the reported Cu values, only three labradorite crystals, one andesine crystal, and one oligoclase crystal were above the Cu detection limit (~170 ppm). Labradorite ranges in Cu concentration from 198 ppm to 225 ppm with an average of 212 ppm, andesine contains 191 ppm, oligoclase contains 170 ppm. See Figure 10 for a microprobe image of a large plagioclase phenocryst that contained copper with the An% plotted in a tract across the crystal.

Olivine

Olivine ranges from Fo_{37}-Fo_{74} with an average of Fo_{57}. In terms of abundance, the majority is forsterite (78%) with the rest being fayalite (22%). See Figure 11 for an olivine ternary diagram plotting the data. Based on the reported Cu values, only three forsterite analyses

and two fayalite analyses were above the Cu detection limit (~107 ppm for forsterite and 113 ppm to 193 ppm for fayalite). Forsterite ranges from 122-135 ppm with an average of 122 ppm and fayalite ranges from 214-430 ppm with an average of 335 ppm. See Figure 12 for a microprobe image of olivine correlating the analysis points with Fo%.

Weathered Olivine

Weathered olivine ranges from Fo_{46}-Fo_{74} with an average of Fo_{60}. In terms of abundance, the majority of weathered olivine is forsteritic (92%) with the rest being fayalitic (8%). See Figure 13 for an olivine ternary diagram plotting the data. Based on the reported Cu ppm values, seven forsteritic analyses were above the Cu detection limit (~185 ppm) and no fayalitic analyses had detectable Cu. The detection limit for fayalitic weathered olivine was ~112 ppm for 24 analyses and 192 ppm for two analyses. Forsteritic weathered olivine ranges from 187-287ppm with an average of 231 ppm. See Figure 14 for a microprobe image of weathered olivine correlating the analysis points with Fo% and Cu (ppm).

Pyroxene

There are 73 pyroxene analyses, the majority, in terms of abundance, being augite (86%) followed by enstatite (5%), diopside (4%) and ferrosillite (4%). See Figure 15 for a pyroxene quadrilateral diagram plotting the data. Based on the reported Cu ppm values, five augite analyses and one enstatite analysis were above the Cu detection limit (~127 ppm or ~181 ppm for augite and 189 ppm for enstatite). The augite analyses range from 141-271 ppm Cu with an average of 211 ppm and the enstatite analysis contains 191 ppm. See Figure 16 for a microprobe image of pyroxene correlating the analysis points and Cu (ppm).

Oxides

52 oxide analyses were deemed acceptable (see the methods section for details). In terms of abundance 44% were magnetite and 56% were ilmenite. 14 magnetite samples and one ilmenite had Cu above the detection limit (~150 ppm). Cu ranges from 316-742 ppm in magnetite and is 178 ppm in ilmenite. Generally, there appears to be more Cu with lower Fe_2O_3 concentrations.

Copper sulfide phases

Copper sulfide phases were only found in MB97-19 and MB97-76C. Three points (all from MB97-76C; see Figure 26A) were successfully analyzed. These analyses range from 94 to 95 wt% CuO and 54 to 55 wt% SO_3. Formula calculations yield the chemical formula $Cu_{1.74}S$ which tends toward the chalcocite formula (Cu_2S) but matches most closely with anilite (Cu_7S_4), a rare mineral first studied at the type locality located at the Ani mines in Akita, Japan (Morimoto et al. 1969). While a detailed geologic description of the mine is unavailable, the location of the copper mine sits on non-alkaline mafic volcanic rocks from the Oligocene to the Miocene (mindat.org, n.d.; Geological Survey of Japan, n.d.). Copper sulfide phases were often found near or within iron oxides or iron-titanium oxides (Figure 18).

Glass

Glass was only found in MB97-76B (Figure 25). The glass analyses are primarily Si-Al glasses. Glass chemistry is reported in Appendix B - (Table 29). None of the analyses contained Cu above the detection limit (~382 ppm). As glass is often used as a proxy for melts, the glass chemistry was plotted on a total alkali vs. silica diagram (Figure 20; after Le Maitre and Bateman, 1989) which reveals that it plots in the rhyolite field.

Amphibole

Amphibole occurs as small "straws" within the glass matrix (Figure 25A-25C). These morphologies will be considered in the discussion section. None of the analyses contained Cu above the detection limit (~340 ppm).

Miscellaneous

In addition, there were three analyses that were run under the oxide protocol that returned with totals <77%. Based on their chemistry they are likely iron sulfide or iron-copper sulfide minerals or quenched melt phases that were previously detected on the EDS spectra during microprobe operation. Because the oxide protocol was not set up to record S concentration, we cannot conclusively determine the mineral chemistry but based on other evidence (primarily EDS) we think these are iron sulfide or iron-copper sulfide mineral or quenched melt phases. These minerals range from 2 to 10 CuO wt% with an average of 6 CuO wt%. The iron sulfides and iron-copper sulfides range in size from sub-1μm to ~20μm and can be found in MB97-19, MB97-76B, and MB97-76C (see Figure 29-Figure 37). Finally, an iron zirconium oxide and one possible zircon were found using the EDS (Figure 31).

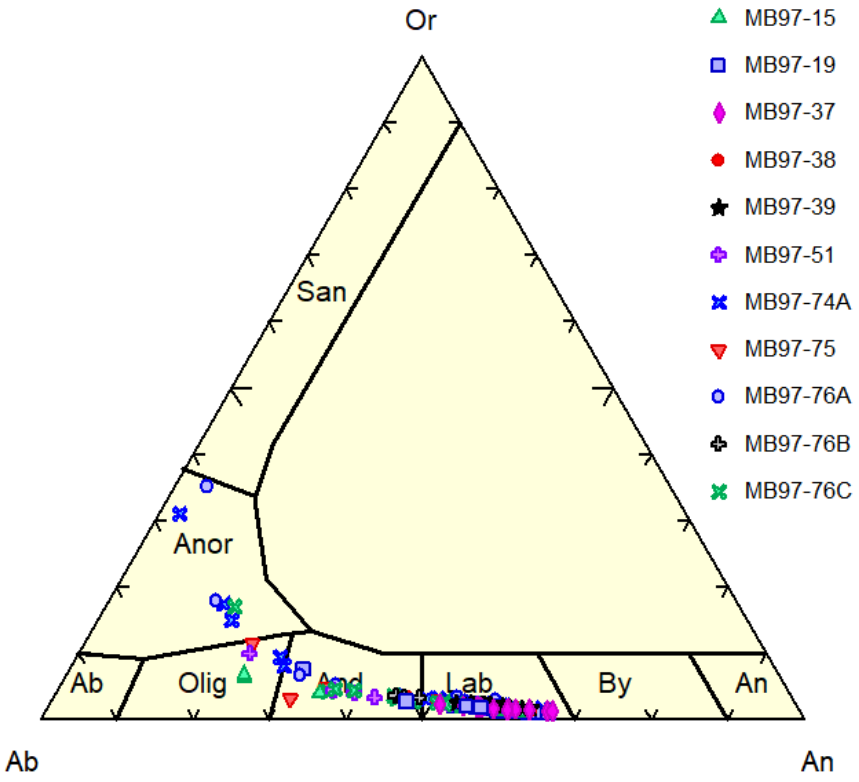

Figure 9: A feldspar ternary diagram of 226 feldspar analyses (220 plagioclase, six alkali feldspar) from the microprobe data. An = anorthite, By = bytonite, Lab = labradorite, And = andesine, Olig = oligoclase, Ab = albite, Anor = anorthite, San = sanidine, Or = orthoclase.

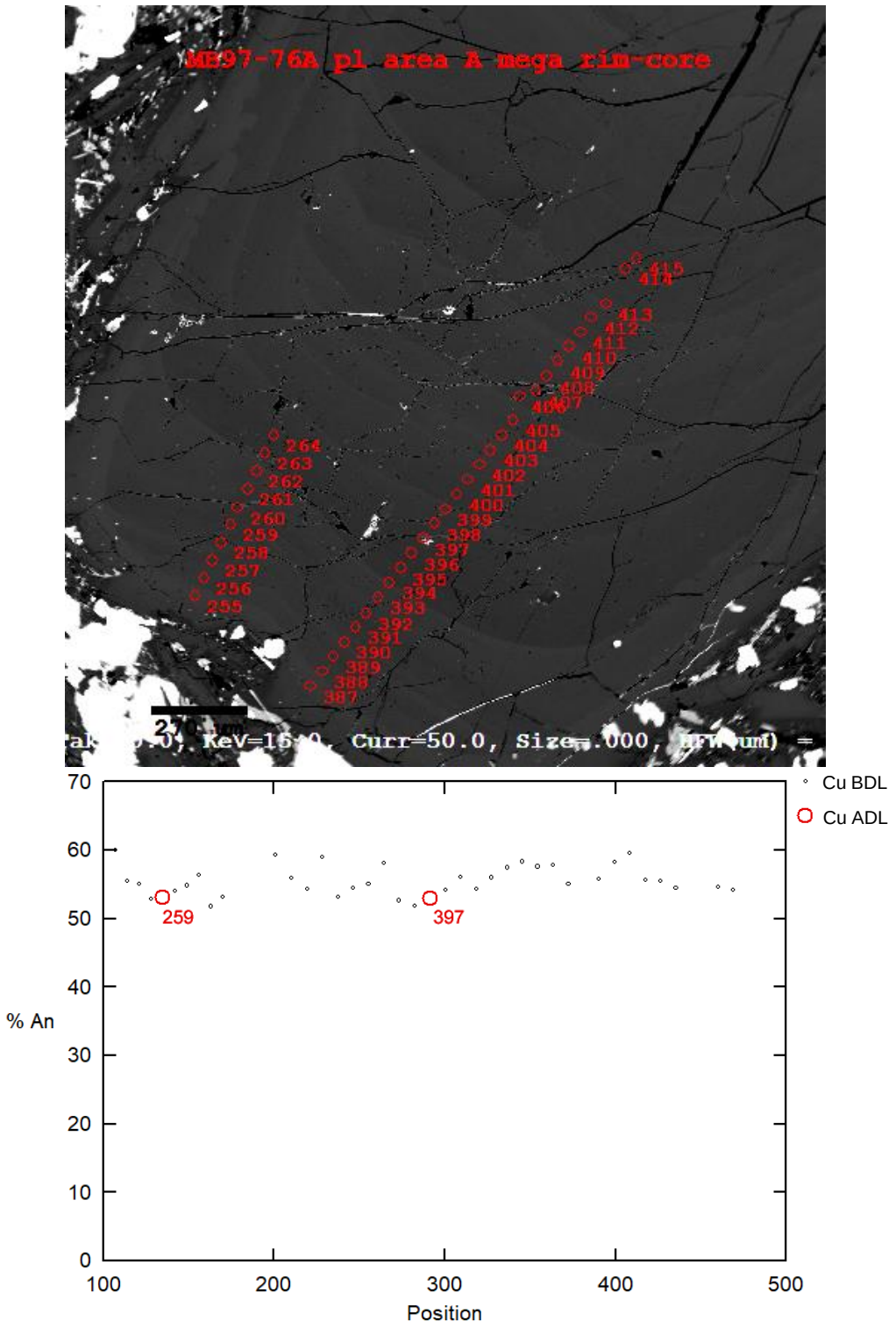

Figure 10: A: A backscattered-electron microprobe (composition mode) image of a single plagioclase crystal in MB97-76A. 39 separate acquisitions were taken in this crystal. Only acquisition 407 has totals too low to be evaluated. B: A plot of the % An of each acquisition arranged by position in the image. Red circles indicate analyses which contained Cu above the detection limit, 259 (213 ppm) and 397 (563 ppm). All other analyses had Cu below the detection limit. It should be noted that 397 may be tainted by the white phase that the

acquisition circle overlaps in 10 (see figure 43 for the same figure without acquisition points obstructing the view).

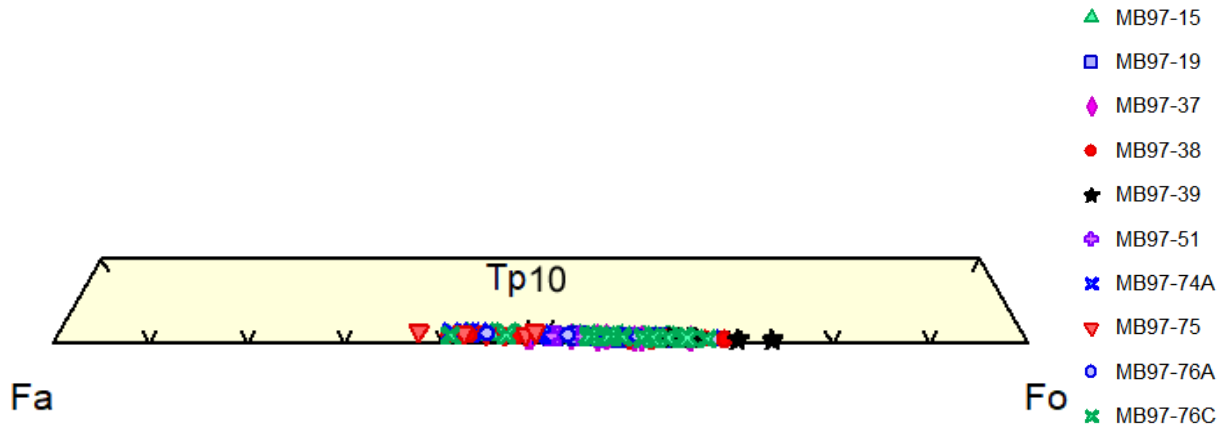

Figure 11: Fayalite (Fa), forsterite (Fo), tephronite (Tp; 10) ternary diagram of 115 olivine analyses from the microprobe data.

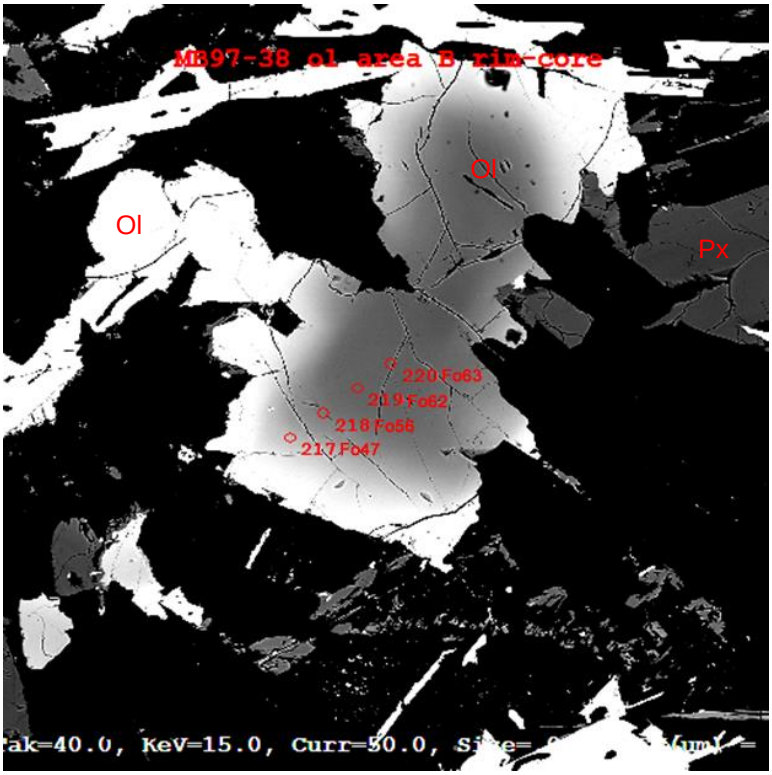

Figure 12: A backscattered-electron microprobe (composition mode) image of olivine in MB97-38 with points indicating the sample information with which they correlate. Forsterite percentage numbers have been added next to the corresponding number. Fo = forsterite, Ol = olivine, Px = pyroxene.

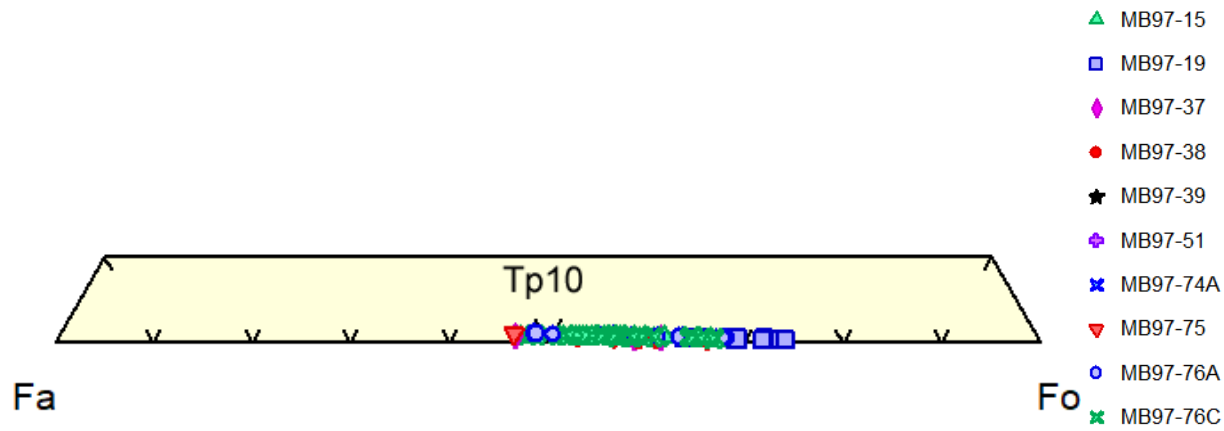

Figure 13: Fayalite (Fa), forsterite (Fo), tephronite (Tp; 10%) ternary diagram of 76 weathered olivine analyses from the microprobe data.

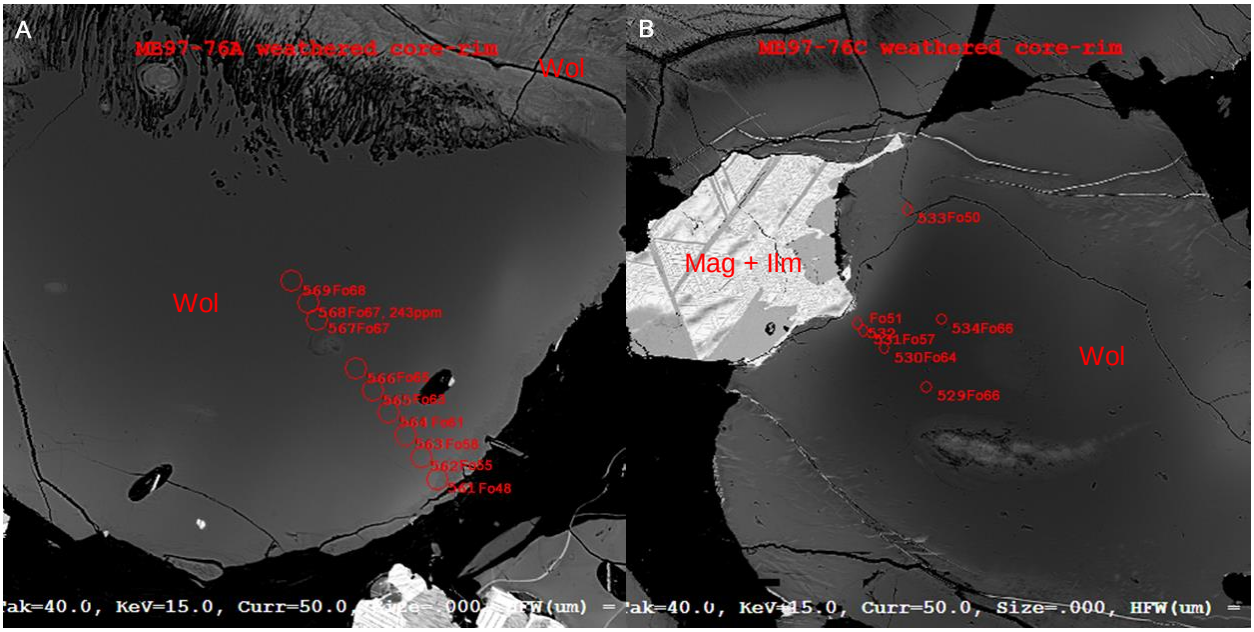

Figure 14: Backscattered-electron microprobe (composition mode) images of weathered olivine with points indicating the sample information with which they correlate. Forsterite percentage numbers have been added next to the corresponding number with ppm Cu if applicable. A: MB97-76A weathered core-rim image. B: MB97-76C weathered core-rim image. Fo = forsterite, Wol = weathered olivine, Mag = magnetite, Ilm = ilmenite.

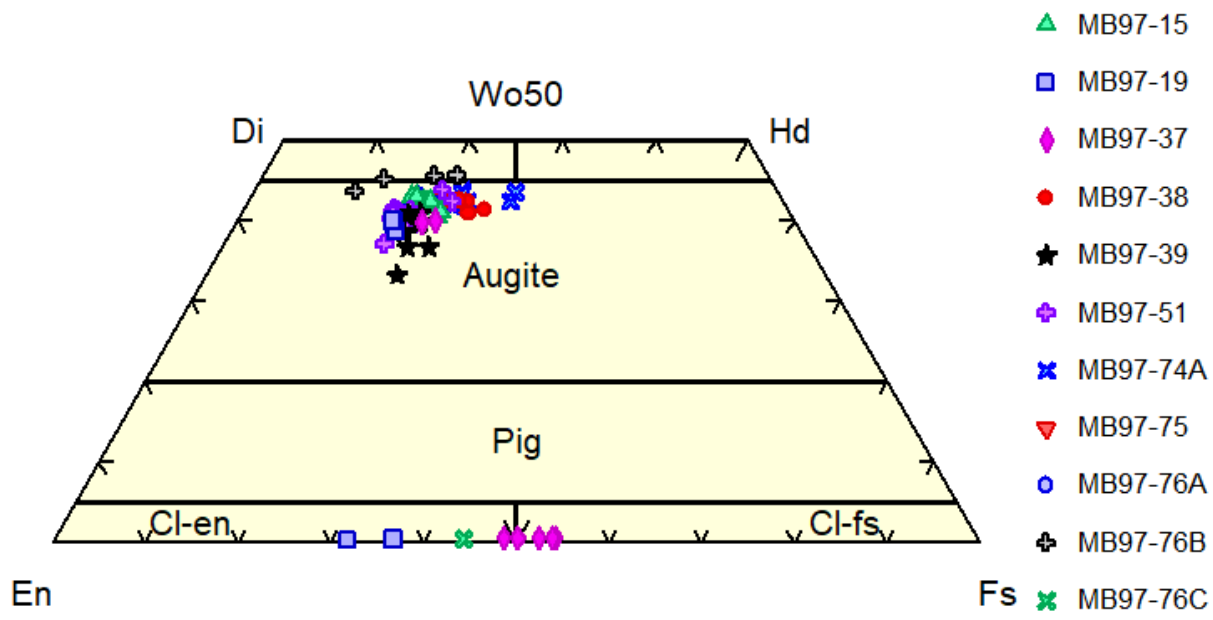

Figure 15: A diagram of the spread of 73 pyroxene analyses from the microprobe data.

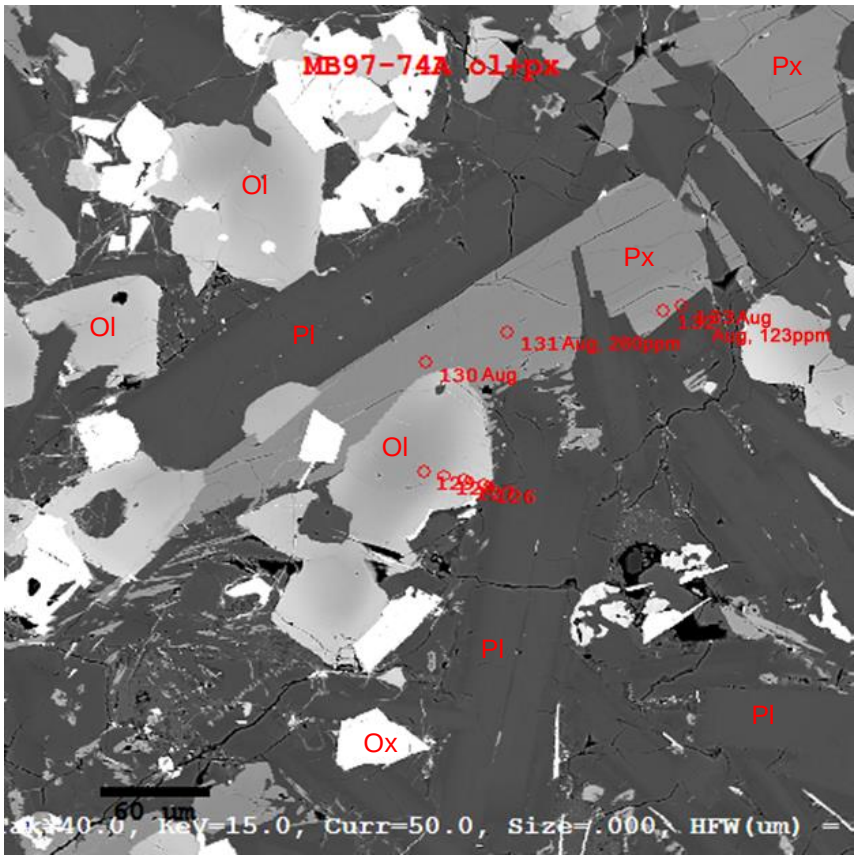

Figure 16: A backscattered-electron microprobe (composition mode) image of a pyroxene crystal next to an olivine crystal in MB97-74A with points indicating the sample information with which they correlate. All pyroxene points are augite (Aug) with ppm Cu added if applicable. Ol = olivine, Ox = oxide, Pl = plagioclase, Px = pyroxene.

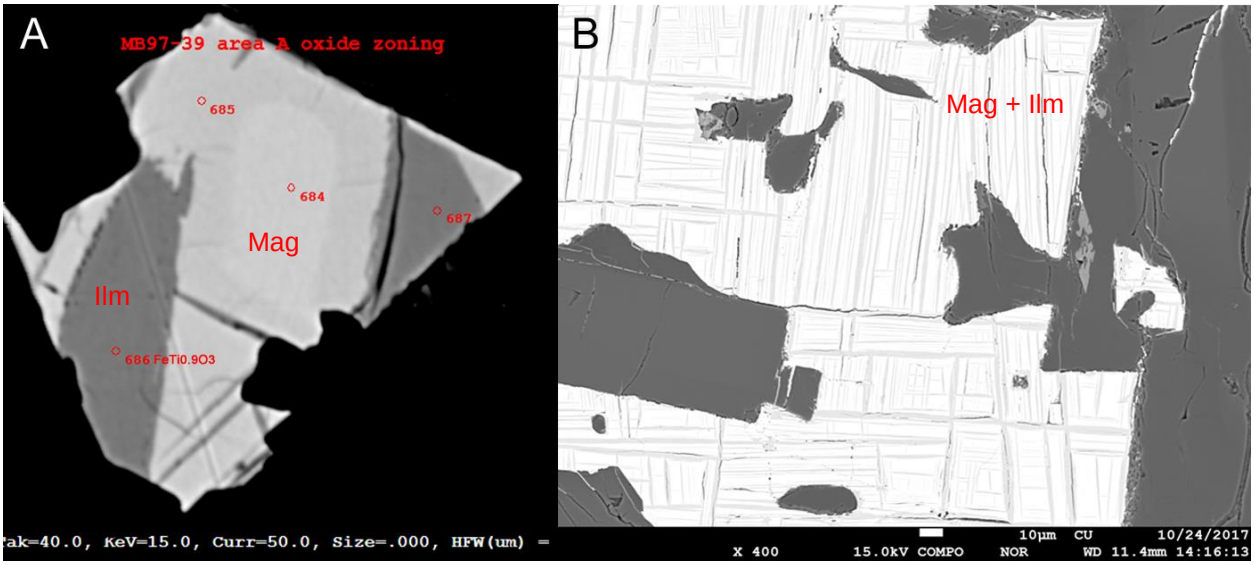

Figure 17: Backscattered-electron microprobe (composition mode) images of oxides. A: An oxide in MB97-39 with points indicating the sample information with which they correlate. An approximate oxide formula (basis of 3 oxygens) has been added next to point 686 which is the only point in this image with high enough totals. B: Another oxide in MB97-15. Note the tartan pattern created by exsolution of iron oxides and iron-titanium oxides.

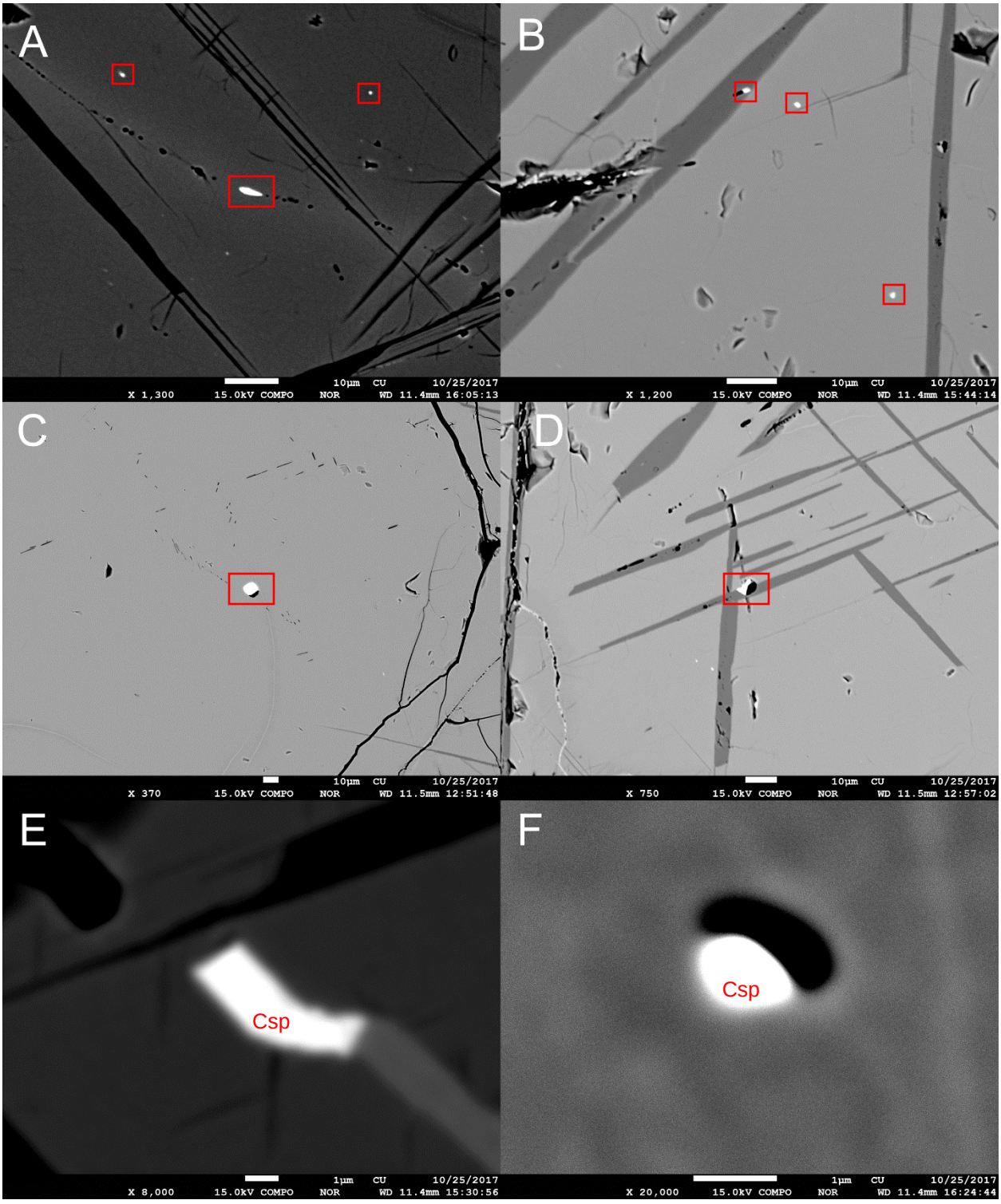

Figure 18: Backscattered-electron microprobe (composition mode) images of copper sulfides from MB97-19 and MB97-76C. The copper sulfides are the bright white blobs (also the more regular, white shape in E) The scale bar for A-D is 10um and the scale bar for E-F is 1um. Copper sulfides in A-F are in oxides. Copper sulfides are outlined in red boxes or have abbreviations. Csp = copper sulfide phase.

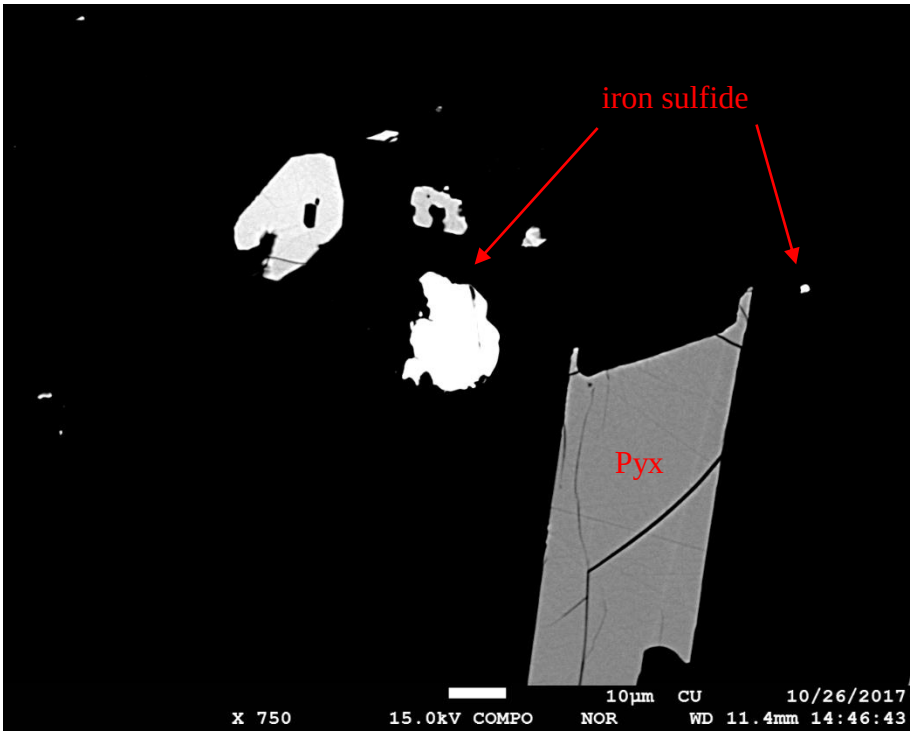

Figure 19: A backscattered-electron microprobe (composition mode) image of iron sulfides in MB97-19. Also note the swallowtail/skeletal morphology of the pyroxene (as in Shea and Hammer, 2013).

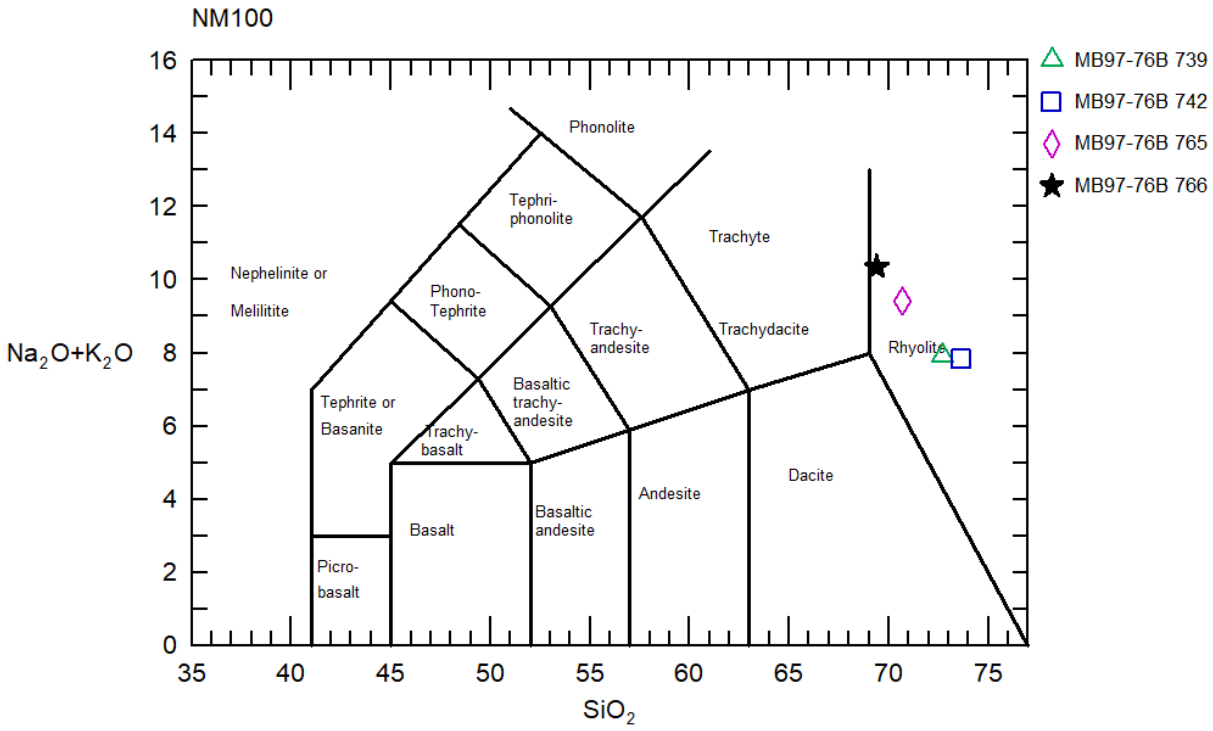

Figure 20: Glass data from MB97-76B plotted on a total alkali silica diagram (after Le Maitre and Bateman, 1989). This plot shows that the residual glass from MB97-76B (a basaltic trachyandesite; see figure 4) plots in the rhyolite field.

Table 3: General summary of the microprobe results as they relate to Cu. Cu mean is the microprobe reported value, Cu max is the maximum possible concentration, Cu min is the minimum possible concentration (which may be below the detection limit). *Only three copper sulfides had acceptable totals.

Mineral	Cu (ppm)	Cu average (ppm)	No. points >DL	wt% CuO	Average Cu DL (ppm)	Average %Err
Plagioclase	170-225	200	5		170	41
Olivine	109-430*	207	5		126	35
Weathered Olivine	187-287	231	7		185	39
Pyroxene	141-271	208	6		165	39
Ilmenite	178	178	1		147	36
Magnetite	316-742	526	14		150	13
Copper Sulfides			3*	94-95	338	0.14

Table 4: Summary of the microprobe results for feldspar as it pertains to Cu. All values are in ppm unless otherwise stated. Line is the analysis number across all samples and phases.

Sample	Mineral	Line	Cu reported (ppm)	Cu %Err	Cu DL (ppm)
MB97-19 (megaphyric)	Labradorite	159	198	41	170
MB97-19	Labradorite	796	225	36	168
MB97-51 (matrix)	Oligoclase	354	170	48	170
MB97-76A (megaphyric)	Labradorite	259	213	38	168
MB97-76B (matrix)	Andesine	781	191	43	172

Table 5: Summary of the microprobe results for olivine as it pertains to Cu. All values are in ppm unless otherwise stated. Line is the analysis number across all samples and phases.

Sample	Mineral	Line	Cu reported (ppm)	Cu %Err	Cu DL (ppm)
MB97-15	Fayalite	347	430	13	113
MB97-74A	Fayalite	118	241	38	193
MB97-74A	Forsterite	125	135	38	109
MB97-76C	Forsterite	254	109	47	107
MB97-76C	Forsterite	326	122	41	107

Table 6: Summary of the microprobe results for pyroxene as it pertains to Cu. All values are in ppm unless otherwise stated. Line is the analysis number across all samples and phases.

Sample	Mineral	Line	Cu reported (ppm)	Cu %Err	Cu DL (ppm)
MB97-37	Augite	717	271	32	181
MB97-38	Augite	222	203	43	184
MB97-51	Augite	380	180	34	127
MB97-74A	Augite	131	260	34	183
MB97-76C	Augite	297	141	43	128
MB97-76C	Enstatite	474	191	47	189

Table 7: Summary of the microprobe results for iron oxides as it pertains to Cu. All values are in ppm unless otherwise stated. Line is the analysis number across all samples and phases.

Sample	Mineral	Line	Cu reported (ppm)	Cu %Err	Cu DL (ppm)
MB97-19	Ilmenite	802	178	36	147
MB97-74A	Magnetite	620	742	9	148
MB97-74A	Magnetite	621	735	9	149
MB97-74A	Magnetite	618	597	11	150
MB97-74A	Magnetite	619	477	14	151
MB97-76C	Magnetite	503	542	12	152
MB97-76C	Magnetite	489	616	11	148
MB97-76C	Magnetite	491	553	12	149
MB97-76C	Magnetite	490	521	13	150
MB97-76C	Magnetite	492	521	13	150
MB97-76C	Magnetite	501	497	13	149
MB97-76C	Magnetite	500	454	14	149
MB97-76C	Magnetite	494	423	15	150
MB97-76C	Magnetite	499	375	18	151
MB97-76C	Magnetite	495	316	21	150

Table 8: Summary of the microprobe results for weathered olivine as it pertains to Cu. All values are in ppm unless otherwise stated. Line is the analysis number across all samples and phases.

Sample	Mineral	Line	Cu mean	Cu %Err	Cu DL
MB97-19	Forsteritic	785	187	47	183
MB97-19	Forsteritic	787	234	38	184
MB97-75	Forsteritic	606	236	38	187
MB97-76A	Forsteritic	568	243	36	182
MB97-76A	Forsteritic	572	234	39	189
MB97-76C	Forsteritic	520	196	45	184
MB97-76C	Forsteritic	536	287	31	187

Table 9: A table detailing the results of the microprobe study for sulfides. Line is the analysis number across all samples and phases. Samples from MB97-19 area B are suspected to be iron sulfides, but this was not confirmed with EDS or microprobe analysis. Note that the totals for the suspected iron sulfides are too low for serious application to the results.

Sample	Mineral	Line	CuO wt%	Cu %err	CuO wt% DL	Total
MB97-76C	Cu sulfide	488	95	0.14	0.03	102.12
MB97-76C	Cu sulfide	622	94	0.14	0.03	101.13
MB97-76C	Cu sulfide	623	94	0.14	0.03	101.71
MB97-19 area B	Fe sulfide	815	6	0.26	0.02	75.42
MB97-19 area B	Fe sulfide	816	2	0.52	0.02	75.32
MB97-19 area B	Fe sulfide	817	10-11	0.19	0.02	76.27

XRD

XRD results are summarized in Table 10. The most common minerals suggested by HighScore Plus were plagioclase, augite (or another pyroxene), and olivine. Other minerals included alkali felspar and iron oxides which were suggested in multiple samples and a selection of other minerals which were only found in one sample. Plagioclase was found in all samples. Augite was found in all but MB97-19 which contained diopside, MB97-38 which had no pyroxene, and MB97-76B which contained diopside. Olivine was found in MB97-19, MB97-37, MB97-38, MB97-39, and MB97-76C (run 2). Alkali felspar was found in MB97-39, MB97-74A, and MB97-76C (run 1). Ilmenite was found in MB97-19 and hematite in MB97-76B. Amphibole was suggested in MB97-76A, and guidottiite (Mn-serpentine; $Mn_2Fe^{3+}(Fe^{3+}SiO_5)(OH)_4$) in MB97-76C (run 1). Other minerals were suggested but are discredited (see the discussion section) as they are found in other geologic environments or systems and not basalt or basaltic andesite magmas.

Table 10: A summary of XRD results. An X indicated the mineral was identified within the sample. A blank entry indicates the mineral was not identified within the sample. All other entries indicate specific minerals.

Sample	Plagioclase	Pyroxene	Olivine	K-spar	Fe-oxide	Other
MB97-15	X	Augite				
MB97-19	X	Diopside	X		Ilmenite	
MB97-37	X	Augite	X			
MB97-38	X		X			
MB97-39	X	Augite	X	X		
MB97-74A	X	Augite		X		
MB97-76A	X	Augite				
MB97-76B	X	Diopside			Hematite	
MB97-76C-1	X	Augite		X		Guidottiite
MB97-76C-2	X	Augite	X			

Raman

MB97-75

Analysis 4-1 peak matching yielded an iron oxyhydroxide answer. Results suggest lepidocrocite, hematite, or ilmenite. Unfortunately, Spectragryph does not provide any additional insight. Lepidocrocite, being the highest ranked hit, will thus be accepted.

Analysis 5-1 (Figure 21) WiRE peak matching suggests olivine, magnetite, and pentlandite (Figure 22A). Spectragryph suggests magnetite (Figure 22B). Since magnetite was identified by both programs, that will be the accepted solution.

WiRE results for analysis 8-3 most closely matches labradorite (Figure 23).

For analysis 13-1, WiRE suggests oligoclase or andesine but oligoclase matches more closely.

MB97-19

For analyses 20-1, 20-2, and 25-1, WiRE suggests mimetite, adamite, and olivine while Spectragryph suggests adamite and fayalite. Mimetite and adamite are unlikely as arsenates in a basalt; for example, mimetite occurs as an epithermal mineral in silver deposits from Morroco (Tuduri et al., 2011), or within alkaline pegmatites of the Kola Peninsula (Lyalina et al., 2010), so olivine is the accepted solution.

For analysis 26-1, WiRE suggests goethite. It is worth noting that Spectragryph suggests chalcocite as a possibility but the reference spectra used a 514 nm laser wavelength and it still doesn't match as well as the Renishaw library goethite spectrum (Figure 24).

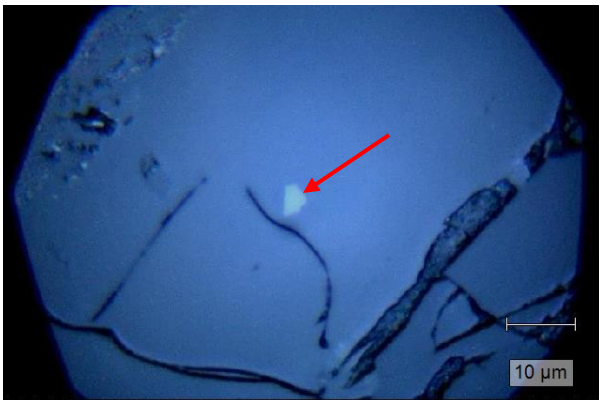

Figure 21: A reflected light imaged captured by the Renishaw InVia Raman Microscope showing a representative target mineral from analysis 5-1. The target is the yellowish crystal near the center of the image indicated by the red arrow.

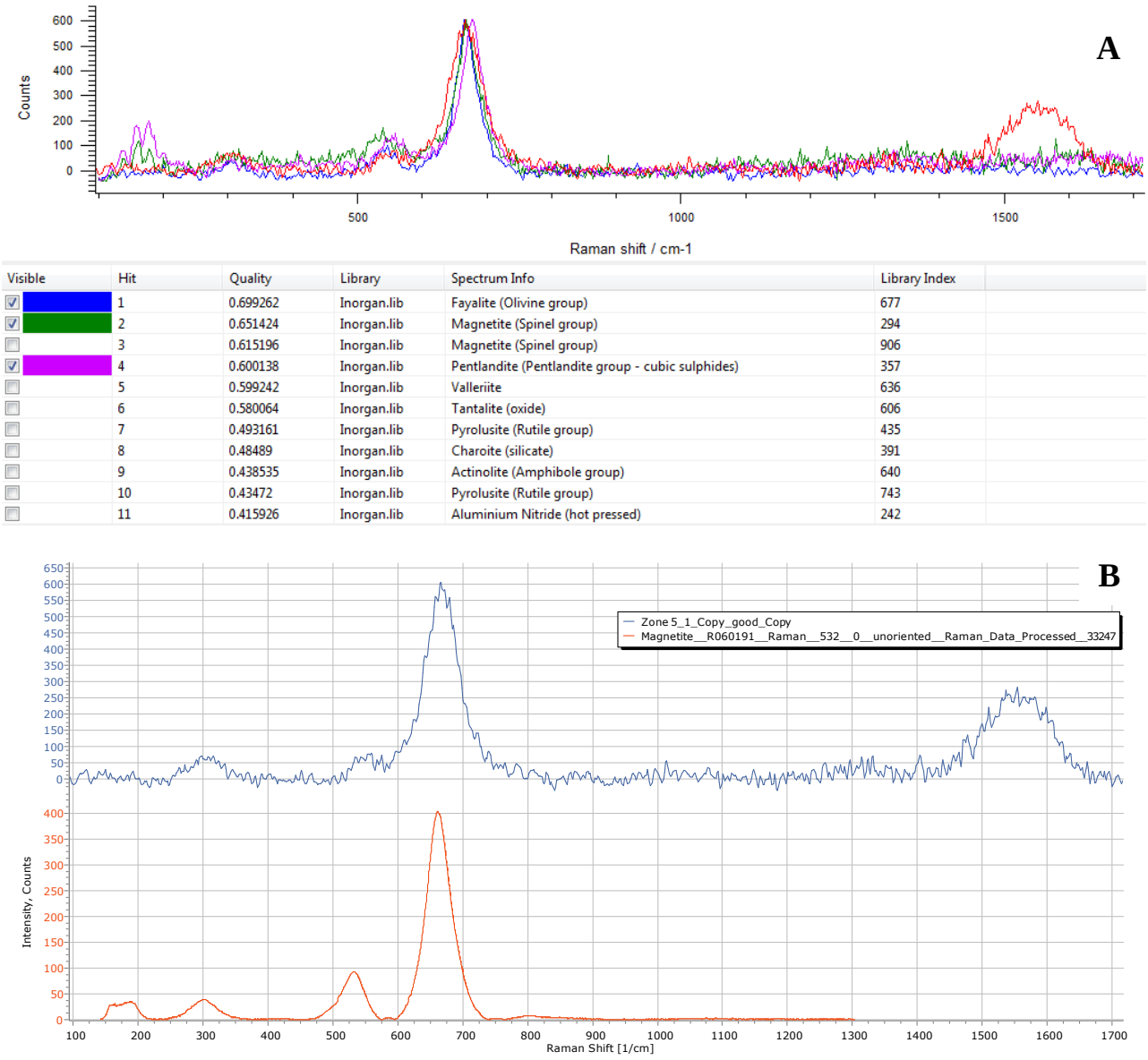

Visible	Hit	Quality	Library	Spectrum Info	Library Index
☑	1	0.699262	Inorgan.lib	Fayalite (Olivine group)	677
☑	2	0.651424	Inorgan.lib	Magnetite (Spinel group)	294
☐	3	0.615196	Inorgan.lib	Magnetite (Spinel group)	906
☑	4	0.600138	Inorgan.lib	Pentlandite (Pentlandite group - cubic sulphides)	357
☐	5	0.599242	Inorgan.lib	Valleriite	636
☐	6	0.580064	Inorgan.lib	Tantalite (oxide)	606
☐	7	0.493161	Inorgan.lib	Pyrolusite (Rutile group)	435
☐	8	0.48489	Inorgan.lib	Charoite (silicate)	391
☐	9	0.438535	Inorgan.lib	Actinolite (Amphibole group)	640
☐	10	0.43472	Inorgan.lib	Pyrolusite (Rutile group)	743
☐	11	0.415926	Inorgan.lib	Aluminium Nitride (hot pressed)	242

Figure 22: Acquired and reference Raman spectra for analysis 5-1. A: An image of the WiRE peak matching tool (Spectrum Search). The sample spectra is in red with reference spectra fayalite (blue), magnetite (green), and pentlandite (magenta). B: A stacked image from Spectragryph showing the sample spectra (blue) and the reference spectra, magnetite (orange).

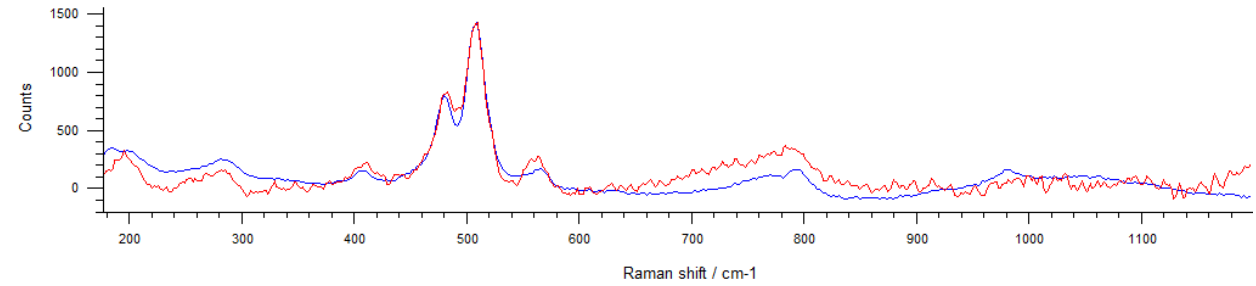

Visible	Hit	Quality	Library	Spectrum Info	Library Index
☐	1	0.798721	Inorgan.lib	Andesine (Feldspar group - An30-50)	493
☐	2	0.787972	Inorgan.lib	Andesine (Feldspar group, An30-50)	163
☑	3	0.767698	Inorgan.lib	Labradorite (Feldspar group, An50-70)	898
☐	4	0.764501	Inorgan.lib	Bytownite (Feldspar group, An70-90)	71
☐	5	0.733616	Inorgan.lib	Oligoclase (Feldspar group - An10-30)	490
☐	6	0.707589	Inorgan.lib	Bytownite (Feldspar group, An70-90)	569
☐	7	0.690685	Inorgan.lib	Oligoclase (Feldspar group, An10-30)	36
☐	8	0.68568	Inorgan.lib	Heliolite	125
☐	9	0.667664	Inorgan.lib	Bytownite (Feldspar group, An70-90)	568
☐	10	0.660203	Inorgan.lib	Moonstone (white) (Feldspar group)	748
☐	11	0.648951	Inorgan.lib	Albite (Feldspar group, An0-10)	724

Figure 23: An image of the WiRE peak matching tool (Spectrum Search) showing acquired (red) and labradorite (blue) reference Raman spectra for analysis 8-3.

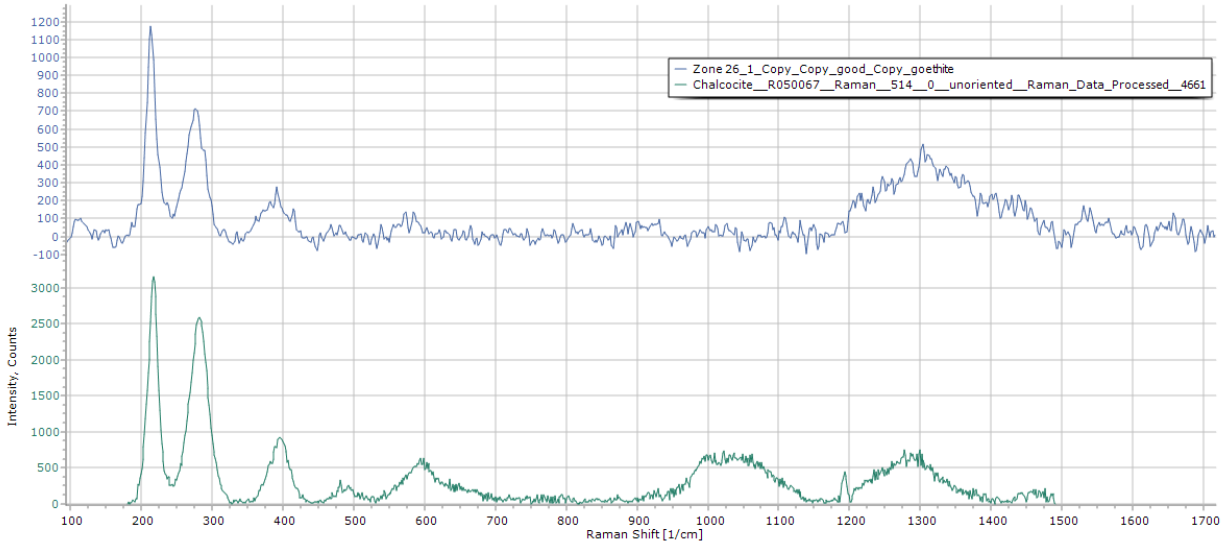

Figure 24: A Spectragryph stacked Raman image showing sample spectra (blue) against chalcocite (green; 514 nm) in analysis 26-1.

Table 11: Summary of Raman results.

Sample	Analysis	Accepted solution
MB97-75	4-1	Lepidocrocite
MB97-75	5-1	Magnetite
MB97-75	8-3	Labradorite
MB97-75	13-1	Oligoclase
MB97-19	20-1	Olivine
MB97-19	20-2	Olivine
MB97-19	25-1	Olivine
MB97-19	26-1	Goethite

Chapter 4 - Discussion

Implications for Copper Partitioning in Steens Basalt magmas

Partitioning Hypotheses

A few options for copper partitioning exist. First, Cu is directly incorporated into the crystal structure of plagioclase and other silcates and oxides. One possibility is that Cu^{+} could substitute for Na^{+} in plagioclase as suggested by LeHuray (1989) and Jensen (1982) or Cu^{2+} substituting for Fe^{2+} in Fe-Ti-oxides and Fe-Mg-silicates (Jensen, 1982). The issue with this hypothesis is that other authors argue that Cu^{+} cannot substitute for Na^{+} due to differences in electronegativity (Ringwood, 1955; Ahrens, 1952; Faure, 1998). It does seem possible that Cu^{2+} could substitute for Fe^{2+} which could explain the higher concentrations of Cu in magnetite, faylitic olivine, and the presence of Cu in copper-iron sulfides (as detected by EDS) but does not explain why the ilmenite had so little Cu considering that publised the K_d value for ilmenite (in basalt) is 1.46 (GERM database; Paster et al., 1974). There is too little data to definitively determine that Cu substitutes for Fe. Evaluating the plagioclase analyses, most Cu-bearing minerals are labradorite; however, this could be biased due to the number of labradorite crystals that were analyzed compared to the other plagioclase compositions. We cannot conclusively show that sodic plagioclase is more likely to incorporate Cu than calcic plagioclase.

Another possibility is that a small amount of Cu could be incorporated due to small pressure and temperature changes that slightly affect Cu relative compatibility (Jensen, 1982; Blundy and Wood, 2003). These small pressure and temperature changes affect partitioning due to causing different strains on the crystal lattice at the lattice site of Cu entry (Blundy and Wood, 2003). Stated differently, partition coefficient (K_d) varies as a function of pressure and temperature, though determining which has the stronger influence requires experimentation on

synthetic systems (Blundy and Wood, 2003). As we did not experimentally determine the pressure nor temperature of the rocks and were we unable to calculate K_d values, we cannot offer much insight into this supposition.

A third suggestion by Hofmeister and Rossman (1985) is that as Cu rises in concentration in the magma, Cu will inevitably increase in concentration in the crystal. There is little evidence, however, that Steens magmas ever had had high Cu concentrations (≥1 wt% CuO). The average Cu concentration for flood basalts is 153 ppm based on the full global flood basalt dataset (4-3008 ppm); even limit the upper bound of Cu to 700 ppm for comparison to Steens rocks, the average only drops to 138 ppm Cu. Average Steens basaltic rocks have 135 ppm Cu, indicating that Steens rocks are not extraordinary regarding Cu concentrations compared to the flood basalt average. This lack of elevated Cu concentrations is supported by our inability to find large (≥1mm) copper sulfide minerals across a range of Steens rocks with varying MgO concentrations.

Plagioclase Cu Nanoparticle Hypothesis

Another hypothesis (proposed here) is that Cu forms nanoparticles that then aggregate onto the growing plagioclase crystal. First, the melting point of Cu (1084.5^{o}C at 1atm; Mirwald and Kennedy, 1979) is lower than the lowest solidus temperature of plagioclase, around 1124^{o}C for pure albite (Greenwood and Hess, 1998). This would mean that normally Cu would still be a liquid when labradorite, andesine, and oligoclase were crystallizing. To get around this melting point issue, the magma would have to be undercooled before the temperature would allow for the precipitation of Cu nanoparticles. During microprobe investigation, evidence of undercooling was found. Minerals in MB97-19, MB97-37, MB97-39, and MB97-76B show swallowtail, skeletal, and hopper morphologies (Figure 25) which is indicative of an undercooled magma

(Shea and Hammer, 2013). Further investigation must be conducted before we can reliably argue that an undercooled mafic magma can cross the melting point of Cu, allowing for the possibility of nanoparticles. Second, Cu seems to be found along crystal lattices (Johnston et al., 1991; Hill, 2009; Xu et al., 2017) which does not support the idea of random Cu nanoparticle aggregation, unless the Cu migrated to the crystal lattice sites later (likely after the intrusion of the magma into a secondary, shallower chamber but before eruption; Hill, 2009; Xu et al., 2017). This hypothesis needs more testing before it can be realistically considered.

Partitioning Conclusion

The first hypothesis, thus, is the more likely; however, Goldschmidt's rules (Faure, 1998), seem to preclude Cu^{+} substituting for Na^{+} and there does not seem to be enough Cu in the magma to allow for the concentration of Cu in the plagioclase crystal. The changes in relative compatibility proposed by Jensen (1982) and Blundy and Wood (2003) seem to be the most probable scenario unless a different mechanism can be proposed.

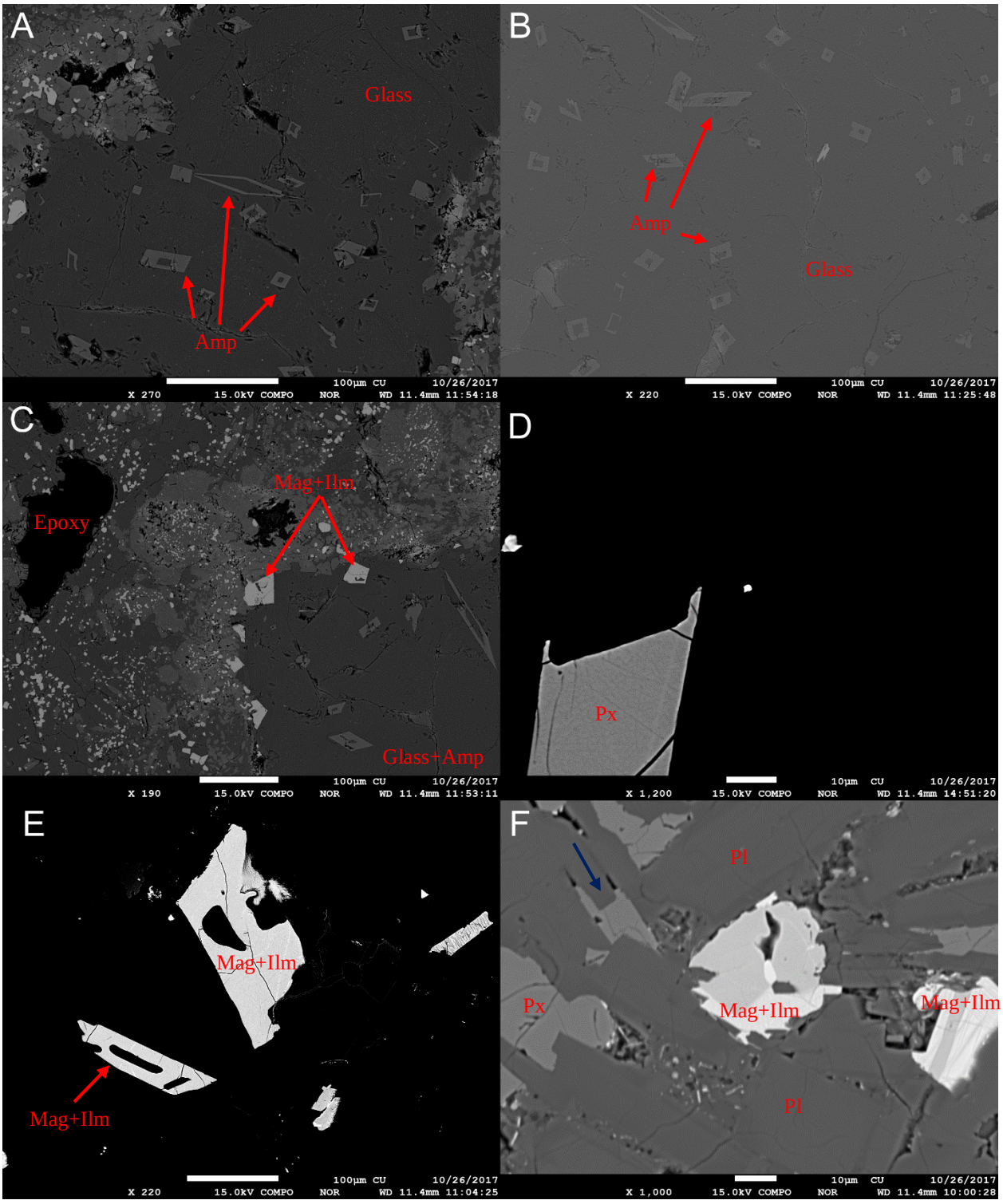

Figure 25: Crystal morphologies indicative of undercooling (Shea and Hammer, 2013). A, B, C: Microprobe images of matrix glass with amphibole "straws" that grew within the glassy matrix from MB97-76B. These "straws" show swallowtail, skeletal, and hopper morphologies and are very similar in appearance to tourmaline straws grown from experimental, pressurized, undercooled peraluminous haplogranite systems (Wierman, et al., unpublished data). D: Iron sulfides in MB97-19. Note the swallowtail and skeletal

morphology of the pyroxene. E: (Ti-rich) oxides in MB97-37 showing hopper morphology. F: A pyroxene (indicated by the blue arrow) in 97-39 showing swallowtail and skeletal morphology. Amp = amphibole, Ilm = ilmenite, Mag = magnetite, Pl = plagioclase, Px = pyroxene.

Immiscible Sulfide Textures

Our first discovery of a copper sulfide was a significant find, not just because it proved copper sulfides were in the Steens basalt, but because of how it appeared (Figure 26A). The discovery is not without complications, however. There is some ambiguity if the copper sulfides, in general, are quenched melt or mineral phases (possibly from the crystallization of the quenched melt). Morphologically, many appear to form blebs and embayed or ribbon-like shapes which are reminiscent of plastic deformation of a liquid or molten phase. A few others, however, appear to have a more defined crystalline structure (see Figure 18E). We found two settings which displayed textures similar to Figure 26A. The first setting is from a meteorite, Katol L6-7 chondrite, which contains a quenched metal-sulfide generated from shear-induced frictional melting (Ray et al. 2017). In the meteorite, there are blebs and deformed droplets of sulfides that look similar to the copper sulfides in MB97-76C (see Figure 26C). While this first example is useful, it is not magmatic. The second example is more applicable to this study. This second setting is magmatic; Cu-Ni-PGE deposits from poikilitic harzburgites and orthopyroxenites in the Mirabela Intrusion of the Santa Rita deposit in northeastern Brazil (Barnes et al., 2017). The reflected light microscopic view (Figure 26B), while being larger than our microprobe view, shows a likeness to our image being similar to the embayed and ribbon-like blebby textures.

The evidence suggests that our phases are from an immiscible sulfide liquid and based on the morphology are quenched melts rather than crystals. This is significant because as above, an immiscible sulfide liquid is often found in layered mafic deposits (Barnes and Ripley, 2016) which are, in turn, often found under flood basalts (Ridley 2013; Song et al., 2011; Starostin and Sorokhtin, 2011).

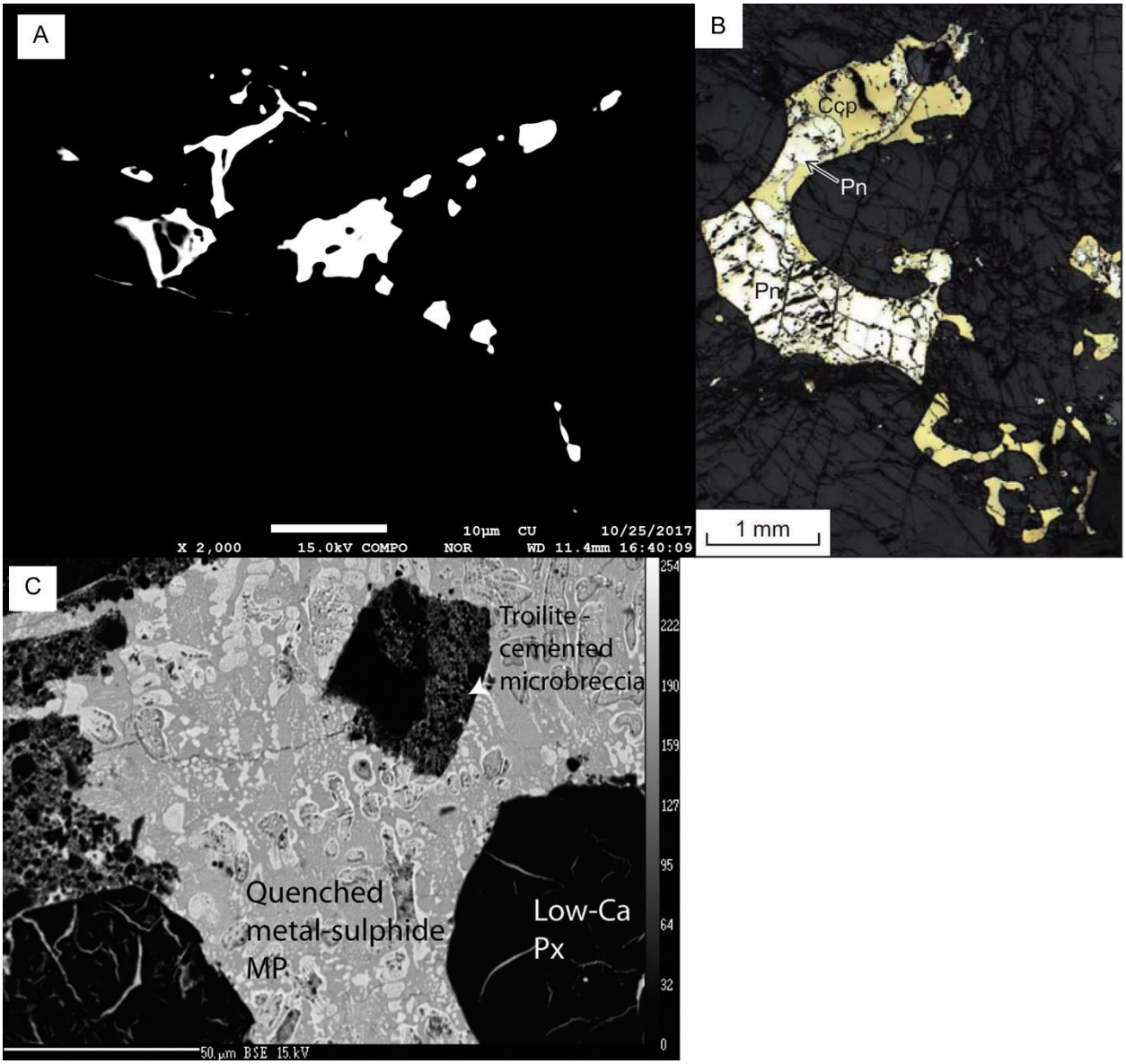

Figure 26: Sulfide textures immiscible melts. A: A microprobe image from MB97-76C showing possible immiscible sulfide quenched liquid textures. The image shows blebs and ribbons of copper sulfides. B: Reflected light view of embayed and ribbon-like sulfides from the Mirabela Intrusion in northeastern Brazil (Barnes et al., 2017). Ccp = chalcopyrite, Pn = pentlandite. C: Blebs, deformed droplets, and ribbons of sulfides from the Katol L6-7 chondrite (Ray et al., 2017). Px = pyroxene, MP = melt pocket.

Raman

Raman analysis did not yield results that could conclusively identify copper sulfides. The carbon coating on the samples proved to have a significant impact on the spectra. Most spectra record a carbon peak which sometimes dominates the spectra or simply obscures it enough that the software cannot accurately generate a mineral match. Analysis 31-1 (Figure 27) shows a good example of this issue. This is particularly unfortunate because the carbon peak occurs in the same Raman shift area as chalcocite which means that if chalcocite was hit by the laser, it is very likely completely obscured by the spectra of the carbon coating. Another issue is that the laser centering was not calibrated due to time and effort which could potentially have caused the laser to miss the target mineral given how small our targets were (approaching 5 μm). The size of the targets was also approaching the spot size of the laser, potentially allowing the spectra to be tainted by other, surrounding minerals. Generally, the Raman reinforced what we already knew, that labradorite, oligoclase, olivine, and iron oxides are present in samples MB97-75 and MB97-19. It is worth mentioning, however, that Spectragryph suggested chalcocite as a possible match for analysis 26-1, albeit at a 514 nm wavelength. Unfortunately, the RRUFF database does not have any useable chalcocite spectra at 532 nm wavelengths; thus, we cannot verify or confidently state that chalcocite is a solution. In addition, it still doesn't match as well as the Renishaw library goethite spectrum that was proposed as the WiRE solution.

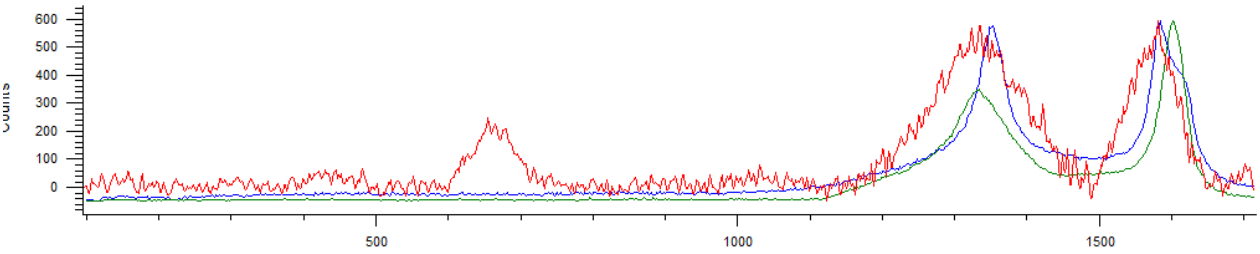

ible	Hit	Quality	Library	Spectrum Info	Library Index
	1	0.709735	Inorgan.lib	Glassy Carbon	596
	2	0.709262	Inorgan.lib	Tucolite	433
	3	0.693221	Inorgan.lib	Glassy Carbon	721
	4	0.677782	Inorgan.lib	Graphite (polycrystalline)	394
	5	0.665001	Inorgan.lib	Anthracite (Organic)	455
	6	0.662632	Inorgan.lib	Lepidocrocite (white) (Fe-hydroxide)	922
	7	0.659143	Inorgan.lib	Zirconolite (Oxide)	29
	8	0.656278	Inorgan.lib	Shungite (Organic)	4
	9	0.655174	Inorgan.lib	Albertite	335
	10	0.642971	Inorgan.lib	Glanzkohle	771
	11	0.62528	Inorgan.lib	Shungite (Organic)	420

Figure 27: Analysis 31-1 showing the peak(s) generated by the carbon coating.

XRD

As with the Raman results, the XRD results also confirmed what we already knew via the microprobe analyses, that plagioclase, pyroxene, olivine, ilmenite and some alkali feldspar and amphibole are present in our samples. The XRD did suggest some additional minerals, but most were eliminated. First, in MB97-19, HighScore Plus suggested a possible match with berezanskite ($KLi_3Ti_2Si_{12}O_{13}$). Berezanskite is a pegmatitic mineral (Martin and Blackburn, 1999), so it would not be in the Steens lavas. Second, in MB97-37, nekrasovite ($Cu_{26}V_2(As, Sn)_6S_{32}$ was suggested. Nekrasovite is found in high-sulfidation epithermal gold-telluride deposits in Uzbekistan (Plotinskaya et al., 2006) as well as porphyry Cu deposits in Serbia where it forms a solid solution with colusite ($Cu_{12}VAs_3S_{16}$; Cvetković et al., 2013). Third, in MB97-38, HighScore Plus suggested a possible match with proustite (Ag_3AsS_3). Prousite is an epithermal mineral (Yuningsih and Matsueda, 2018), so it is likely not in the Steens lavas themselves. Fourth, in MB97-74A, garnet (between andradite and uvarovite) is suggested. Garnets may be found in residual ultrabasic mantle (Baksi, 1995), but our rocks are basic. Fifth, hematite as the iron-oxide in MB97-76B. This makes sense for MB97-76B because it is the most weathered Steens lava sample chosen for analysis. Sixth, in MB97-76C (run 1) guidottiite (Mn-serpentine) is suggested. Serpentine occurs from the hydration of ultrabasic minerals, so it is possible (Scott et al., 2017).

Chapter 5 - Conclusions and Future Work

Conclusions

1) Cu sulfide phases were found in MB97-19 and MB97-76C and Fe sulfides in MB97-19, MB97-76B, and MB97-76C. Other possible sulfides were found but unverified in MB97-75 and MB97-76A.
2) There appears to be a weak correlation between whole rock Cu concentration and the presence of (Cu) sulfides. MB97-19 and MB97-76B contain moderate concentrations of Cu while MB97-76C is the sample with the highest Cu concentration.
3) Cu can be found in all analyzed phases, except glass and amphibole. Cu is most abundant in the sulfide phases. Based on average Cu concentration for the non-sulfides, magnetite contains the most, followed by (forsteritic) weathered olivine, pyroxene, olivine, plagioclase, and ilmenite. Felspar is observed to be below all other silicates in Cu concentration, which is unexpected based on the evidence of the Oregon Sunstones (Hofmeister and Rossman, 1985; Johnston et al., 1991).
4) A lack of glass with detectable Cu precludes the ability to calculate partition coefficients (K_d).
5) We could not confirm the presence of sulfides using either the XRD or the Raman.
6) Cu sulfide phases are most likely quenched melts as they appear to resemble quenched metal-sulfide melts in the Katol L6-7 chondrite meteorite (Ray et al., 2017) and quenched sulfides in the Mirabela Intrusion in northeastern Brazil (Barnes et al., 2017).

7) Hopper, swallowtail, and skeletal crystal morphologies were detected in MB97-19, MB97-37, MB97-39, and MB97-76B which indicate that at least some Steens lavas could be undercooled (Shea and Hammer, 2013).
8) Of the several hypotheses summarized in this work, none are confirmed. Cu^{+} cannot be verified to substitute for Na^{+} as suggested by LeHuray (1989) and Jensen (1982) and disputed by Ahrens (1952), Ringwood (1955), and Faure (1998). Cu^{2+} may substitute for Fe^{2+} as suggested by Jensen (1982), but due to analytical limitations this is not definitive.
9) A new hypothesis centered on the idea of nanoparticles is proposed but due to issues with temperature and crystallographic location is also unconfirmed.
10) Despite being untested in this work, the changes in relative compatibility proposed by Jensen (1982) and Blundy and Wood (2003) seem to be the most likely hypothesis to explain Cu concentrations in silicate minerals.

Future Work

Given that we only found a few, mostly small, copper sulfide phases in Steens lavas, it would be foolishly ambitious to speculate about the existence of larger copper sulfide deposits in a potential mafic intrusion beneath the Steens Basalt. We think that further scientific investigation is warranted, however. One such future study would be to drill into the subsurface of the Steens Basalt to search for more evidence of copper sulfides at depth, with the hope that further down, there may be more and larger phases. If that investigation yields fruitful results, then the possibility of economic deposits of copper may then be considered. As it is, the results are not conclusive enough for contemplation.

Other studies we would like to see would done would be an experimental determination of Cu partition coefficients in basalts and basaltic andesites over a range of pressure and

temperature conditions and a microprobe investigation of the Oregon Sunstone crystals themselves to suppliment the work on plagioclase and other silicate phases presented here.

References

Ahrens, L.H., 1952, The use of ionization potentials Part 1. Ionic radii of the elements: Geochimica et Cosmochimica Acta, v. 2, no. 3, p. 155-169

Barnes, S. and Ripley, E. M., 2016, Highly siderophile and strongly chalcophile elements in magmatic ore deposits in Harvey, J. and Day, J. M. D., eds., Highly siderophile and strongly chalcophile elements in high temperature geochemistry and cosmochemistry: Reviews in mineralogy and geochemistry, vol. 81, p. 725-744.

Barnes, S.J., Mungall, J.E., Le Vaillant, M., Godel, B., Lesher, C.M., Holwell, D., Lightfoot, P.C., Krivolutskaya, N., and Wei, B., 2017, Sulfide-silicate textures in magmatic Ni-Cu-PGE sulfide ore deposits: Disseminated and net-textured ores: American Mineralogist, v. 102, p. 473–506

Blundy, J., and Wood, B., 2003, Partitioning of trace elements between crystals and melts: Earth and Planetary Science Letters, v. 210, p. 383-397

Bondre, N. and Hart, W., 2008, Morphological and textural diversity of the Steens Basalt lava flows, Southeastern Oregon, USA: implications for emplacement style and nature of eruptive episodes: Bulletin of Volcanology, v.70, no. 8, p. 999-1019

Bougault, H. and Hekinian, R., 1974, Rift valley in the Atlantic Ocean near 36°50'N: petrology and geochemistry of basalt rocks: Earth and Planetary Science Letters, v. 24, no. 2, p. 249-261

Brueseke, M.E., 2010, Magmatism and mineralization in the Oregon Plateau and northern Great Basin: Mid-Miocene volcanism and associated bonanza ore deposits and their relations to the inception of the Yellowstone hotspot.

Brueseke, M.E., Callicoat, J.S., Hames, W., and Larson, P.B., 2014, Mid-Miocene rhyolite volcanism in northeastern Nevada: The Jarbidge Rhyolite and its relationship to the Cenozoic evolution of the northern Great Basin (USA): GSA Bull., 21 p.

Brueseke, M.E., Hart, W.K., and Heizler, M.E., 2008, Diverse mid-Miocene silicic volcanism associated with the Yellowstone–Newberry thermal anomaly: Bull. Volcanol, 18 p.

Brueseke, M.E., Heizler, M.T., Hart, W.K., and Mertzman, S.A., 2007, Distribution and geochronology of Oregon Plateau (U.S.A.) flood basalt volcanism: The Steens Basalt revisited: J. Volcanology and Geothermal Research, v. 161, p. 187-214

Camp, V.E. and Ross, M.E., 2004, Mantle dynamics and genesis of mafic magmatism in the intermontane Pacific Northwest: Journal of Geophysical Research, v. 109, no. B08204, 14 p.

Camp, V.E., Ross, M.E., Duncan, R.A., Jarboe, N.A., Coe, R.S., Hanan, B.B., and Johnson, J.A., 2013, The Steens Basalt: Earliest lavas of the Columbia River Basalt Group, *in* Reidel, S.P., Camp, V.E., Ross, M.E., Wolff, J.A., Martin, B.S., Tolan, T.L., and Wells, R.E., eds., The Columbia River Flood Basalt Province: Geological Society of America Special Paper 497, p. 87–116

Carlson, R.W. and Hart, W.K., 1987, Crustal genesis on the Oregon Plateau: Journal of Geophysical Research, v. 92, no. B7, p. 6191-6206.

Casey, J.F., Banerji, D., and Zarian, P., 2007, Leg 179 synthesis: geochemistry, stratigraphy, and structure of gabbroic rocks drilled in ODP Hole 1105A, Southwest Indian Ridge. *In* Casey, J.F., and Miller, D.J. (Eds.), Proc. ODP, Sci. Results, 179: College Station, TX (Ocean Drilling Program), p. 1–125

Chamberlain, C.P., Mix, H.T., Mulch, A., Hren, M.T., Kent-Corson, M.L., Davis, S.J., Horton, T.W., and Graham, S.A., 2012, The Cenozoic climatic and topographic evolution of the western North American Cordillera: American Journal of Science, v. 312, p. 213-262

Colgan, J.P. and Henry, C.D., 2009, Rapid middle Miocene collapse of the Mesozoic orogenic plateau in north-central Nevada: International Geology Review, v. 51, p. 920-961

Cvetković, L., Pačevski, A., and Tončić, T., 2013, Occurrence of Sn-bearing colusite in the ore-body "T" of the Bor copper deposit, Serbia: Geology of Ore Deposits, v. 55, no. 4, p. 298–304.

Degen, T., Sadki, M., Bron, E., König, U., and Nénert, G., 2014, The HighScore suite: Powder Diffraction, v. 29, s. S2, p. S13-S18

Doe, B.R., 1994, Zinc, copper, and lead in mid-ocean ridge basalts and the source rock control on Zn/Pb in ocean-ridge hydrothermal deposits: Geochimica Acta, v. 58, no. 10, p. 2215-2223

Dostal, J., Dupuy, C., Carron, J.P., Dekerneizon, M.L., and Maury, R.C., 1983, Partition coefficients of trace elements: Application to volcanic rocks of St. Vincent, West Indies: Geochimica et Cosmochimica Acta, v. 47, no. 3, p. 525-533

Esperança, S., Carlson, R.W., Shirey, S.B., and Smith, D., 1997, Dating crust-mantle separation: Re-OS isotopic study of mafic xenoliths from central Arizona: Geology, v. 25, p. 651-654

Ewart, A., Bryan, W.B., and Gill, J.B., 1973, Mineralogy and geochemistry of the younger volcanic islands of Tonga, S. W. Pacific: Journal of Petrology, v. 14, no. 3, p. 429-465

Faure, G., 1998, Principles and Applications of Geochemistry (second edition): New Jersey, Prentice-Hall, 600 p.

Gaetani, G.A. and Grove, T.L., 1997, Partitioning of moderately siderophile elements among olivine, silicate melt, and sulfide melt: Constraints on core formation in the Earth and Mars: Geochimica et Cosmochimica Acta, v. 61, no. 9, p. 1829-1846

Geochemical Earth Reference Model, n.d., GERM partition coefficient (Kd) database: https://earthref.org/KDD/e:29/ (accessed April 2017)

Geological Society of Japan, n.d., Online Geological Map of Japan: https://www.gsj.jp/en/education/geomap-e/online-map.html (accessed October 2018)

Gill, R., 2010, Igneous rocks and processes: a practical guide: West Sussex, UK, Wiley-Blackwell, 428 p.

Goldschmidt, V.M., 1937, The principles of distribution of chemical elements in minerals and rocks, Journal of the Chemical Society (Resumed), 1937, 655-673.

Gunn, B.M., and Watkins, N.D., 1970, Geochemistry of the Steens Mountain Basalts, Oregon: GSA Bull, v. 81, p. 1497-1516

Hart, S.R. and Dunn, T., 1993, Experimental cpx/melt partitioning of 24 trace elements: Contributions to Mineralogy and Petrology, v. 113, p. 1-8.

Hart, W.K and Carlson, R.W., 1985, Distribution and geochronology of Steens Mountain-type basalts from the northwestern Great Basin: Isocron/West, no. 43, p. 5-10

Heinrich, C.A., Driesner, T., Stefánsson, A., and Seward, T.M., 2004, Magmatic vapor contraction and the transport of gold from the porphyry environment to epithermal ore deposits: Geology, v. 32, no. 9, p. 761–764

Heinrich, C.A., Ryan, C.G., Mernagh, T.P., and Eadington, P.J., 1992, Segregation of ore metals between magmatic brine and vapor—a fluid inclusion study using pixe microanalysis: Economic Geology, v. 87, p. 1566–1583.

Henry, C.D., Hinz, N.H., Faulds, J.E., Colgan, J.P., John, D.A., Brooks, E.R., Cassel, E.J., Garside, L.J., Davis, D.A., and Castor, S.B., 2012, Eocene–Early Miocene paleotopography of the Sierra Nevada–Great Basin–Nevadaplano based on widespread ash-flow tuffs and paleovalleys: Geosphere v. 8, no. 1, p. 1-27

Hill, T.R., 2009, High-resolution transmission electron microscopy investigation of nano-crystals of pyroxene and copper in Oregon sunstones [M.S. thesis]: University of Wisconsin-Madison, 77 p.

Hofmeister, A.M., and Rossman, G.R. 1985, Exsolution of metallic copper from Lake County labradorite: GEOLOGY, v. 13, p. 644-647

Irvine T.N. and Baragar, W.R.A., 1971, A guide to the chemical classification of the common volcanic rocks: Can J Earth Sci, v. 8, p. 523–548

Jensen, A., 1982. The distribution of Cu across three basaltic lava flows from the Faroe Islands. Bull. Geol. Soc. Den., v. 31, p. 1-10

John, D.A., 2001, Miocene and early Pliocene epithermal gold-silver deposits of the northern Great Basin, western United States: Characteristics, distribution and relation to magmatism: Economic Geology, v. 96, p. 1827–1853

Johnson, J., Nielsen, R.L., and Fisk, M.R., 1996, Plagioclase-hosted melt inclusions in the Steens Basalt, Southeastern Oregon: Petrology, v. 4, no. 3, p. 247-255

Johnston, C.L., Gunter, M.E., and Knowles, C.R., 1991, Sunstone labradorite from the Ponderosa Mine, Oregon: Gems&Gemology, v. 27, no. 4, p. 220-233

Kamenov, G.D., Saunders, J.A., Hames, W.E., and Unger, D.L., 2007, Mafic magmas as sources for gold in middle Miocene epithermal deposits of the Northern Great Basin, United States: evidence from Pb isotope compositions of native gold: Econ Geology, v. 102, no. 7, p. 1191–1195

Kloeck, W. and Palme, H., 1988, Partitioning of siderophile and chalcophile elements between sulfide, olivine, and glass in a naturally reduced basalt from Disko Island, Greenland, *in* Ryder, G., eds., Proceedings, Lunar and Planetary Science Conference, 18th, Houston, 1987, p. 471-483.

Lafuente, B., Downs, R.T., Yang, H., and, Stone N., 2015, The power of databases: the RRUFF project, *in* Armbruster, T., and Danisi, R.M., eds., Highlights in Mineralogical Crystallography, p. 1-30 http://rruff.info/about/downloads/HMC1-30.pdf (accessed August 2018)

Le Maitre, R. and Bateman, P., 1989, A classification of igneous rocks and glossary of terms: Recommendations of the International Union of Geological Sciences Subcommission on the Systematics of Igneous Rocks: Oxford; Boston, Blackwell, 193 p.

LeHuray A.P., 1989, Native Copper in ODP Site 642 tholeiites: Proceedings of the Ocean Drilling Program, v. 104, p. 411-417

Lemarchand, F., Benoit, V., and Calais, G., 1987, Trace element distribution coefficients in alkaline series: Geochimica et Cosmochimica Acta, v. 51, p. 1071-1081

Liu, X., Xiong. X. Audetat, A., Li, Y., Song, M., Li, L. Sun, W., Ding, X., 2014, Partitioning of copper between olivine, orthopyroxene, clinopyroxene, spinel, garnet and silicate melts at upper mantle conditions: Geochimica et Cosmochimica Acta, v. 125, p. 1-22

Lyalina, L.M., Savchenko, Ye.E., Selivanova, E.A., and Zozulya, D.R., 2010, Behoite and mimetite from the Saharjok alkaline intrusion, Kola Peninsula: Geology of Ore Deposits, v. 52, no. 7, p. 641–645

Martin, R.F. and Blackburn, W.H., 1999, Encyclopedia of mineral names; first update: The Canadian Mineralogist v. 37, no. 4, p. 1045-1078.

Maynard, A.L., 2016, Copper isotope compositions of Cenozoic mafic-intermediate rocks of the Northern Great Basin and Snake River Plain (USA) [M.S. thesis]: Kansas State University, 79 p.

Menges, F., 2018, Spectragryph - optical spectroscopy software, Version 1.2.9, 2018, http://www.effemm2.de/spectragryph/

Mindat.org, n.d., Ani Mine, Ani-machi, Kitaakita City, Akita Prefecture, Tohoku Region, Honshu Island, Japan: https://www.mindat.org/loc-2175.html (accessed October 2018)

Mirwald, P. W. and Kennedy, G.C., 1979, The melting curve of gold, silver, and copper to 60-kbar pressure: a reinvestigation: Journal of Geophysical Research, v. 84, no. B12, p. 6750-6756

Morimoto, N., Koto, K., and Shimazaki, Y., 1969, Anilite, Cu_7S_4, a new mineral: American Mineralogist, v. 54, no. 9-10, p. 1256-1268

Paster, T.P., Schauwecker, D.S., and Haskin, L.A., 1974, The behavior of some trace elements during solidification of the Skaergaard layered series: Geochimica et Cosmochimica Acta, v. 38 no. 10, p. 1549-1577

Pedersen, A.K., 1979, Basaltic Glass with High-Temperature Equilibrated Immiscible Sulfide Bodies with Native Iron from Disko, Central West Greenland: Contributions to Mineralogy and Petrology, v. 69, no. 4, p. 397-407

Perkins, D. and Brady, J., n.d., Binary Phase Diagrams: Science Education Resource Center, https://serc.carleton.edu/research_education/equilibria/binary_diagrams.html (accessed October 2018)

Plotinskaya, O. Yu., Kovalenker V. A., Seltmann, R., and Stanley, C. J., 2006, Te and Se mineralogy of the high-sulfidation Kochbulak and Kairagach epithermal gold-telluride deposits (Kurama Ridge, Middle Tien Shan, Uzbekistan): Mineralogy and Petrology, v. 87, p. 187–207

Rajamani, V. and Naldrett, A.J., 1978, Partitioning of Fe, Co, Ni, and Cu between Sulfide Liquid and Basaltic Melts and Composition of Ni-Cu Sulfide Deposits: Economic Geology and the Bulletin of the Society of Economic Geologists, v. 73, no. 1, p. 82-93.

Ray, D., Ghosh, S., and Murty, S.V.S., 2017, On the possible origin of troilite-metal nodules in the Katol chondrite (L6-7): Meteoritics & Planetary Science v. 52, no. 1, p. 72–88

Ridley, J., 2013, Ore Deposit Geology: New York, Cambridge University Press, 398 p.

Ringwood, A.E., 1955, The principles governing trace element distribution during magmatic crystallization Part I: The influence of electronegativity: Geochimica et Cosmochimica Acta, v. 7, no. 3, p. 189-202

Saunders, J.A., and Brueseke, M.E., 2012, Volatility of Se and Te during subduction-related distillation and the geochemistry of epithermal ores of the western United States: Econ Geology v. 107, p. 165-172

Saunders, J.A., Mathur, R., Kamenov, G.D., Shimizu, T., and Brueseke, M.E., 2016, New isotopic evidence bearing on bonanza (Au-Ag) epithermal ore-forming processes: Miner Deposita, v. 51, no. 1, p1-11

Saunders, J.A., Unger D.L., Kamenov, G.D., Fayek, M., Hames, W.E., and Utterback, W.C., 2008, Genesis of Middle Miocene Yellowstone hotspot-related bonanza epithermal Au–Ag deposits, Northern Great Basin, USA: Miner Deposita, 20 p.

Schulz, K.J., Chandler, V.W., Nicholson, S.W., Piatak, Nadine, Seall, II, R.R., Woodruff, L.G., and Zientek, M.L., 2010, Magmatic sulfide-rich nickel-copper deposits related to picrite and (or) tholeiitic basalt dike-sill complexes—A preliminary deposit model: USGS Open-File Report 2010–1179, 25 p.

Scott, S.R., Sims, K.W.W., Frost, B.R., Kelemen, P.B., Evans, K.A., and Swapp, S.M., 2017, On the hydration of olivine in ultramafic rocks: Implications from Fe isotopes in serpentinites: Geochimica et Cosmochimica Acta, v. 215, p. 105–121

Shea, T. and Hammer, J.E., 2013, Kinetics of cooling- and decompression-induced crystallization in hydrous mafic-intermediate magmas: Journal of Volcanology and Geothermal Research, v. 260, p. 127–145

Song, X. Wang, Y., and Chen, L., 2011, Magmatic Ni-Cu-(PGE) deposits in magma plumbing systems: Features, formation and exploration: Geoscience Frontiers, v. 2, no. 3, p. 375-384

Starostin, V.I. and Sorokhtin, O.G., 2011, A new interpretation for the origin of the Norilsk type PGE–Cu–Ni sulfide deposits: Geoscience Frontiers, v. 2, no. 4, p. 583-591

Stolper, E. and Walker, D., 1980, Melt density and the average composition of basalt: Contributions to Mineralogy and Petrology, v. 74, no. 1, p. 7-12

Tuduri, J., Pourret, O., Chauvet, A., Barbanson, L., Abdelaziz, G., and Ennaciri, A., 2011, Rare earth elements as proxies of supergene alteration processes from the giant Imiter silver

deposit (Morocco), in Proceedings, Biennal meeting SGA, 11th: Antofagasta, Chile, p. 982, <hal-00601984>

Williams-Jones, A.E. and Heinrich, C.A., 2005, Vapor transport of metals and the formation of magmatic-hydrothermal ore deposits: Economic Geology, v. 100, no. 7, p. 1287-1312

Xu, H., Hill, T.R., Konishi, H., and Farfan, G., 2017, Protoenstatite: A new mineral in Oregon sunstones with “watermelon” colors: American Mineralogist, v. 102, p. 2146–2149

Yuningsih, E.T. and Matsueda, H., 2018, Study on the Cu–As–Sb–Ag–Bi–Pb–Te sulfosalt minerals from the hydrothermal system of southwestern Hokkaido, Japan: Resource Geology, v. 68, no.3, p. 209-226

Zajacz, Z. and Halter, W., 2009, Copper transport by high temperature, sulfur-rich magmatic vapor: Evidence from silicate melt and vapor inclusions in a basaltic andesite from the Villarrica volcano (Chile): Earth and Planetary Science Letters, v. 282, p. 115-121

Appendix A - Supplemental Figures and Images

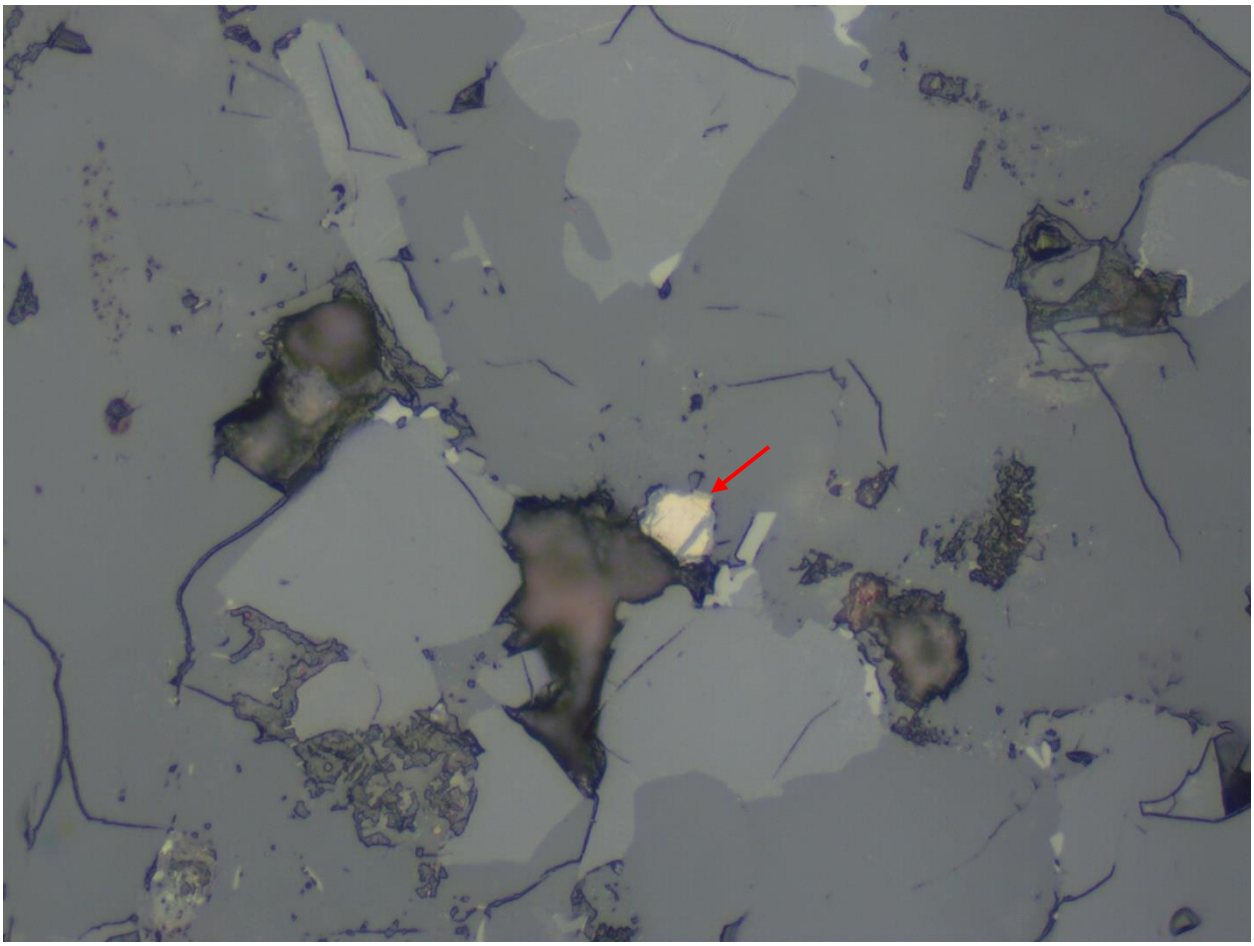

Figure 28: Reflected light image of a magnetite crystal in MB97-19 (indicated by red arrow). 50x field of view.

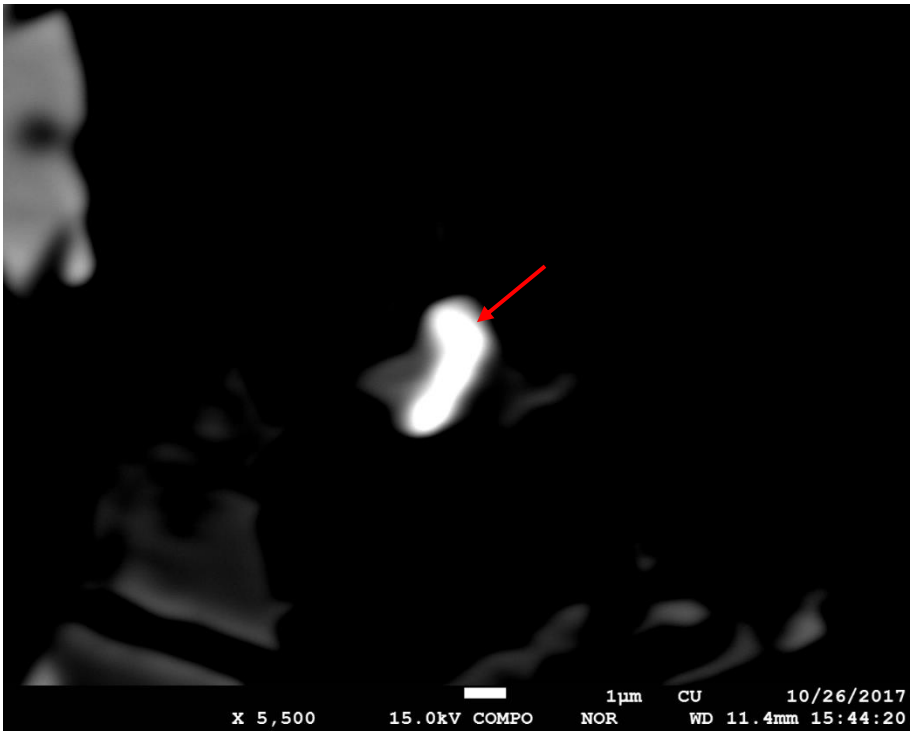

Figure 29: MB97-19 iron-copper sulfide (indicated by red arrow).

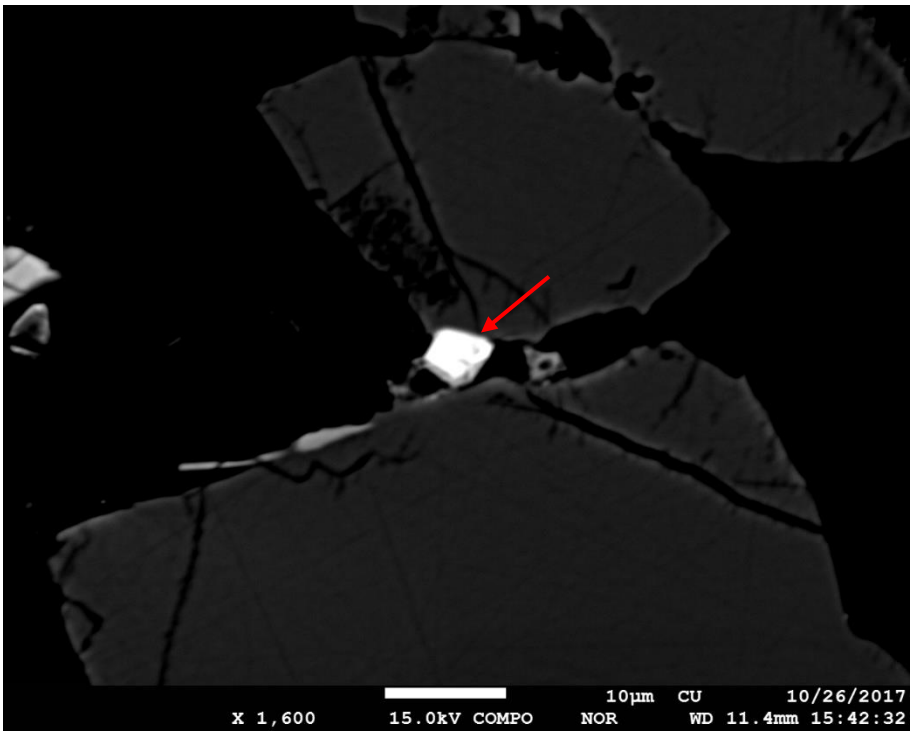

Figure 30: MB97-19 pyrite (indicated by red arrow).

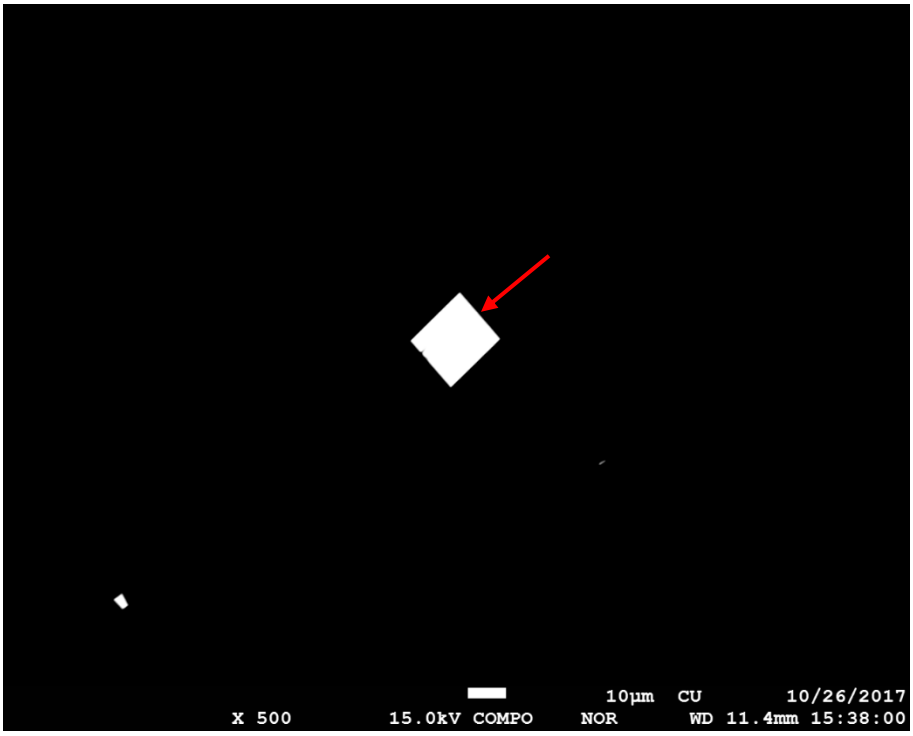

Figure 31: MB97-19 zircon (indicated by red arrow).

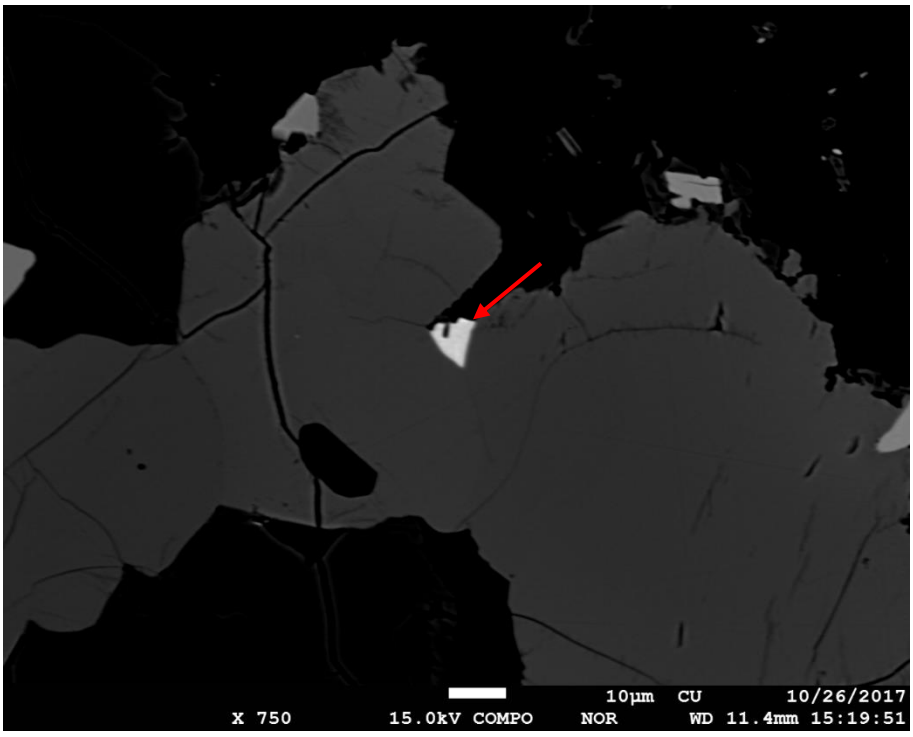

Figure 32: MB97-19 copper iron sulfide (indicated by red arrow).

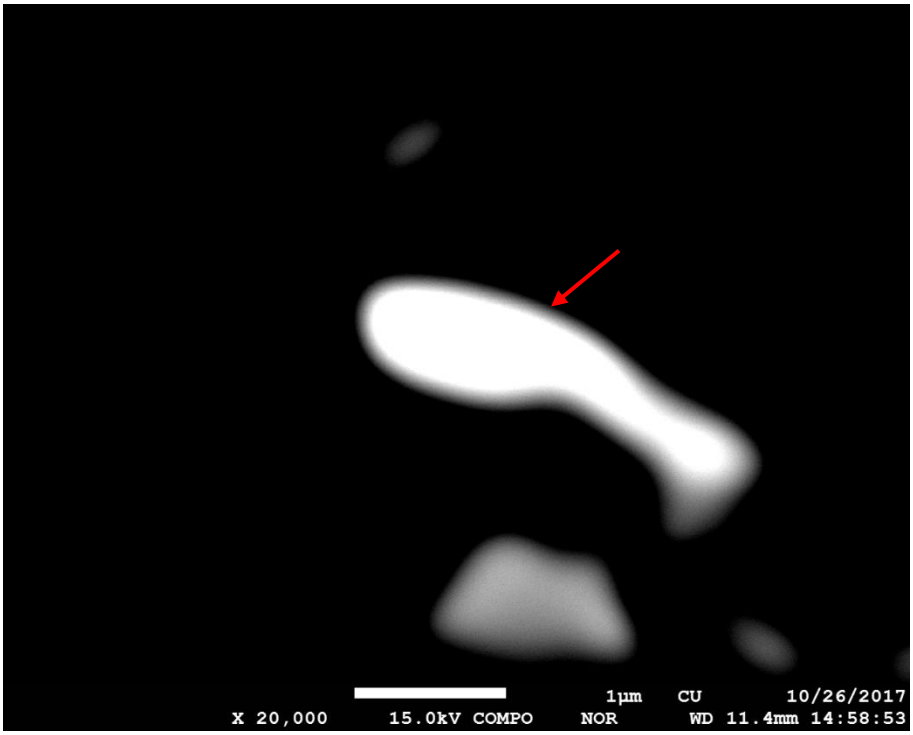

Figure 33: 97-19 iron sulfide (indicated by red arrow).

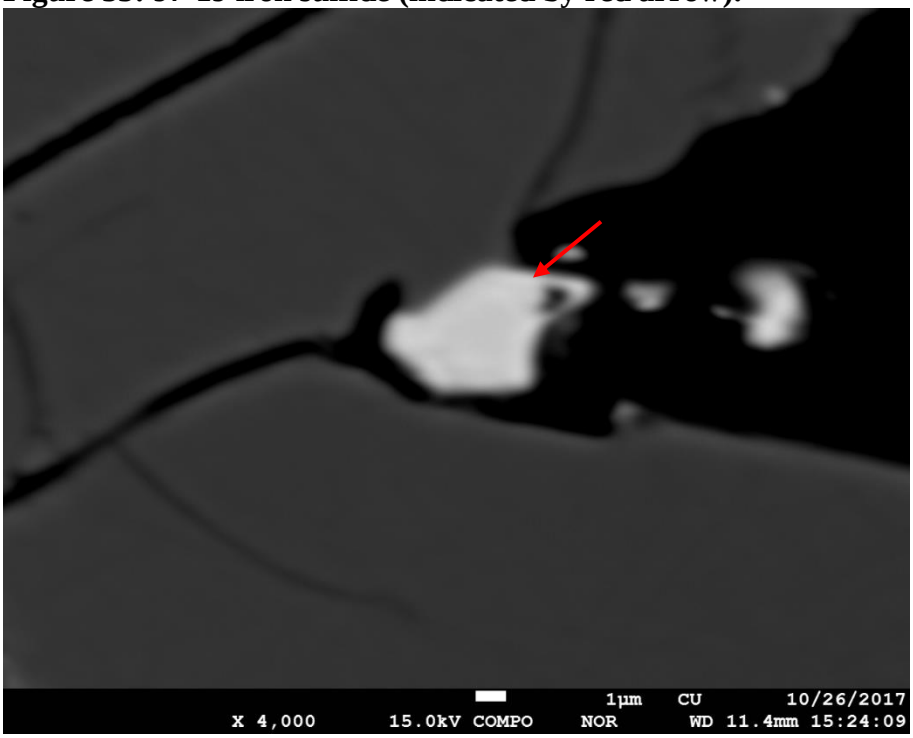

Figure 34: 97-19 iron sulfide (indicated by red arrow).

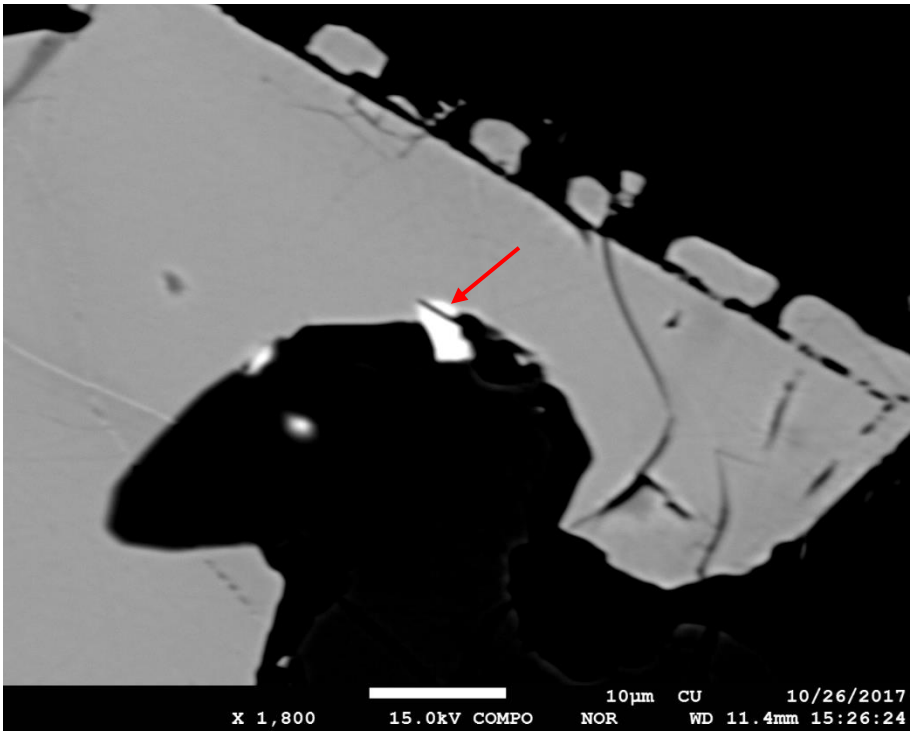

Figure 35: 97-19 iron sulfide (indicated by red arrow).

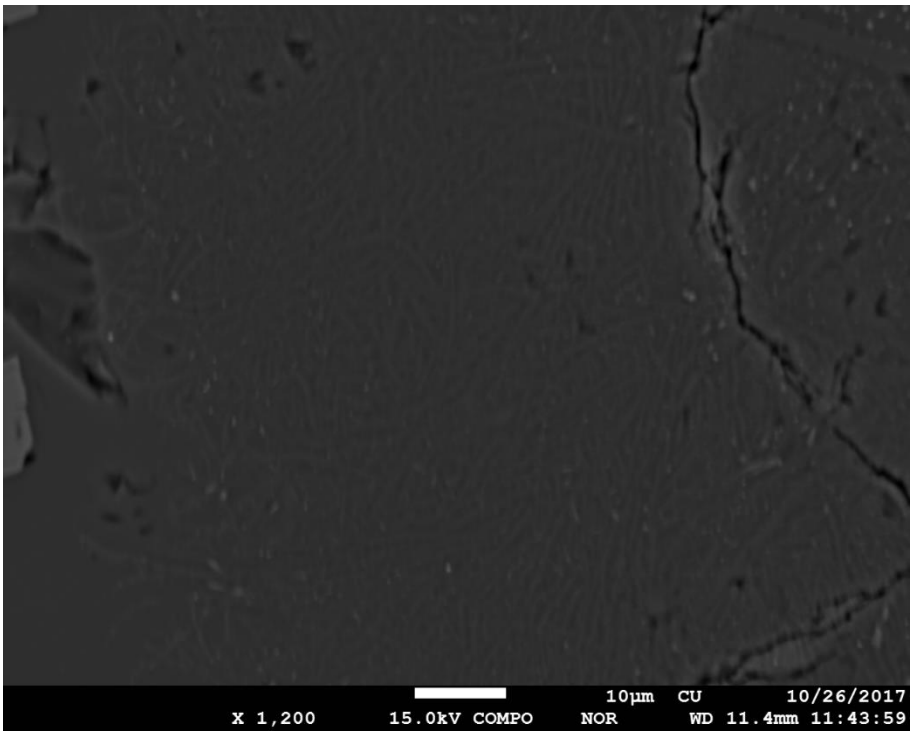

Figure 36: 97-76B glass texture.

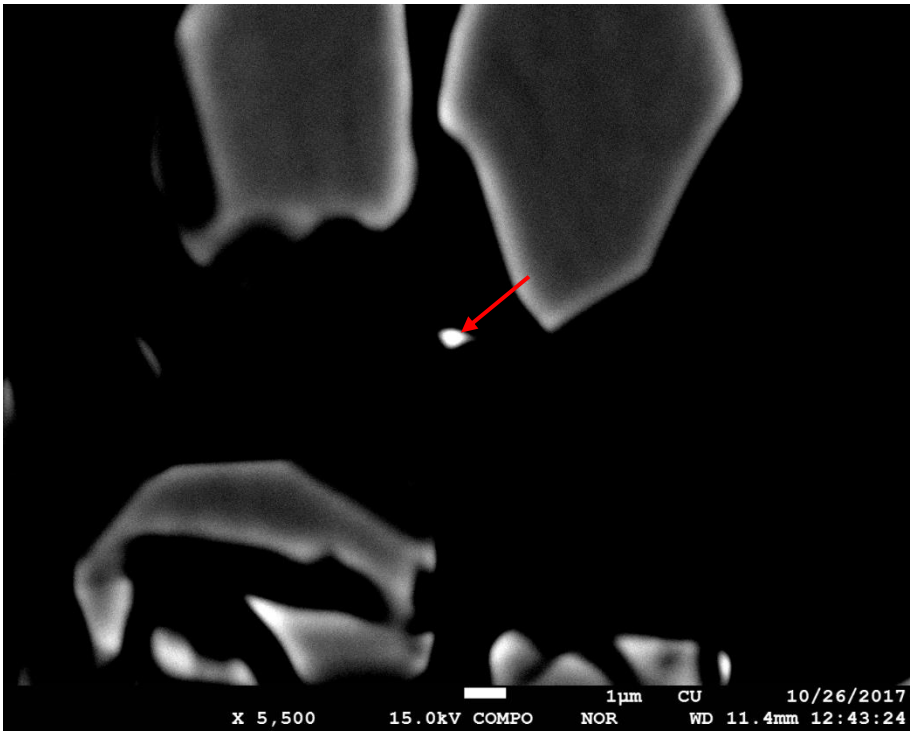

Figure 37: 97-76B iron sulfide (indicated by red arrow).

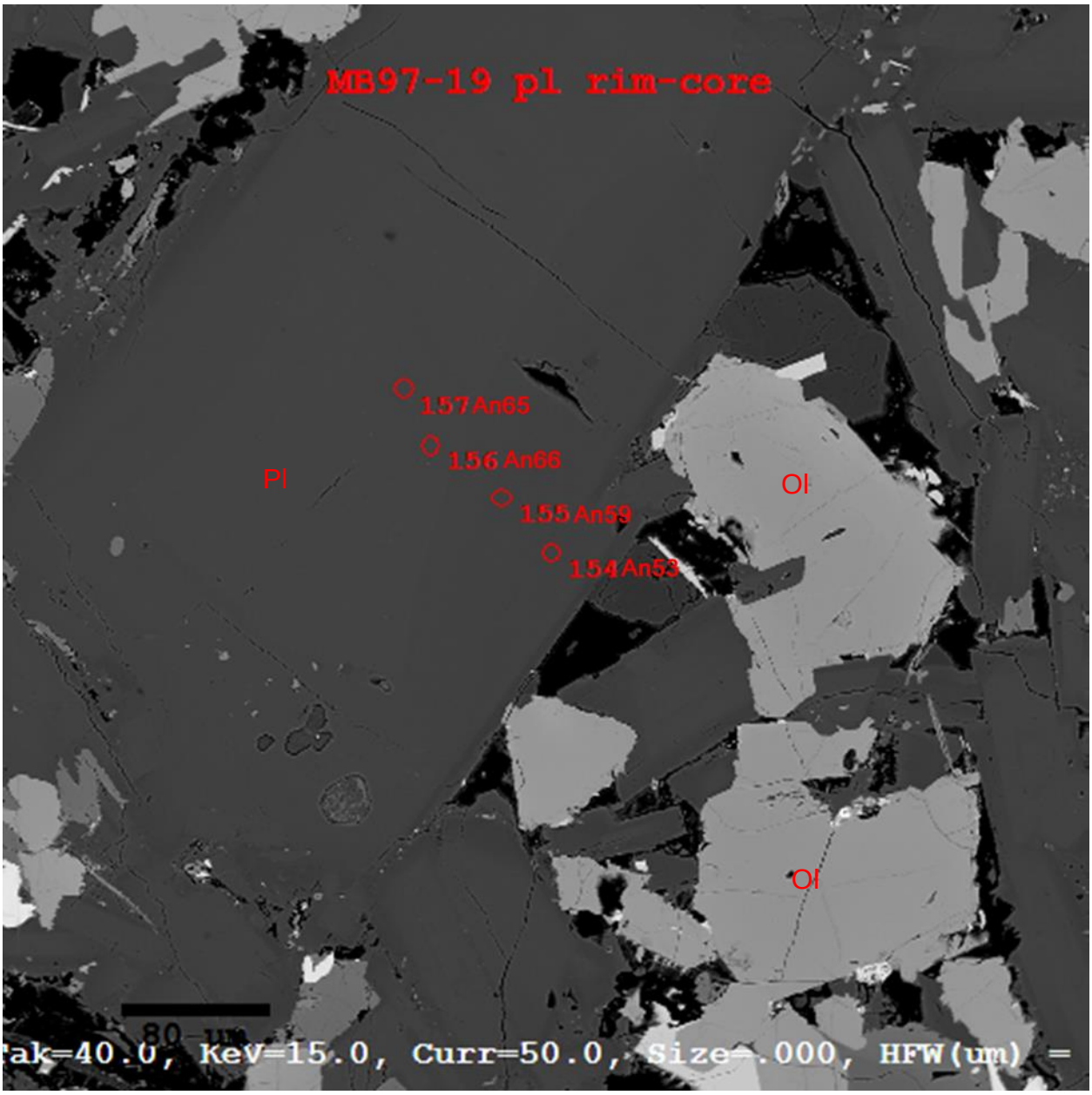

Figure 38: MB97-19 plagioclase rim to core transect with An% noted next to analysis point. Ol = olivine, Pl = plagioclase.

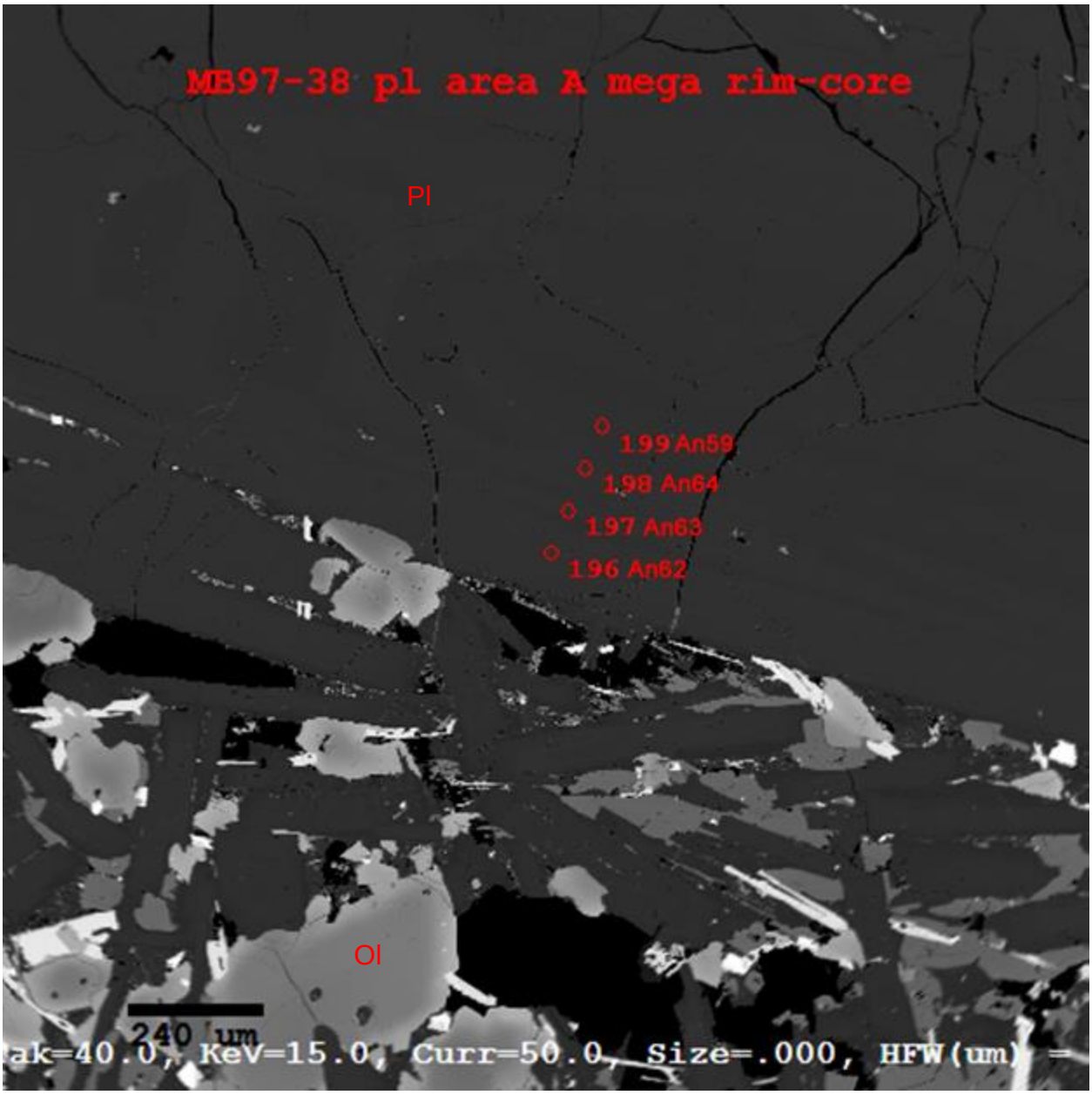

Figure 39: MB97-38 plagioclase rim to core transect with An% noted next to analysis point. Ol = olivine, Pl = plagioclase.

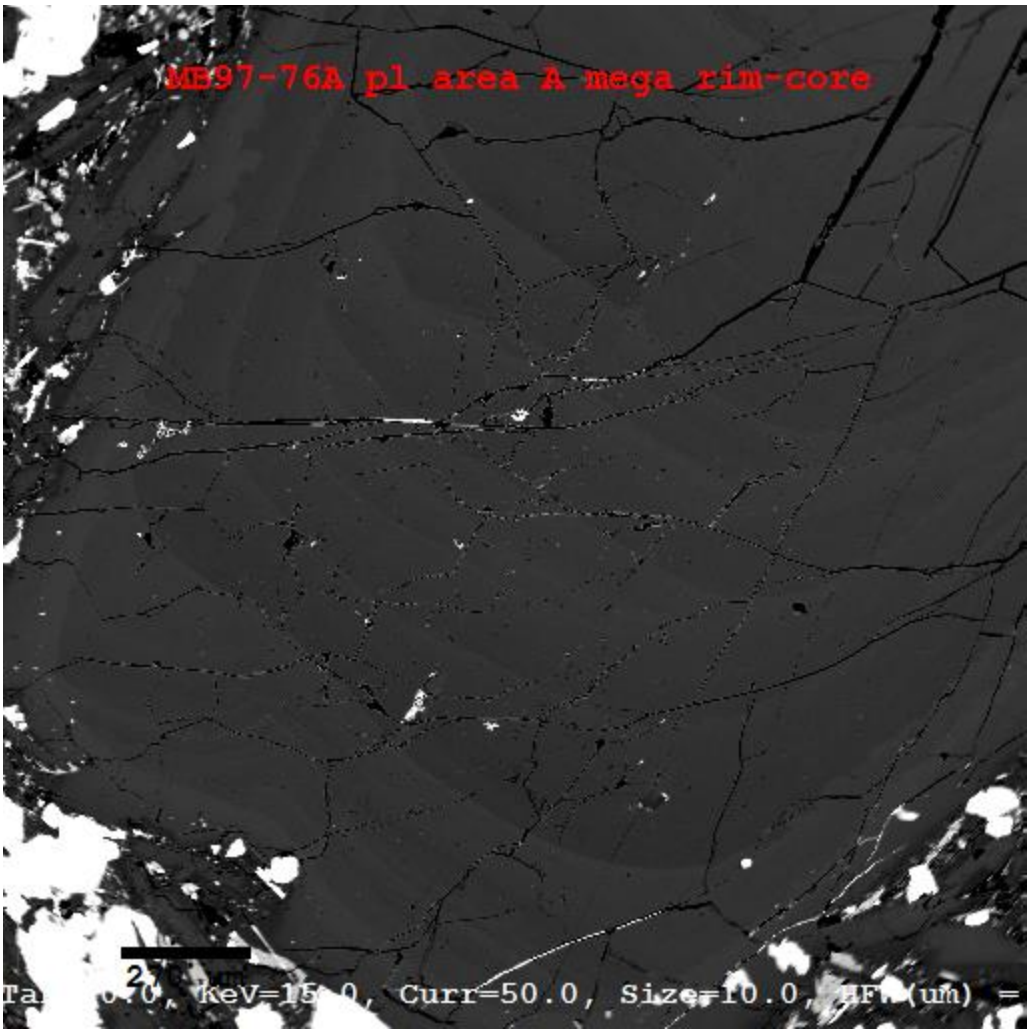

Figure 40: MB97-76A plagioclase megacryst rim to core transect. Same as Figure 10A but with the points removed for clearer viewing.

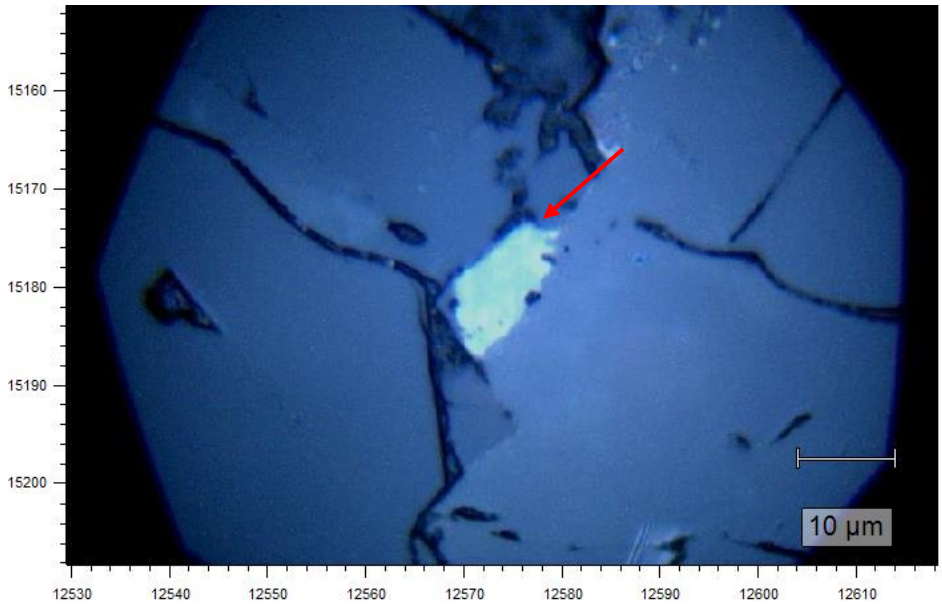

Figure 41: Raman reflected light, analysis 4-1 (target mineral indicated by the red arrow).

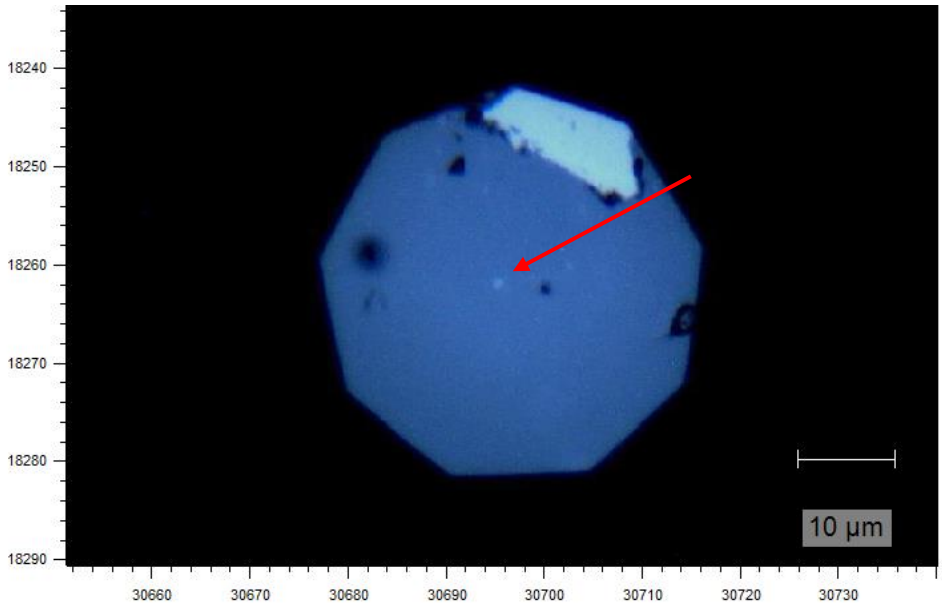

Figure 42: Raman reflected light, analysis 11-1. Possible copper sulfide noted by arrow.

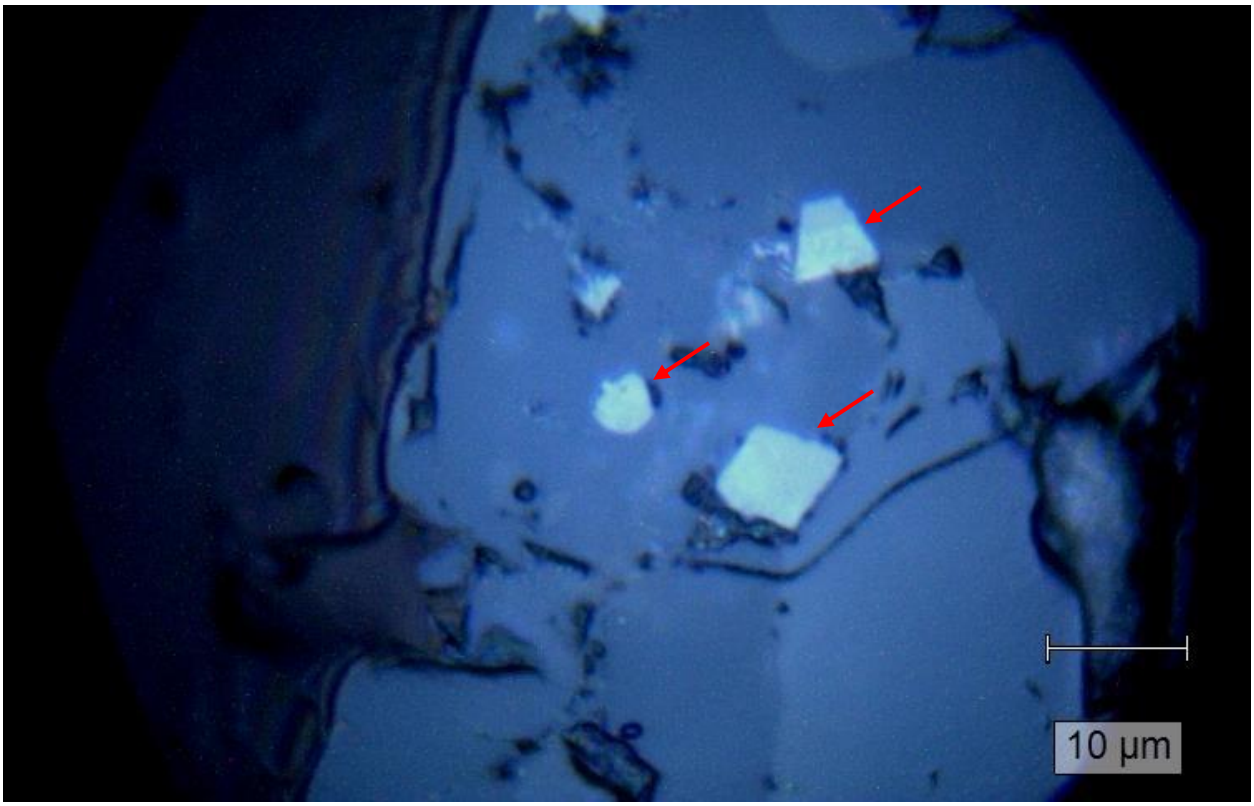

Figure 43: Raman reflected light, analysis 2-1, 2-2, and 2-3 (target minerals indicated by red arrows).

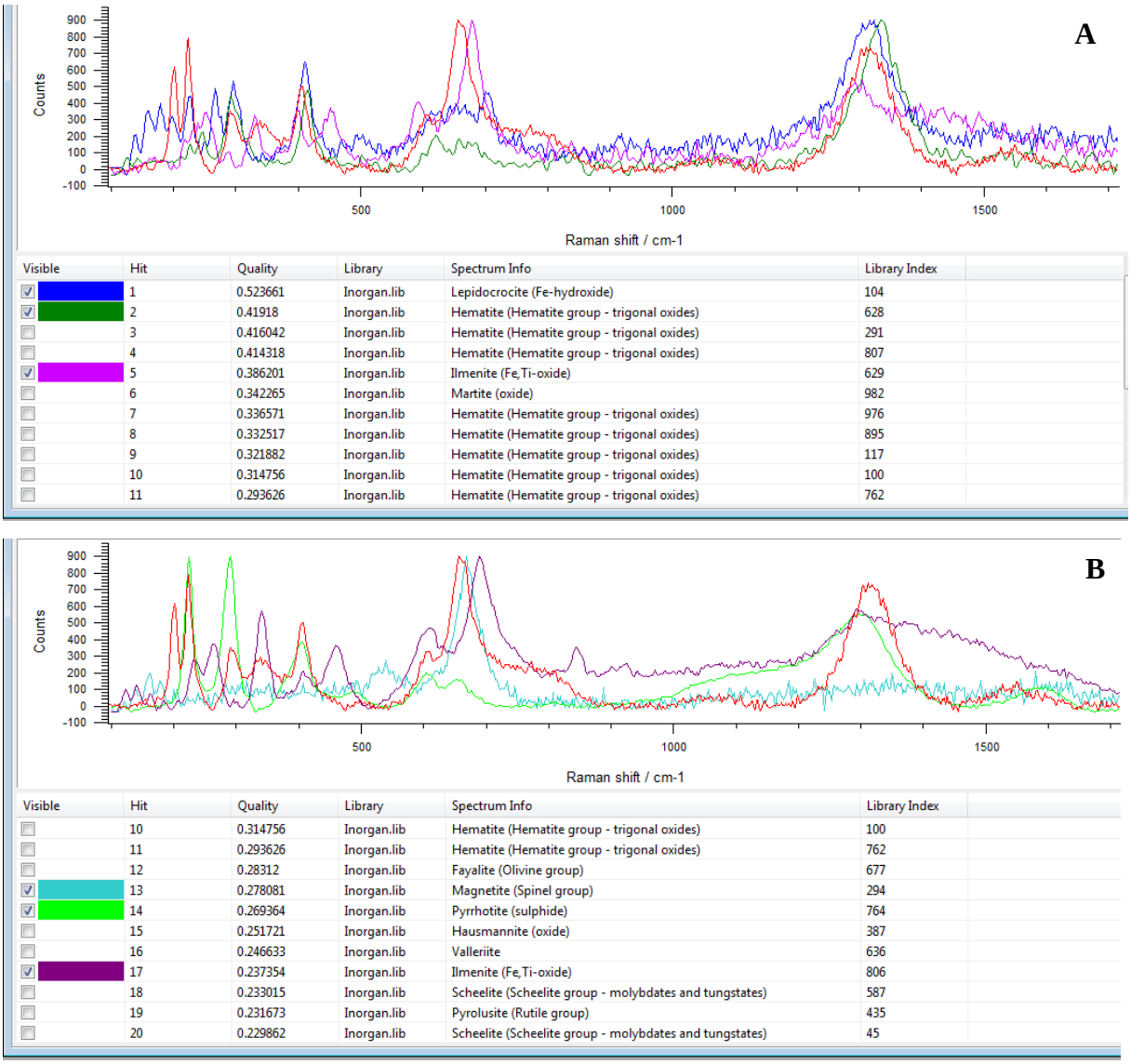

Visible	Hit	Quality	Library	Spectrum Info	Library Index
☑	1	0.523661	Inorgan.lib	Lepidocrocite (Fe-hydroxide)	104
☑	2	0.41918	Inorgan.lib	Hematite (Hematite group - trigonal oxides)	628
☐	3	0.416042	Inorgan.lib	Hematite (Hematite group - trigonal oxides)	291
☐	4	0.414318	Inorgan.lib	Hematite (Hematite group - trigonal oxides)	807
☑	5	0.386201	Inorgan.lib	Ilmenite (Fe,Ti-oxide)	629
☐	6	0.342265	Inorgan.lib	Martite (oxide)	982
☐	7	0.336571	Inorgan.lib	Hematite (Hematite group - trigonal oxides)	976
☐	8	0.332517	Inorgan.lib	Hematite (Hematite group - trigonal oxides)	895
☐	9	0.321882	Inorgan.lib	Hematite (Hematite group - trigonal oxides)	117
☐	10	0.314756	Inorgan.lib	Hematite (Hematite group - trigonal oxides)	100
☐	11	0.293626	Inorgan.lib	Hematite (Hematite group - trigonal oxides)	762

Visible	Hit	Quality	Library	Spectrum Info	Library Index
☐	10	0.314756	Inorgan.lib	Hematite (Hematite group - trigonal oxides)	100
☐	11	0.293626	Inorgan.lib	Hematite (Hematite group - trigonal oxides)	762
☐	12	0.28312	Inorgan.lib	Fayalite (Olivine group)	677
☑	13	0.278081	Inorgan.lib	Magnetite (Spinel group)	294
☑	14	0.269364	Inorgan.lib	Pyrrhotite (sulphide)	764
☐	15	0.251721	Inorgan.lib	Hausmannite (oxide)	387
☐	16	0.246633	Inorgan.lib	Valleriite	636
☑	17	0.237354	Inorgan.lib	Ilmenite (Fe,Ti-oxide)	806
☐	18	0.233015	Inorgan.lib	Scheelite (Scheelite group - molybdates and tungstates)	587
☐	19	0.231673	Inorgan.lib	Pyrolusite (Rutile group)	435
☐	20	0.229862	Inorgan.lib	Scheelite (Scheelite group - molybdates and tungstates)	45

Figure 44: WiRE Spectra searchs for analysis 4-1.

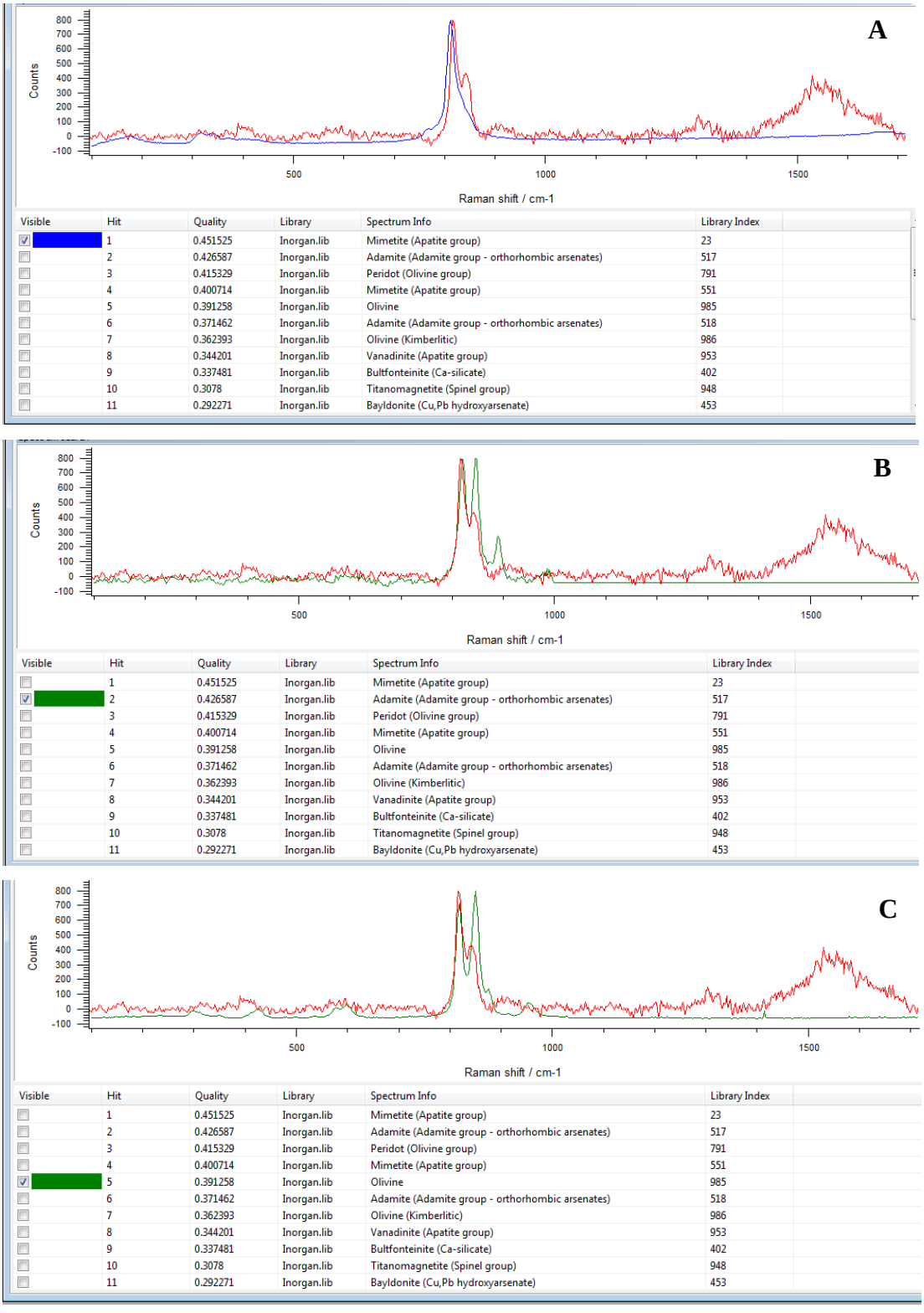

Figure 45: WiRE Spectra search for analysis 20-1.

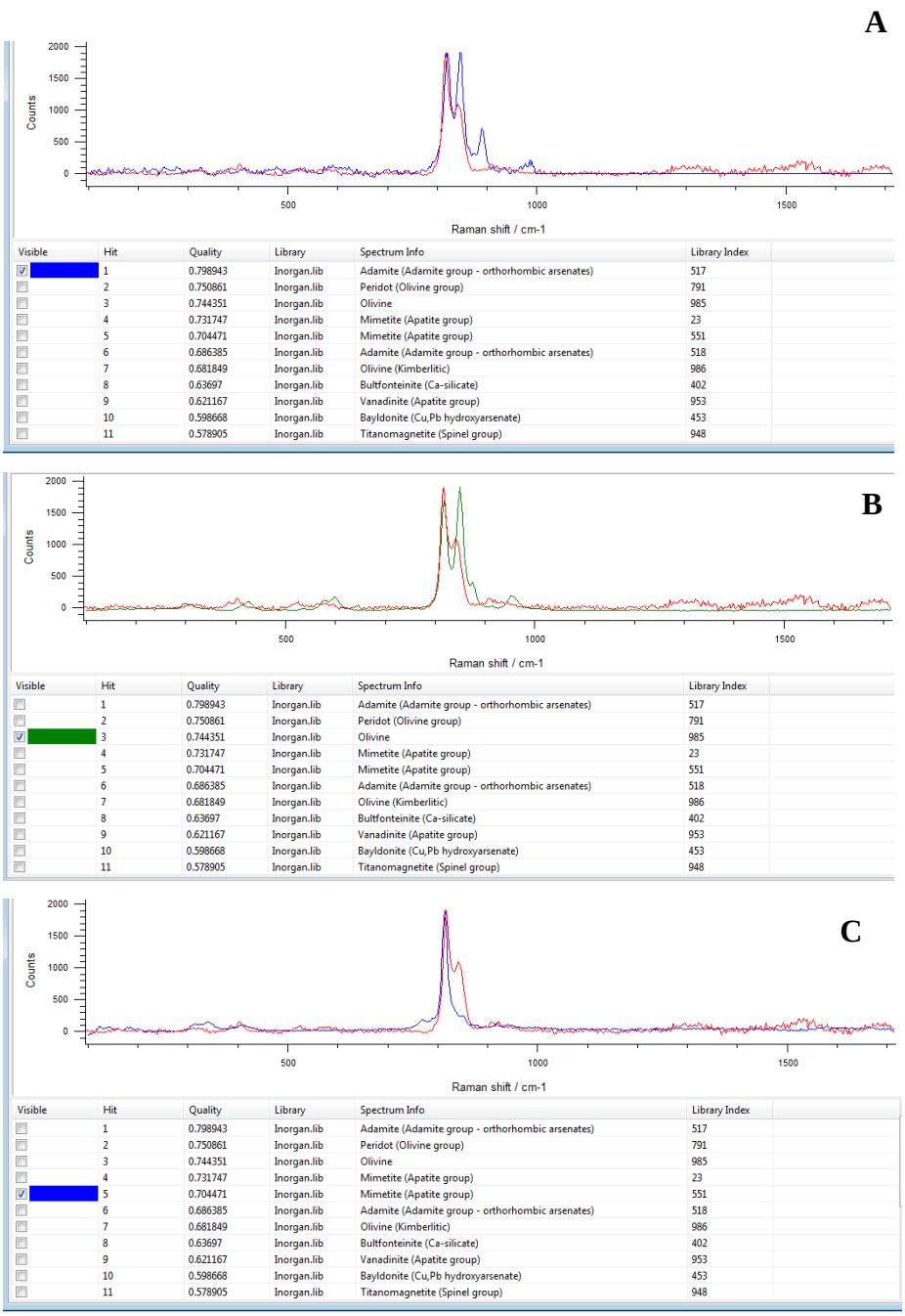

Visible	Hit	Quality	Library	Spectrum Info	Library Index
☑	1	0.798943	Inorgan.lib	Adamite (Adamite group - orthorhombic arsenates)	517
☐	2	0.750861	Inorgan.lib	Peridot (Olivine group)	791
☐	3	0.744351	Inorgan.lib	Olivine	985
☐	4	0.731747	Inorgan.lib	Mimetite (Apatite group)	23
☐	5	0.704471	Inorgan.lib	Mimetite (Apatite group)	551
☐	6	0.686385	Inorgan.lib	Adamite (Adamite group - orthorhombic arsenates)	518
☐	7	0.681849	Inorgan.lib	Olivine (Kimberlitic)	986
☐	8	0.63697	Inorgan.lib	Bultfonteinite (Ca-silicate)	402
☐	9	0.621167	Inorgan.lib	Vanadinite (Apatite group)	953
☐	10	0.598668	Inorgan.lib	Bayldonite (Cu,Pb hydroxyarsenate)	453
☐	11	0.578905	Inorgan.lib	Titanomagnetite (Spinel group)	948

Visible	Hit	Quality	Library	Spectrum Info	Library Index
☐	1	0.798943	Inorgan.lib	Adamite (Adamite group - orthorhombic arsenates)	517
☐	2	0.750861	Inorgan.lib	Peridot (Olivine group)	791
☑	3	0.744351	Inorgan.lib	Olivine	985
☐	4	0.731747	Inorgan.lib	Mimetite (Apatite group)	23
☐	5	0.704471	Inorgan.lib	Mimetite (Apatite group)	551
☐	6	0.686385	Inorgan.lib	Adamite (Adamite group - orthorhombic arsenates)	518
☐	7	0.681849	Inorgan.lib	Olivine (Kimberlitic)	986
☐	8	0.63697	Inorgan.lib	Bultfonteinite (Ca-silicate)	402
☐	9	0.621167	Inorgan.lib	Vanadinite (Apatite group)	953
☐	10	0.598668	Inorgan.lib	Bayldonite (Cu,Pb hydroxyarsenate)	453
☐	11	0.578905	Inorgan.lib	Titanomagnetite (Spinel group)	948

Visible	Hit	Quality	Library	Spectrum Info	Library Index
☐	1	0.798943	Inorgan.lib	Adamite (Adamite group - orthorhombic arsenates)	517
☐	2	0.750861	Inorgan.lib	Peridot (Olivine group)	791
☐	3	0.744351	Inorgan.lib	Olivine	985
☐	4	0.731747	Inorgan.lib	Mimetite (Apatite group)	23
☑	5	0.704471	Inorgan.lib	Mimetite (Apatite group)	551
☐	6	0.686385	Inorgan.lib	Adamite (Adamite group - orthorhombic arsenates)	518
☐	7	0.681849	Inorgan.lib	Olivine (Kimberlitic)	986
☐	8	0.63697	Inorgan.lib	Bultfonteinite (Ca-silicate)	402
☐	9	0.621167	Inorgan.lib	Vanadinite (Apatite group)	953
☐	10	0.598668	Inorgan.lib	Bayldonite (Cu,Pb hydroxyarsenate)	453
☐	11	0.578905	Inorgan.lib	Titanomagnetite (Spinel group)	948

Figure 46: WiRE Spectra search for analysis 20-2.

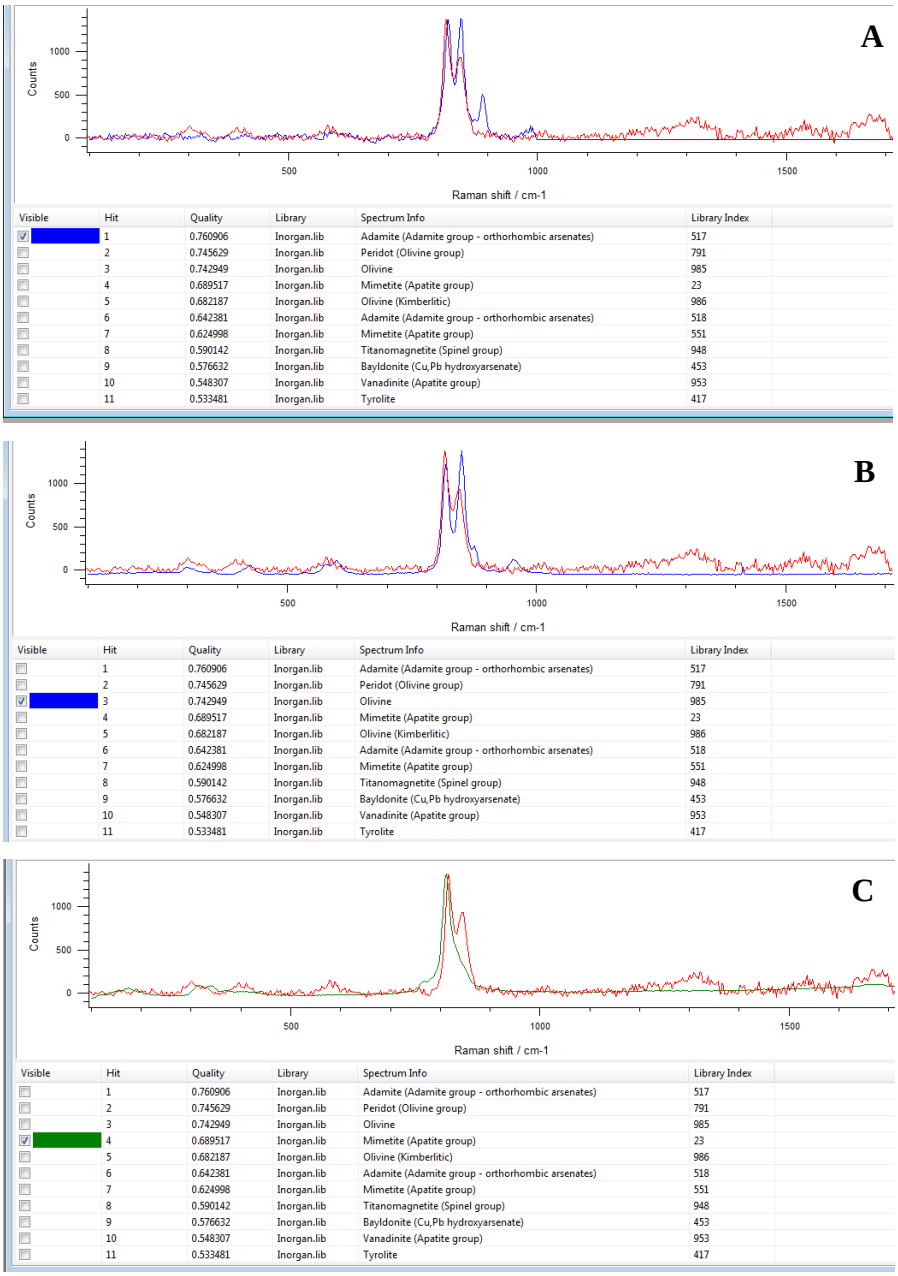

Visible	Hit	Quality	Library	Spectrum Info	Library Index
☑	1	0.760906	Inorgan.lib	Adamite (Adamite group - orthorhombic arsenates)	517
☐	2	0.745629	Inorgan.lib	Peridot (Olivine group)	791
☐	3	0.742949	Inorgan.lib	Olivine	985
☐	4	0.689517	Inorgan.lib	Mimetite (Apatite group)	23
☐	5	0.682187	Inorgan.lib	Olivine (Kimberlitic)	986
☐	6	0.642381	Inorgan.lib	Adamite (Adamite group - orthorhombic arsenates)	518
☐	7	0.624998	Inorgan.lib	Mimetite (Apatite group)	551
☐	8	0.590142	Inorgan.lib	Titanomagnetite (Spinel group)	948
☐	9	0.576632	Inorgan.lib	Bayldonite (Cu,Pb hydroxyarsenate)	453
☐	10	0.548307	Inorgan.lib	Vanadinite (Apatite group)	953
☐	11	0.533481	Inorgan.lib	Tyrolite	417

Visible	Hit	Quality	Library	Spectrum Info	Library Index
☐	1	0.760906	Inorgan.lib	Adamite (Adamite group - orthorhombic arsenates)	517
☐	2	0.745629	Inorgan.lib	Peridot (Olivine group)	791
☑	3	0.742949	Inorgan.lib	Olivine	985
☐	4	0.689517	Inorgan.lib	Mimetite (Apatite group)	23
☐	5	0.682187	Inorgan.lib	Olivine (Kimberlitic)	986
☐	6	0.642381	Inorgan.lib	Adamite (Adamite group - orthorhombic arsenates)	518
☐	7	0.624998	Inorgan.lib	Mimetite (Apatite group)	551
☐	8	0.590142	Inorgan.lib	Titanomagnetite (Spinel group)	948
☐	9	0.576632	Inorgan.lib	Bayldonite (Cu,Pb hydroxyarsenate)	453
☐	10	0.548307	Inorgan.lib	Vanadinite (Apatite group)	953
☐	11	0.533481	Inorgan.lib	Tyrolite	417

Visible	Hit	Quality	Library	Spectrum Info	Library Index
☐	1	0.760906	Inorgan.lib	Adamite (Adamite group - orthorhombic arsenates)	517
☐	2	0.745629	Inorgan.lib	Peridot (Olivine group)	791
☐	3	0.742949	Inorgan.lib	Olivine	985
☑	4	0.689517	Inorgan.lib	Mimetite (Apatite group)	23
☐	5	0.682187	Inorgan.lib	Olivine (Kimberlitic)	986
☐	6	0.642381	Inorgan.lib	Adamite (Adamite group - orthorhombic arsenates)	518
☐	7	0.624998	Inorgan.lib	Mimetite (Apatite group)	551
☐	8	0.590142	Inorgan.lib	Titanomagnetite (Spinel group)	948
☐	9	0.576632	Inorgan.lib	Bayldonite (Cu,Pb hydroxyarsenate)	453
☐	10	0.548307	Inorgan.lib	Vanadinite (Apatite group)	953
☐	11	0.533481	Inorgan.lib	Tyrolite	417

Figure 47: WiRE Spectra search for analysis 25-1.

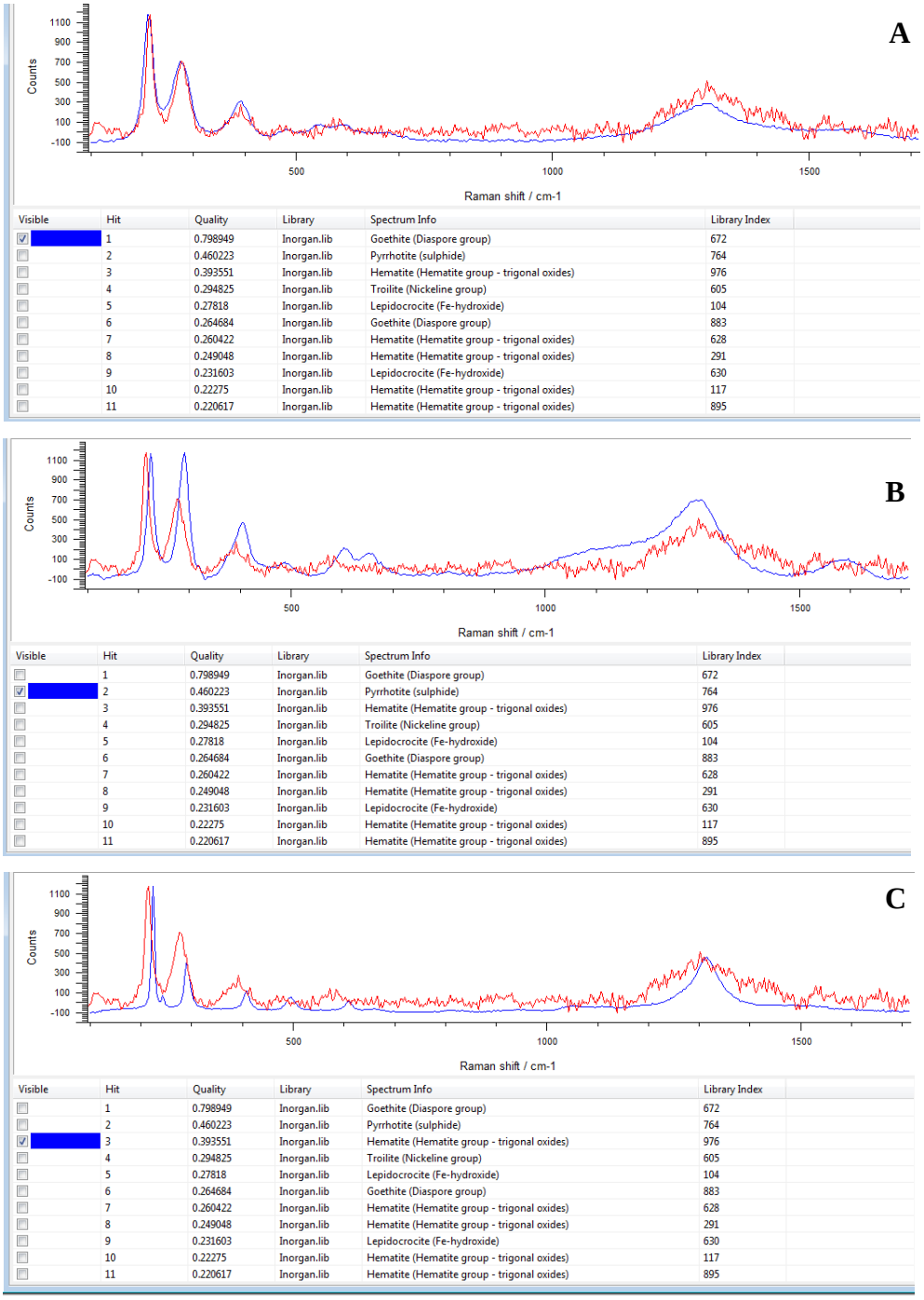

Visible	Hit	Quality	Library	Spectrum Info	Library Index
☑	1	0.798949	Inorgan.lib	Goethite (Diaspore group)	672
☐	2	0.460223	Inorgan.lib	Pyrrhotite (sulphide)	764
☐	3	0.393551	Inorgan.lib	Hematite (Hematite group - trigonal oxides)	976
☐	4	0.294825	Inorgan.lib	Troilite (Nickeline group)	605
☐	5	0.27818	Inorgan.lib	Lepidocrocite (Fe-hydroxide)	104
☐	6	0.264684	Inorgan.lib	Goethite (Diaspore group)	883
☐	7	0.260422	Inorgan.lib	Hematite (Hematite group - trigonal oxides)	628
☐	8	0.249048	Inorgan.lib	Hematite (Hematite group - trigonal oxides)	291
☐	9	0.231603	Inorgan.lib	Lepidocrocite (Fe-hydroxide)	630
☐	10	0.22275	Inorgan.lib	Hematite (Hematite group - trigonal oxides)	117
☐	11	0.220617	Inorgan.lib	Hematite (Hematite group - trigonal oxides)	895

Visible	Hit	Quality	Library	Spectrum Info	Library Index
☐	1	0.798949	Inorgan.lib	Goethite (Diaspore group)	672
☑	2	0.460223	Inorgan.lib	Pyrrhotite (sulphide)	764
☐	3	0.393551	Inorgan.lib	Hematite (Hematite group - trigonal oxides)	976
☐	4	0.294825	Inorgan.lib	Troilite (Nickeline group)	605
☐	5	0.27818	Inorgan.lib	Lepidocrocite (Fe-hydroxide)	104
☐	6	0.264684	Inorgan.lib	Goethite (Diaspore group)	883
☐	7	0.260422	Inorgan.lib	Hematite (Hematite group - trigonal oxides)	628
☐	8	0.249048	Inorgan.lib	Hematite (Hematite group - trigonal oxides)	291
☐	9	0.231603	Inorgan.lib	Lepidocrocite (Fe-hydroxide)	630
☐	10	0.22275	Inorgan.lib	Hematite (Hematite group - trigonal oxides)	117
☐	11	0.220617	Inorgan.lib	Hematite (Hematite group - trigonal oxides)	895

Visible	Hit	Quality	Library	Spectrum Info	Library Index
☐	1	0.798949	Inorgan.lib	Goethite (Diaspore group)	672
☐	2	0.460223	Inorgan.lib	Pyrrhotite (sulphide)	764
☑	3	0.393551	Inorgan.lib	Hematite (Hematite group - trigonal oxides)	976
☐	4	0.294825	Inorgan.lib	Troilite (Nickeline group)	605
☐	5	0.27818	Inorgan.lib	Lepidocrocite (Fe-hydroxide)	104
☐	6	0.264684	Inorgan.lib	Goethite (Diaspore group)	883
☐	7	0.260422	Inorgan.lib	Hematite (Hematite group - trigonal oxides)	628
☐	8	0.249048	Inorgan.lib	Hematite (Hematite group - trigonal oxides)	291
☐	9	0.231603	Inorgan.lib	Lepidocrocite (Fe-hydroxide)	630
☐	10	0.22275	Inorgan.lib	Hematite (Hematite group - trigonal oxides)	117
☐	11	0.220617	Inorgan.lib	Hematite (Hematite group - trigonal oxides)	895

Figure 48: WiRE Spectra search for analysis 26-1.

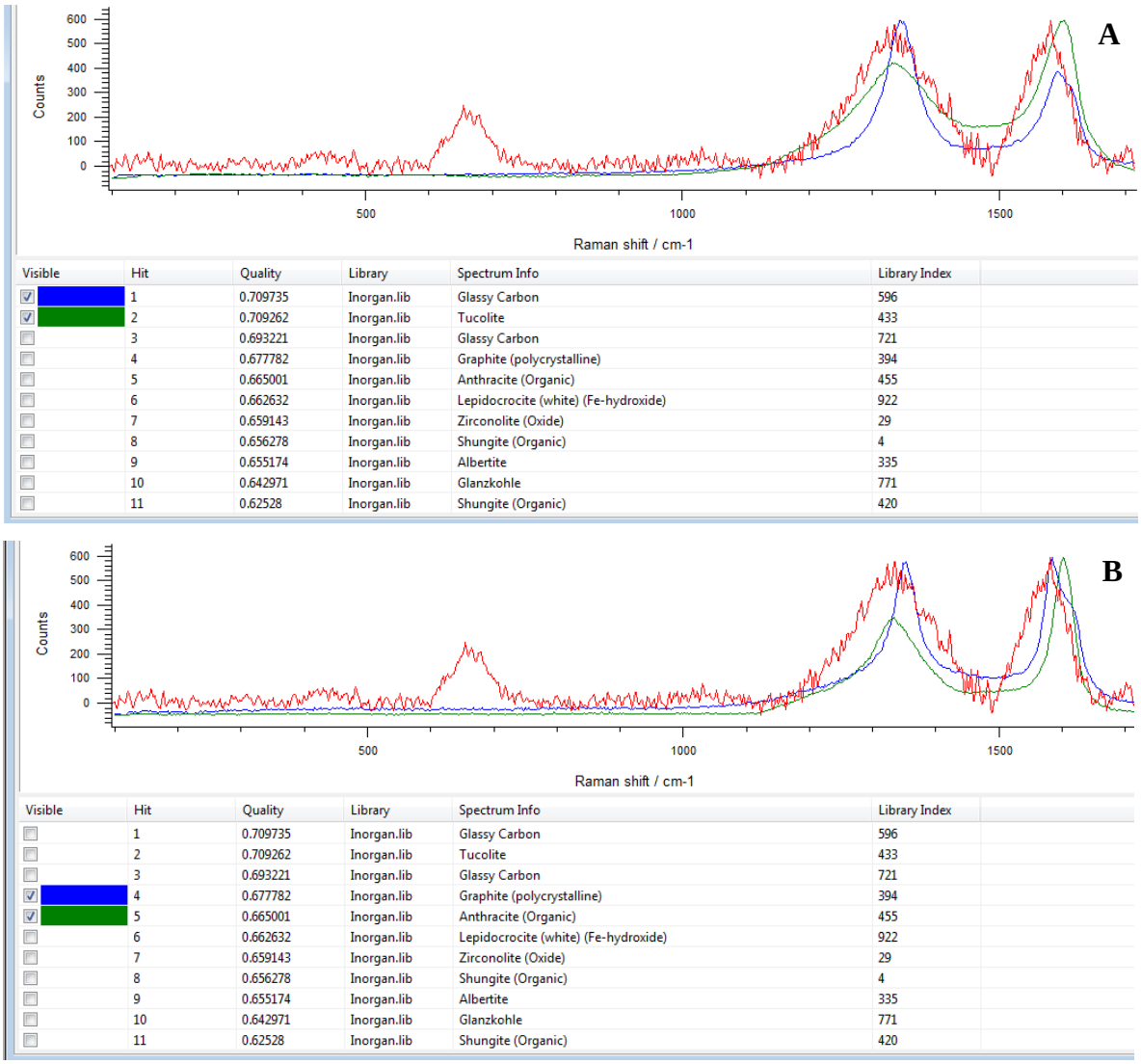

Visible	Hit	Quality	Library	Spectrum Info	Library Index
☑	1	0.709735	Inorgan.lib	Glassy Carbon	596
☑	2	0.709262	Inorgan.lib	Tucolite	433
☐	3	0.693221	Inorgan.lib	Glassy Carbon	721
☐	4	0.677782	Inorgan.lib	Graphite (polycrystalline)	394
☐	5	0.665001	Inorgan.lib	Anthracite (Organic)	455
☐	6	0.662632	Inorgan.lib	Lepidocrocite (white) (Fe-hydroxide)	922
☐	7	0.659143	Inorgan.lib	Zirconolite (Oxide)	29
☐	8	0.656278	Inorgan.lib	Shungite (Organic)	4
☐	9	0.655174	Inorgan.lib	Albertite	335
☐	10	0.642971	Inorgan.lib	Glanzkohle	771
☐	11	0.62528	Inorgan.lib	Shungite (Organic)	420

Visible	Hit	Quality	Library	Spectrum Info	Library Index
☐	1	0.709735	Inorgan.lib	Glassy Carbon	596
☐	2	0.709262	Inorgan.lib	Tucolite	433
☐	3	0.693221	Inorgan.lib	Glassy Carbon	721
☑	4	0.677782	Inorgan.lib	Graphite (polycrystalline)	394
☑	5	0.665001	Inorgan.lib	Anthracite (Organic)	455
☐	6	0.662632	Inorgan.lib	Lepidocrocite (white) (Fe-hydroxide)	922
☐	7	0.659143	Inorgan.lib	Zirconolite (Oxide)	29
☐	8	0.656278	Inorgan.lib	Shungite (Organic)	4
☐	9	0.655174	Inorgan.lib	Albertite	335
☐	10	0.642971	Inorgan.lib	Glanzkohle	771
☐	11	0.62528	Inorgan.lib	Shungite (Organic)	420

Figure 49: WiRE Spectra search for analysis 31-1.

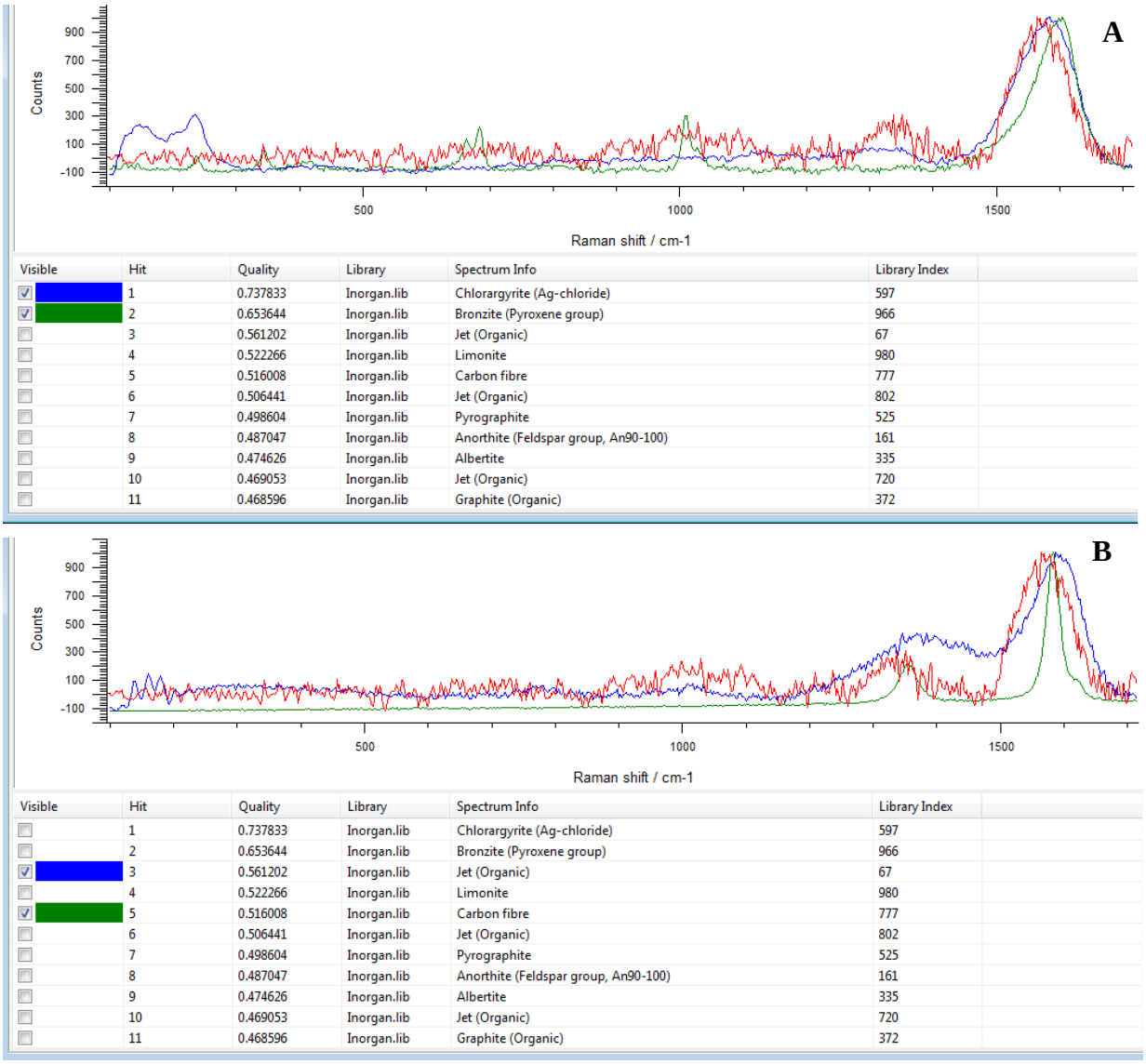

Visible	Hit	Quality	Library	Spectrum Info	Library Index
☑	1	0.737833	Inorgan.lib	Chlorargyrite (Ag-chloride)	597
☑	2	0.653644	Inorgan.lib	Bronzite (Pyroxene group)	966
☐	3	0.561202	Inorgan.lib	Jet (Organic)	67
☐	4	0.522266	Inorgan.lib	Limonite	980
☐	5	0.516008	Inorgan.lib	Carbon fibre	777
☐	6	0.506441	Inorgan.lib	Jet (Organic)	802
☐	7	0.498604	Inorgan.lib	Pyrographite	525
☐	8	0.487047	Inorgan.lib	Anorthite (Feldspar group, An90-100)	161
☐	9	0.474626	Inorgan.lib	Albertite	335
☐	10	0.469053	Inorgan.lib	Jet (Organic)	720
☐	11	0.468596	Inorgan.lib	Graphite (Organic)	372

Visible	Hit	Quality	Library	Spectrum Info	Library Index
☐	1	0.737833	Inorgan.lib	Chlorargyrite (Ag-chloride)	597
☐	2	0.653644	Inorgan.lib	Bronzite (Pyroxene group)	966
☑	3	0.561202	Inorgan.lib	Jet (Organic)	67
☐	4	0.522266	Inorgan.lib	Limonite	980
☑	5	0.516008	Inorgan.lib	Carbon fibre	777
☐	6	0.506441	Inorgan.lib	Jet (Organic)	802
☐	7	0.498604	Inorgan.lib	Pyrographite	525
☐	8	0.487047	Inorgan.lib	Anorthite (Feldspar group, An90-100)	161
☐	9	0.474626	Inorgan.lib	Albertite	335
☐	10	0.469053	Inorgan.lib	Jet (Organic)	720
☐	11	0.468596	Inorgan.lib	Graphite (Organic)	372

Figure 50: WiRE Spectra search for analysis 32-1.

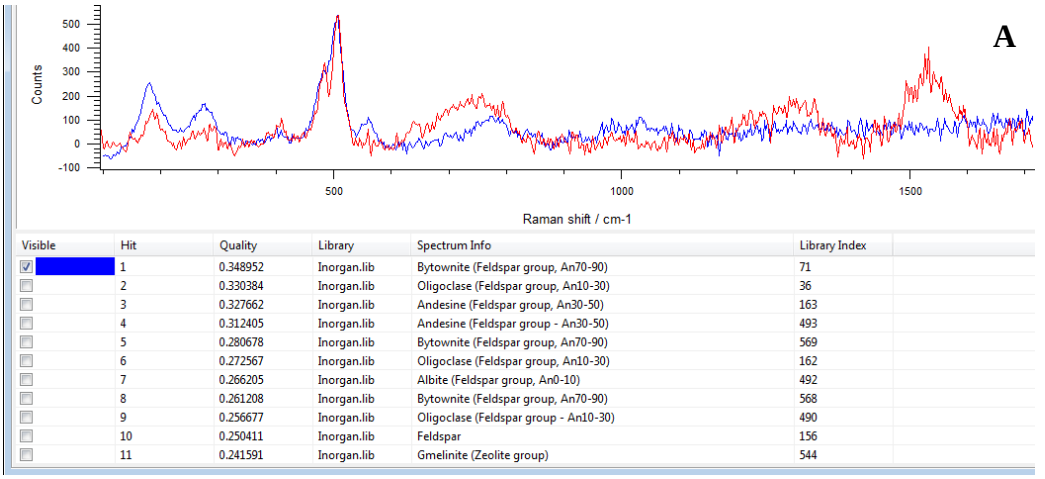

Visible	Hit	Quality	Library	Spectrum Info	Library Index
☑	1	0.348952	Inorgan.lib	Bytownite (Feldspar group, An70-90)	71
☐	2	0.330384	Inorgan.lib	Oligoclase (Feldspar group, An10-30)	36
☐	3	0.327662	Inorgan.lib	Andesine (Feldspar group, An30-50)	163
☐	4	0.312405	Inorgan.lib	Andesine (Feldspar group - An30-50)	493
☐	5	0.280678	Inorgan.lib	Bytownite (Feldspar group, An70-90)	569
☐	6	0.272567	Inorgan.lib	Oligoclase (Feldspar group, An10-30)	162
☐	7	0.266205	Inorgan.lib	Albite (Feldspar group, An0-10)	492
☐	8	0.261208	Inorgan.lib	Bytownite (Feldspar group, An70-90)	568
☐	9	0.256677	Inorgan.lib	Oligoclase (Feldspar group - An10-30)	490
☐	10	0.250411	Inorgan.lib	Feldspar	156
☐	11	0.241591	Inorgan.lib	Gmelinite (Zeolite group)	544

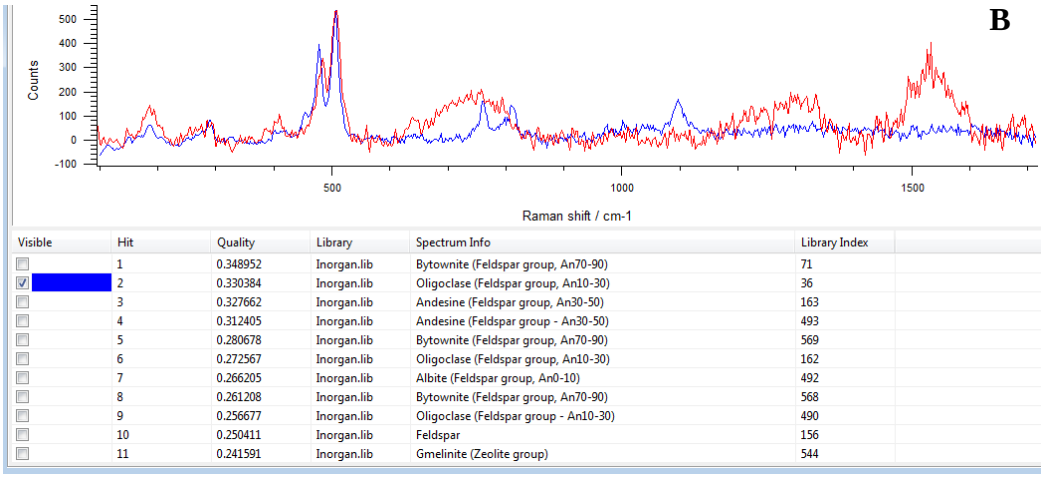

Visible	Hit	Quality	Library	Spectrum Info	Library Index
☐	1	0.348952	Inorgan.lib	Bytownite (Feldspar group, An70-90)	71
☑	2	0.330384	Inorgan.lib	Oligoclase (Feldspar group, An10-30)	36
☐	3	0.327662	Inorgan.lib	Andesine (Feldspar group, An30-50)	163
☐	4	0.312405	Inorgan.lib	Andesine (Feldspar group - An30-50)	493
☐	5	0.280678	Inorgan.lib	Bytownite (Feldspar group, An70-90)	569
☐	6	0.272567	Inorgan.lib	Oligoclase (Feldspar group, An10-30)	162
☐	7	0.266205	Inorgan.lib	Albite (Feldspar group, An0-10)	492
☐	8	0.261208	Inorgan.lib	Bytownite (Feldspar group, An70-90)	568
☐	9	0.256677	Inorgan.lib	Oligoclase (Feldspar group - An10-30)	490
☐	10	0.250411	Inorgan.lib	Feldspar	156
☐	11	0.241591	Inorgan.lib	Gmelinite (Zeolite group)	544

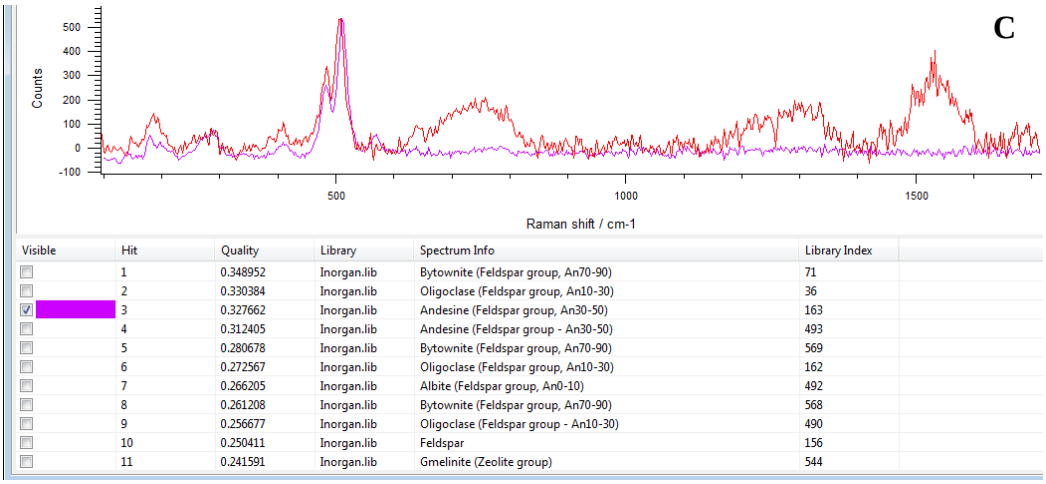

Visible	Hit	Quality	Library	Spectrum Info	Library Index
☐	1	0.348952	Inorgan.lib	Bytownite (Feldspar group, An70-90)	71
☐	2	0.330384	Inorgan.lib	Oligoclase (Feldspar group, An10-30)	36
☑	3	0.327662	Inorgan.lib	Andesine (Feldspar group, An30-50)	163
☐	4	0.312405	Inorgan.lib	Andesine (Feldspar group - An30-50)	493
☐	5	0.280678	Inorgan.lib	Bytownite (Feldspar group, An70-90)	569
☐	6	0.272567	Inorgan.lib	Oligoclase (Feldspar group, An10-30)	162
☐	7	0.266205	Inorgan.lib	Albite (Feldspar group, An0-10)	492
☐	8	0.261208	Inorgan.lib	Bytownite (Feldspar group, An70-90)	568
☐	9	0.256677	Inorgan.lib	Oligoclase (Feldspar group - An10-30)	490
☐	10	0.250411	Inorgan.lib	Feldspar	156
☐	11	0.241591	Inorgan.lib	Gmelinite (Zeolite group)	544

Figure 51: WiRE Spectra search for analysis 13-1.

Appendix B - Microprobe Data

Plagioclase

Oxide concentrations

Table 12: Plagioclase chemical data (oxide concentrations)

Sample	Line	wt% SiO2	wt% Al2O3	wt% FeO	wt% MgO	wt% CaO	wt% Na2O	wt% K2O	Cu (ppm)	Total
MB97-15 pl area A matrix	327	53.26	29.42	0.50	0.08	12.36	4.40	0.22	BDL	100.24
MB97-15 pl area A matrix	328	62.41	23.12	0.41	0.04	4.92	8.10	1.11	BDL	100.10
MB97-15 pl area A matrix	329	54.42	28.23	0.53	0.10	11.23	5.01	0.28	BDL	99.81
MB97-15 pl area A matrix	330	59.43	24.96	0.47	0.06	7.22	7.09	0.68	BDL	99.90
MB97-15 pl area B matrix	341	52.58	29.61	0.42	0.11	12.82	4.09	0.18	BDL	99.82
MB97-15 pl area B matrix	342	52.94	29.60	0.50	0.09	12.63	4.26	0.21	BDL	100.23
MB97-15 pl area B matrix	343	62.38	23.17	0.98	0.05	4.91	8.12	1.18	BDL	100.81
MB97-15 pl area B matrix	344	52.70	29.58	0.46	0.13	12.75	4.14	0.18	BDL	99.93
MB97-19 pl area A matrix rim-core	154	55.24	27.89	0.66	0.15	10.86	5.04	0.34	BDL	100.19
MB97-19 pl area A matrix rim-core	155	53.90	29.09	0.45	0.13	12.11	4.47	0.24	BDL	100.40
MB97-19 pl area A matrix rim-core	156	52.23	30.48	0.42	0.14	13.51	3.73	0.16	BDL	100.69
MB97-19 pl area A matrix rim-core	157	52.16	30.12	0.42	0.13	13.36	3.81	0.16	BDL	100.17
MB97-19 pl area A mega	150	54.03	29.29	0.42	0.15	12.19	4.41	0.21	BDL	100.68
MB97-19 pl area A mega	151	53.50	29.46	0.41	0.15	12.50	4.24	0.19	BDL	100.45
MB97-19 pl area A mega	152	53.83	29.39	0.41	0.15	12.35	4.32	0.20	BDL	100.66
MB97-19 pl area A mega	153	52.75	30.13	0.41	0.14	13.17	3.87	0.17	BDL	100.64
MB97-19 pl area B matrix	163	54.09	28.99	0.75	0.08	11.78	4.66	0.30	BDL	100.65
MB97-19 pl area B matrix	164	60.55	24.13	0.74	0.06	6.37	7.09	1.33	BDL	100.27
MB97-19 pl area B matrix	165	53.85	29.22	0.56	0.08	12.06	4.54	0.28	BDL	100.59
MB97-19 pl area B matrix	166	54.37	28.58	0.60	0.11	11.54	4.77	0.30	BDL	100.25
MB97-19 pl area B mega	159	52.95	29.90	0.39	0.14	12.96	3.99	0.18	198.13	100.53
MB97-19 pl area B mega	158	53.66	29.32	0.38	0.14	12.36	4.31	0.21	BDL	100.39
MB97-19 pl area B mega	160	53.83	29.18	0.41	0.15	12.15	4.43	0.21	BDL	100.36
MB97-19 pl area B mega	161	51.73	30.28	0.40	0.14	13.40	3.70	0.16	BDL	99.80
MB97-19 pl area B mega	162	53.97	29.11	0.43	0.15	12.06	4.43	0.21	BDL	100.36
MB97-19 pl area B multi	796	53.74	28.47	0.57	0.11	11.67	4.70	0.30	224.58	99.57
MB97-19 pl area B multi	797	56.41	26.68	0.65	0.10	9.63	5.77	0.47	BDL	99.71
MB97-19 pl area B multi	798	54.32	28.16	0.92	0.11	11.22	4.89	0.35	BDL	99.96
MB97-37 pl area A matrix	725	55.04	27.30	0.61	0.10	10.55	5.32	0.39	BDL	99.31
MB97-37 pl area A matrix	726	53.78	28.36	0.65	0.10	11.64	4.73	0.31	BDL	99.57
MB97-37 pl area A matrix	727	53.84	28.29	0.63	0.09	11.55	4.76	0.33	BDL	99.49

MB97-37 pl area A mega	705	52.68	29.39	0.33	0.11	12.57	4.19	0.25	BDL	99.52
MB97-37 pl area A mega	706	52.73	29.01	0.47	0.13	12.44	4.33	0.24	BDL	99.35
MB97-37 pl area A mega	707	52.12	29.66	0.31	0.11	12.89	3.97	0.24	BDL	99.31
MB97-37 pl area B matrix	703	54.43	27.95	0.77	0.10	11.16	4.96	0.35	BDL	99.73
MB97-37 pl area B matrix	704	51.41	30.15	0.57	0.07	13.51	3.64	0.21	BDL	99.55
MB97-37 pl area B mega	693	54.05	28.60	0.37	0.14	11.65	4.69	0.30	BDL	99.80
MB97-37 pl area B mega	694	53.65	28.93	0.29	0.11	11.98	4.50	0.28	BDL	99.74
MB97-37 pl area B mega	695	51.58	30.24	0.29	0.10	13.37	3.70	0.21	BDL	99.50
MB97-37 pl area B mega	696	54.08	28.22	0.43	0.13	11.53	4.75	0.31	BDL	99.46
MB97-37 pl area B mega	697	53.03	29.08	0.41	0.12	12.37	4.29	0.25	BDL	99.57
MB97-38 pl area A matrix	200	53.42	29.62	0.33	0.13	12.59	4.22	0.26	BDL	100.56
MB97-38 pl area A matrix	201	53.16	29.71	0.31	0.12	12.67	4.12	0.26	BDL	100.35
MB97-38 pl area A matrix	202	54.06	28.70	0.33	0.12	11.66	4.68	0.32	BDL	99.87
MB97-38 pl area A mega rim-core	196	53.30	29.95	0.29	0.12	12.69	4.14	0.24	BDL	100.72
MB97-38 pl area A mega rim-core	197	52.97	30.14	0.32	0.13	12.90	3.98	0.23	BDL	100.65
MB97-38 pl area A mega rim-core	198	52.86	30.21	0.31	0.13	12.98	3.95	0.22	BDL	100.67
MB97-38 pl area A mega rim-core	199	54.16	29.32	0.31	0.13	12.11	4.44	0.27	BDL	100.75
MB97-38 pl area B matrix	209	55.84	27.59	0.57	0.11	10.46	5.29	0.45	BDL	100.32
MB97-38 pl area B matrix	210	54.04	29.28	0.41	0.12	12.11	4.46	0.30	BDL	100.72
MB97-38 pl area B matrix	211	54.03	29.21	0.36	0.12	12.05	4.47	0.28	BDL	100.50
MB97-38 pl area B mega	203	54.69	28.34	0.37	0.13	11.37	4.85	0.32	BDL	100.08
MB97-38 pl area B mega	204	53.01	29.91	0.34	0.12	12.80	4.08	0.24	BDL	100.50
MB97-38 pl area B mega	205	54.28	28.67	0.35	0.13	11.67	4.68	0.30	BDL	100.08
MB97-38 pl area B mega	206	52.89	29.96	0.32	0.12	12.88	4.00	0.24	BDL	100.40
MB97-38 pl area B mega	207	53.13	29.73	0.37	0.12	12.69	4.12	0.24	BDL	100.40
MB97-38 pl area B mega	208	55.04	28.42	0.36	0.12	11.28	4.85	0.31	BDL	100.39
MB97-39 pl area A matrix	670	52.39	29.46	0.79	0.09	12.78	4.07	0.29	BDL	99.87
MB97-39 pl area A matrix	671	52.01	29.49	0.90	0.12	12.96	3.95	0.28	BDL	99.70
MB97-39 pl area A matrix	672	53.93	27.82	1.13	0.15	11.43	4.75	0.40	BDL	99.62
MB97-39 pl area A matrix	673	54.17	27.99	0.85	0.09	11.25	4.92	0.35	BDL	99.61
MB97-39 pl area B matrix	680	53.68	28.48	0.83	0.10	11.81	4.57	0.36	BDL	99.80
MB97-39 pl area B matrix	681	53.23	28.84	0.88	0.12	12.18	4.35	0.35	BDL	99.97
MB97-39 pl area B matrix	682	53.79	28.66	0.68	0.12	11.89	4.54	0.37	BDL	100.05
MB97-39 pl area B matrix	683	53.87	28.29	0.85	0.12	11.70	4.66	0.38	BDL	99.85
MB97-39 pl area B mega	640	53.73	28.93	0.50	0.09	11.88	4.48	0.35	BDL	99.96
MB97-39 pl area B mega	641	53.72	28.63	0.52	0.08	11.65	4.58	0.38	BDL	99.55
MB97-39 pl area B mega	642	54.57	28.43	0.48	0.08	11.32	4.81	0.41	BDL	100.09
MB97-39 pl area B mega	643	53.95	28.98	0.52	0.08	11.86	4.50	0.35	BDL	100.21
MB97-39 pl area B mega	644	54.99	27.96	0.53	0.08	10.94	5.01	0.44	BDL	99.97
MB97-39 pl area B mega	645	53.15	28.99	0.73	0.15	12.43	4.25	0.32	BDL	100.02

MB97-39 pl area B mega	646	53.94	28.53	0.54	0.10	11.68	4.63	0.37	BDL	99.79
MB97-51 pl area A matrix	375	58.55	25.68	0.83	0.13	8.20	6.56	0.68	BDL	100.64
MB97-51 pl area A matrix	376	53.92	28.45	0.97	0.08	11.68	4.67	0.36	BDL	100.10
MB97-51 pl area A matrix	377	53.50	28.19	1.16	0.22	11.59	4.62	0.35	BDL	99.62
MB97-51 pl area A matrix	378	57.18	25.93	0.87	0.11	8.76	6.25	0.57	BDL	99.67
MB97-51 pl area A mega	371	54.48	28.87	0.41	0.12	11.75	4.69	0.30	BDL	100.62
MB97-51 pl area A mega	372	53.04	29.33	0.41	0.12	12.49	4.30	0.26	BDL	99.96
MB97-51 pl area A mega	373	54.01	28.78	0.42	0.13	11.75	4.66	0.30	BDL	100.05
MB97-51 pl area A mega	374	52.65	29.17	0.44	0.16	12.44	4.28	0.23	BDL	99.37
MB97-51 pl area B matrix	354	62.36	22.66	0.75	0.03	4.72	7.81	1.75	170.39	100.10
MB97-51 pl area B matrix	353	53.41	28.85	0.91	0.07	12.09	4.48	0.33	BDL	100.14
MB97-51 pl area B matrix	355	54.67	27.64	1.01	0.07	10.87	5.16	0.41	BDL	99.83
MB97-51 pl area B matrix	356	58.63	24.91	0.94	0.19	7.49	6.78	0.76	BDL	99.69
MB97-51 pl area B mega	367	53.64	28.83	0.69	0.11	12.04	4.51	0.30	BDL	100.12
MB97-51 pl area B mega	368	54.98	27.76	0.43	0.10	10.74	5.18	0.45	BDL	99.64
MB97-51 pl area B mega	369	54.21	28.39	0.50	0.12	11.54	4.73	0.39	BDL	99.88
MB97-51 pl area B mega	370	54.91	27.63	0.41	0.11	10.71	5.21	0.44	BDL	99.42
MB97-74A pl area A	115	54.19	27.64	0.53	0.11	10.95	4.97	0.43	BDL	98.83
MB97-74A pl area A	116	51.43	29.80	0.54	0.09	13.20	3.75	0.27	BDL	99.10
MB97-74A pl area A	117	53.17	28.67	0.60	0.10	12.08	4.35	0.35	BDL	99.30
MB97-74A pl area A core matrix	134	53.92	28.51	0.66	0.10	11.61	4.66	0.40	BDL	99.84
MB97-74A pl area A core matrix	135	54.65	28.17	0.67	0.11	11.21	4.87	0.41	BDL	100.07
MB97-74A pl area A core matrix	136	54.72	28.08	0.68	0.12	11.23	4.92	0.42	BDL	100.17
MB97-74A pl area A core matrix	137	54.65	27.92	0.70	0.12	11.03	4.96	0.45	BDL	99.82
MB97-74A pl area A rim 5um matrix	138	64.49	21.68	0.54	0.03	3.19	7.72	3.03	BDL	100.70
MB97-74A pl area A rim 5um matrix	139	61.65	23.53	0.55	0.05	5.50	7.24	1.62	BDL	100.15
MB97-74A pl area A rim 5um matrix	140	61.62	23.97	0.52	0.04	5.75	7.30	1.39	BDL	100.60
MB97-74A pl area A rim 5um matrix	141	63.88	22.08	0.70	0.03	3.67	7.77	2.61	BDL	100.74
MB97-74A pl area B matrix 5um	146	67.13	19.14	0.45	0.01	0.58	7.53	5.36	BDL	100.19
MB97-74A pl area B matrix 5um	147	55.12	27.93	0.66	0.10	10.93	5.06	0.45	BDL	100.26
MB97-74A pl area B matrix 5um	148	54.43	28.05	0.66	0.12	11.21	4.89	0.40	BDL	99.77
MB97-74A pl area B matrix 5um	149	56.10	27.25	0.96	0.10	10.12	5.46	0.53	BDL	100.51
MB97-74A pl area B mega	142	55.96	27.44	0.54	0.09	10.33	5.23	0.53	BDL	100.13
MB97-74A pl area B mega	143	55.51	28.12	0.56	0.10	10.90	5.00	0.46	BDL	100.64
MB97-74A pl area B mega	144	54.62	28.74	0.59	0.11	11.64	4.61	0.38	BDL	100.69
MB97-74A pl area B mega	145	53.46	29.08	0.59	0.11	12.18	4.30	0.34	BDL	100.06
MB97-75 pl area A matrix	171	63.25	22.86	0.53	0.05	4.58	7.59	1.97	BDL	100.83
MB97-75 pl area A matrix	172	57.17	26.77	0.83	0.11	9.50	5.79	0.62	BDL	100.81
MB97-75 pl area A matrix	173	59.89	25.25	0.61	0.05	7.28	6.86	0.81	157.07	100.76

MB97-75 pl area A mega	167	54.01	29.19	0.60	0.11	12.09	4.42	0.35	BDL	100.77
MB97-75 pl area A mega	168	54.62	28.80	0.58	0.11	11.65	4.65	0.38	BDL	100.78
MB97-75 pl area A mega	169	55.17	28.31	0.54	0.11	11.17	4.90	0.42	BDL	100.62
MB97-75 pl area A mega	170	54.26	28.98	0.60	0.11	11.94	4.48	0.36	BDL	100.72
MB97-75 pl area B matrix	182	54.52	28.66	0.67	0.11	11.55	4.71	0.39	BDL	100.61
MB97-75 pl area B matrix	183	55.83	27.69	0.63	0.11	10.46	5.28	0.51	BDL	100.49
MB97-75 pl area B matrix	184	59.51	24.18	0.69	0.22	6.25	7.28	0.53	BDL	98.66
MB97-75 pl area B mega	174	55.73	28.06	0.54	0.10	10.87	5.01	0.44	BDL	100.74
MB97-75 pl area B mega	175	54.27	28.93	0.60	0.12	11.89	4.49	0.36	BDL	100.65
MB97-75 pl area B mega	176	53.94	28.99	0.58	0.11	12.07	4.40	0.35	BDL	100.45
MB97-75 pl area B mega	177	55.62	28.33	0.55	0.11	11.05	4.94	0.45	BDL	101.06
MB97-75 pl area B mega	178	56.13	27.78	0.51	0.10	10.53	5.20	0.49	BDL	100.73
MB97-75 pl area B mega	179	54.94	28.24	0.58	0.10	11.23	4.82	0.42	BDL	100.33
MB97-75 pl area B mega	180	55.05	28.37	0.56	0.10	11.26	4.86	0.42	BDL	100.62
MB97-75 pl area B mega	181	53.56	29.22	0.60	0.11	12.17	4.36	0.35	BDL	100.36
MB97-76A pl area A matrix	265	52.63	28.67	0.60	0.09	12.15	4.39	0.35	BDL	98.88
MB97-76A pl area A matrix	266	58.86	25.02	0.61	0.06	7.49	6.73	0.91	BDL	99.67
MB97-76A pl area A matrix	267	54.73	27.27	0.70	0.10	10.59	5.22	0.49	BDL	99.10
MB97-76A pl area A matrix	268	63.95	21.18	0.45	0.02	2.96	7.85	3.13	BDL	99.55
MB97-76A pl area A mega rim-core	259	54.60	27.70	0.54	0.10	10.94	5.04	0.45	213.30	99.40
MB97-76A pl area A mega rim-core	255	53.04	28.85	0.60	0.10	12.27	4.30	0.33	BDL	99.50
MB97-76A pl area A mega rim-core	256	54.08	28.01	0.55	0.11	11.39	4.79	0.39	BDL	99.31
MB97-76A pl area A mega rim-core	257	53.99	27.91	0.56	0.10	11.33	4.85	0.41	BDL	99.16
MB97-76A pl area A mega rim-core	258	54.70	27.57	0.52	0.10	10.86	5.05	0.46	BDL	99.26
MB97-76A pl area A mega rim-core	260	54.24	27.73	0.54	0.11	11.11	4.94	0.44	BDL	99.11
MB97-76A pl area A mega rim-core	261	54.34	28.06	0.57	0.10	11.24	4.84	0.42	BDL	99.58
MB97-76A pl area A mega rim-core	262	53.19	28.13	0.55	0.10	11.53	4.67	0.40	BDL	98.57
MB97-76A pl area A mega rim-core	263	54.69	27.46	0.54	0.10	10.65	5.17	0.48	BDL	99.07
MB97-76A pl area A mega rim-core	264	54.25	27.37	0.74	0.18	10.77	4.94	0.47	BDL	98.73
MB97-76A pl area A mega zoning points	397	53.78	25.58	2.19	0.70	9.86	4.49	0.52	562.72	97.18
MB97-76A pl area A mega zoning points	387	53.19	28.82	0.58	0.10	12.11	4.38	0.33	BDL	99.53
MB97-76A pl area A mega zoning points	388	53.65	27.99	0.60	0.12	11.46	4.74	0.38	BDL	98.93
MB97-76A pl area A mega zoning points	389	53.92	27.78	0.65	0.13	11.18	4.90	0.43	BDL	98.99
MB97-76A pl area A mega zoning points	390	52.91	28.61	0.62	0.11	12.08	4.42	0.35	BDL	99.11
MB97-76A pl area A mega zoning points	391	54.62	27.72	0.54	0.10	10.93	5.03	0.46	BDL	99.39
MB97-76A pl area A mega zoning points	392	54.28	27.91	0.58	0.10	11.19	4.88	0.43	BDL	99.36
MB97-76A pl area A mega zoning points	393	54.22	27.92	0.71	0.16	11.23	4.77	0.45	BDL	99.47

MB97-76A pl area A mega zoning points	394	53.09	28.30	0.64	0.12	11.84	4.38	0.50	BDL	98.86
MB97-76A pl area A mega zoning points	395	54.83	27.59	0.56	0.10	10.84	5.09	0.45	BDL	99.47
MB97-76A pl area A mega zoning points	396	54.92	27.40	0.53	0.10	10.65	5.17	0.47	BDL	99.24
MB97-76A pl area A mega zoning points	398	54.51	27.95	0.59	0.10	11.18	4.94	0.42	BDL	99.67
MB97-76A pl area A mega zoning points	399	53.84	28.20	0.56	0.10	11.53	4.73	0.39	BDL	99.35
MB97-76A pl area A mega zoning points	400	54.08	27.84	0.59	0.10	11.14	4.90	0.43	BDL	99.08
MB97-76A pl area A mega zoning points	401	54.05	28.11	0.59	0.10	11.49	4.73	0.40	BDL	99.45
MB97-76A pl area A mega zoning points	402	53.55	28.34	0.60	0.10	11.75	4.56	0.37	BDL	99.28
MB97-76A pl area A mega zoning points	403	53.21	28.54	0.60	0.10	11.94	4.48	0.36	BDL	99.20
MB97-76A pl area A mega zoning points	404	53.43	28.34	0.59	0.10	11.80	4.56	0.37	BDL	99.19
MB97-76A pl area A mega zoning points	405	53.29	28.31	0.58	0.10	11.86	4.55	0.36	BDL	99.05
MB97-76A pl area A mega zoning points	406	54.04	27.88	0.54	0.10	11.30	4.82	0.41	BDL	99.07
MB97-76A pl area A mega zoning points	408	53.66	28.05	0.57	0.10	11.40	4.74	0.41	BDL	98.93
MB97-76A pl area A mega zoning points	409	53.28	28.54	0.60	0.10	11.96	4.50	0.36	BDL	99.33
MB97-76A pl area A mega zoning points	410	52.89	28.80	0.60	0.10	12.16	4.34	0.34	BDL	99.24
MB97-76A pl area A mega zoning points	411	53.61	28.08	0.57	0.11	11.42	4.76	0.41	BDL	98.95
MB97-76A pl area A mega zoning points	412	53.95	28.17	0.55	0.10	11.42	4.79	0.40	BDL	99.38
MB97-76A pl area A mega zoning points	413	54.20	27.99	0.55	0.11	11.20	4.89	0.43	BDL	99.35
MB97-76A pl area A mega zoning points	414	54.16	27.93	0.56	0.10	11.18	4.86	0.42	BDL	99.21
MB97-76A pl area A mega zoning points	415	54.22	27.71	0.57	0.10	11.09	4.92	0.43	BDL	99.01
MB97-76A pl area B matrix	282	60.75	24.33	0.57	0.05	6.41	7.23	1.16	BDL	100.49
MB97-76A pl area B matrix	283	53.02	28.60	0.69	0.10	12.12	4.45	0.34	BDL	99.31
MB97-76A pl area B matrix	284	56.60	26.55	0.61	0.09	9.45	5.85	0.63	134.55	99.79
MB97-76A pl area B matrix	285	66.07	19.26	0.54	0.01	0.90	6.95	6.13	BDL	99.87
MB97-76A pl area B mega	278	52.92	28.76	0.59	0.10	12.24	4.35	0.34	BDL	99.30
MB97-76A pl area B mega	279	54.74	27.84	0.58	0.11	11.03	4.95	0.43	BDL	99.67
MB97-76A pl area B mega	280	53.85	28.16	0.56	0.11	11.55	4.71	0.39	BDL	99.31
MB97-76A pl area B mega	281	53.82	28.35	0.57	0.10	11.62	4.66	0.38	BDL	99.49
MB97-76A pl area B mega zoning points	416	53.75	28.18	0.53	0.11	11.44	4.84	0.39	BDL	99.25
MB97-76A pl area B mega zoning points	417	53.38	28.42	0.61	0.11	11.86	4.60	0.36	BDL	99.35
MB97-76A pl area B mega zoning points	418	54.59	27.82	0.61	0.12	11.02	5.02	0.43	BDL	99.62
MB97-76A pl area B mega zoning points	419	53.60	28.46	0.59	0.11	11.80	4.62	0.38	BDL	99.56
MB97-76A pl area B mega zoning points	420	54.52	27.91	0.54	0.11	11.10	4.98	0.43	BDL	99.56
MB97-76A pl area B mega zoning points	421	53.25	28.17	0.63	0.13	11.76	4.60	0.37	BDL	98.91
MB97-76A pl area B mega zoning points	422	53.94	28.02	0.56	0.11	11.38	4.84	0.41	BDL	99.26

MB97-76A pl area B mega zoning points	423	53.06	28.68	0.59	0.11	12.08	4.41	0.34	BDL	99.29
MB97-76A pl area B mega zoning points	424	52.99	28.73	0.62	0.12	12.16	4.38	0.34	BDL	99.36
MB97-76A pl area B mega zoning points	425	52.66	28.82	0.58	0.12	12.33	4.27	0.33	BDL	99.10
MB97-76A pl area B mega zoning points	426	53.98	27.99	0.57	0.11	11.42	4.79	0.39	BDL	99.24
MB97-76A pl area B mega zoning points	427	52.71	28.96	0.60	0.11	12.37	4.27	0.33	BDL	99.33
MB97-76A pl area B mega zoning points	428	53.84	27.99	0.56	0.11	11.43	4.79	0.39	BDL	99.11
MB97-76A pl area B mega zoning points	429	53.76	27.99	0.58	0.12	11.39	4.78	0.40	BDL	99.00
MB97-76A pl area B mega zoning points	430	53.22	28.53	0.59	0.12	11.91	4.53	0.35	BDL	99.24
MB97-76A pl area B mega zoning points	431	53.05	28.34	0.57	0.12	11.80	4.57	0.36	BDL	98.80
MB97-76A pl area B mega zoning points	432	52.64	28.71	0.57	0.11	12.16	4.36	0.33	BDL	98.88
MB97-76A pl area B mega zoning points	433	52.62	28.36	0.55	0.11	11.97	4.45	0.34	BDL	98.42
MB97-76A pl area B mega zoning points	434	53.32	28.08	0.56	0.11	11.60	4.68	0.38	BDL	98.72
MB97-76A pl area B mega zoning points	435	52.89	28.59	0.57	0.11	12.00	4.41	0.34	BDL	98.93
MB97-76A pl area B mega zoning points	436	53.59	28.56	0.56	0.11	11.81	4.58	0.36	BDL	99.56
MB97-76A pl area B mega zoning points	437	52.65	28.98	0.56	0.11	12.34	4.26	0.31	BDL	99.21
MB97-76A pl area B mega zoning points	438	52.91	28.57	0.60	0.13	12.00	4.44	0.34	BDL	99.00
MB97-76A pl area B mega zoning points	439	53.72	28.16	0.56	0.11	11.49	4.74	0.38	BDL	99.17
MB97-76A pl area B mega zoning points	440	53.23	28.82	0.57	0.12	12.12	4.40	0.34	BDL	99.60
MB97-76A pl area B mega zoning points	441	53.91	28.17	0.54	0.11	11.47	4.77	0.39	BDL	99.35
MB97-76A pl area B mega zoning points	442	54.08	28.00	0.54	0.11	11.31	4.85	0.40	BDL	99.30
MB97-76A pl area B mega zoning points	443	54.57	27.90	0.55	0.11	11.11	4.97	0.43	BDL	99.65
MB97-76A pl area B mega zoning points	444	53.80	28.42	0.57	0.11	11.62	4.67	0.37	BDL	99.59
MB97-76A pl area B mega zoning points	445	54.14	28.01	0.56	0.11	11.33	4.83	0.41	BDL	99.38
MB97-76B pl area A matrix	781	56.25	26.68	0.82	0.05	9.53	5.80	0.56	191.25	99.73
MB97-76B pl area A matrix	779	56.71	26.36	0.98	0.07	9.30	5.92	0.61	BDL	99.96
MB97-76B pl area B	737	56.26	26.41	1.14	0.09	9.74	5.45	0.55	BDL	99.63
MB97-76C pl area A	319	54.97	27.70	0.64	0.08	10.77	5.16	0.42	BDL	99.75
MB97-76C pl area A	320	55.21	27.78	0.63	0.09	10.74	5.14	0.43	BDL	100.01
MB97-76C pl area A	321	55.22	27.58	0.63	0.09	10.65	5.19	0.46	BDL	99.82
MB97-76C pl area A	322	59.52	25.03	0.47	0.05	7.36	6.88	0.71	BDL	100.02
MB97-76C pl area B	304	54.59	27.80	0.66	0.07	10.89	5.12	0.40	146.69	99.55
MB97-76C pl area B	305	56.84	26.58	0.66	0.04	9.23	5.95	0.62	BDL	99.92
MB97-76C pl area B	306	54.98	27.54	0.67	0.08	10.63	5.26	0.44	BDL	99.60
MB97-76C pl area B	307	53.99	28.31	0.64	0.09	11.48	4.76	0.38	BDL	99.64
MB97-76C pl area B transect	453	54.69	27.35	0.66	0.07	10.64	5.24	0.42	BDL	99.07
MB97-76C pl area B transect	454	63.12	21.19	0.46	0.02	3.58	7.67	2.99	BDL	99.03

MB97-76C pl area B transect	455	56.13	26.43	0.76	0.06	9.37	5.95	0.54	BDL	99.21
MB97-76C pl area B transect	456	54.81	27.35	0.76	0.07	10.51	5.36	0.42	BDL	99.27
MB97-76C pl area B transect	457	55.28	26.75	0.64	0.06	9.83	5.68	0.47	139.15	98.73
MB97-76C pl area B transect	458	58.31	25.08	0.46	0.05	7.60	6.80	0.79	BDL	99.08
MB97-76C pl area B transect	459	57.78	25.48	0.50	0.06	8.08	6.51	0.76	BDL	99.17
MB97-76C pl area B transect	460	53.41	28.28	0.60	0.08	11.59	4.75	0.37	BDL	99.09
MB97-76C pl area B transect	461	53.85	27.91	0.63	0.08	11.23	4.91	0.39	BDL	99.01
MB97-76C pl area B transect	462	54.55	27.39	0.71	0.06	10.71	5.23	0.39	BDL	99.02

Formula weights and minerals

Table 13: Plagioclase formula weights and mineral determination

Sample	Line	Ca FORMULA	Na FORMULA	K FORMULA	Mineral
MB97-15 pl area A matrix	327	0.60	0.39	0.01	Labradorite
MB97-15 pl area A matrix	328	0.23	0.70	0.06	Oligoclase
MB97-15 pl area A matrix	329	0.55	0.44	0.02	Labradorite
MB97-15 pl area A matrix	330	0.35	0.62	0.04	Andesine
MB97-15 pl area B matrix	341	0.63	0.36	0.01	Labradorite
MB97-15 pl area B matrix	342	0.61	0.37	0.01	Labradorite
MB97-15 pl area B matrix	343	0.23	0.70	0.07	Oligoclase
MB97-15 pl area B matrix	344	0.62	0.36	0.01	Labradorite
MB97-19 pl area A matrix rim-core	154	0.53	0.44	0.02	Labradorite
MB97-19 pl area A matrix rim-core	155	0.59	0.39	0.01	Labradorite
MB97-19 pl area A matrix rim-core	156	0.65	0.33	0.01	Labradorite
MB97-19 pl area A matrix rim-core	157	0.65	0.34	0.01	Labradorite
MB97-19 pl area A mega	150	0.59	0.39	0.01	Labradorite
MB97-19 pl area A mega	151	0.61	0.37	0.01	Labradorite
MB97-19 pl area A mega	152	0.60	0.38	0.01	Labradorite
MB97-19 pl area A mega	153	0.64	0.34	0.01	Labradorite
MB97-19 pl area B matrix	163	0.57	0.41	0.02	Labradorite
MB97-19 pl area B matrix	164	0.31	0.61	0.08	Andesine
MB97-19 pl area B matrix	165	0.58	0.40	0.02	Labradorite
MB97-19 pl area B matrix	166	0.56	0.42	0.02	Labradorite
MB97-19 pl area B mega	159	0.63	0.35	0.01	Labradorite
MB97-19 pl area B mega	158	0.60	0.38	0.01	Labradorite
MB97-19 pl area B mega	160	0.59	0.39	0.01	Labradorite
MB97-19 pl area B mega	161	0.65	0.33	0.01	Labradorite
MB97-19 pl area B mega	162	0.58	0.39	0.01	Labradorite
MB97-19 pl area B multi	796	0.57	0.41	0.02	Labradorite
MB97-19 pl area B multi	797	0.47	0.51	0.03	Andesine
MB97-19 pl area B multi	798	0.54	0.43	0.02	Labradorite

MB97-37 pl area A matrix	725	0.51	0.47	0.02	Labradorite
MB97-37 pl area A matrix	726	0.57	0.42	0.02	Labradorite
MB97-37 pl area A matrix	727	0.56	0.42	0.02	Labradorite
MB97-37 pl area A mega	705	0.61	0.37	0.01	Labradorite
MB97-37 pl area A mega	706	0.61	0.38	0.01	Labradorite
MB97-37 pl area A mega	707	0.63	0.35	0.01	Labradorite
MB97-37 pl area B matrix	703	0.54	0.44	0.02	Labradorite
MB97-37 pl area B matrix	704	0.66	0.32	0.01	Labradorite
MB97-37 pl area B mega	693	0.57	0.41	0.02	Labradorite
MB97-37 pl area B mega	694	0.58	0.40	0.02	Labradorite
MB97-37 pl area B mega	695	0.65	0.33	0.01	Labradorite
MB97-37 pl area B mega	696	0.56	0.42	0.02	Labradorite
MB97-37 pl area B mega	697	0.60	0.38	0.01	Labradorite
MB97-38 pl area A matrix	200	0.61	0.37	0.01	Labradorite
MB97-38 pl area A matrix	201	0.61	0.36	0.02	Labradorite
MB97-38 pl area A matrix	202	0.57	0.41	0.02	Labradorite
MB97-38 pl area A mega rim-core	196	0.61	0.36	0.01	Labradorite
MB97-38 pl area A mega rim-core	197	0.62	0.35	0.01	Labradorite
MB97-38 pl area A mega rim-core	198	0.63	0.35	0.01	Labradorite
MB97-38 pl area A mega rim-core	199	0.58	0.39	0.02	Labradorite
MB97-38 pl area B matrix	209	0.50	0.46	0.03	Labradorite
MB97-38 pl area B matrix	210	0.58	0.39	0.02	Labradorite
MB97-38 pl area B matrix	211	0.58	0.39	0.02	Labradorite
MB97-38 pl area B mega	203	0.55	0.43	0.02	Labradorite
MB97-38 pl area B mega	204	0.62	0.36	0.01	Labradorite
MB97-38 pl area B mega	205	0.57	0.41	0.02	Labradorite
MB97-38 pl area B mega	206	0.62	0.35	0.01	Labradorite
MB97-38 pl area B mega	207	0.61	0.36	0.01	Labradorite
MB97-38 pl area B mega	208	0.54	0.42	0.02	Labradorite
MB97-39 pl area A matrix	670	0.62	0.36	0.02	Labradorite
MB97-39 pl area A matrix	671	0.63	0.35	0.02	Labradorite
MB97-39 pl area A matrix	672	0.56	0.42	0.02	Labradorite
MB97-39 pl area A matrix	673	0.55	0.43	0.02	Labradorite
MB97-39 pl area B matrix	680	0.57	0.40	0.02	Labradorite
MB97-39 pl area B matrix	681	0.59	0.38	0.02	Labradorite
MB97-39 pl area B matrix	682	0.58	0.40	0.02	Labradorite
MB97-39 pl area B matrix	683	0.57	0.41	0.02	Labradorite
MB97-39 pl area B mega	640	0.58	0.39	0.02	Labradorite
MB97-39 pl area B mega	641	0.57	0.40	0.02	Labradorite
MB97-39 pl area B mega	642	0.55	0.42	0.02	Labradorite
MB97-39 pl area B mega	643	0.57	0.39	0.02	Labradorite

MB97-39 pl area B mega	644	0.53	0.44	0.03	Labradorite
MB97-39 pl area B mega	645	0.60	0.37	0.02	Labradorite
MB97-39 pl area B mega	646	0.57	0.41	0.02	Labradorite
MB97-51 pl area A matrix	375	0.39	0.57	0.04	Andesine
MB97-51 pl area A matrix	376	0.57	0.41	0.02	Labradorite
MB97-51 pl area A matrix	377	0.57	0.41	0.02	Labradorite
MB97-51 pl area A matrix	378	0.42	0.55	0.03	Andesine
MB97-51 pl area A mega	371	0.57	0.41	0.02	Labradorite
MB97-51 pl area A mega	372	0.61	0.38	0.01	Labradorite
MB97-51 pl area A mega	373	0.57	0.41	0.02	Labradorite
MB97-51 pl area A mega	374	0.61	0.38	0.01	Labradorite
MB97-51 pl area B matrix	354	0.23	0.67	0.10	Oligoclase
MB97-51 pl area B matrix	353	0.59	0.39	0.02	Labradorite
MB97-51 pl area B matrix	355	0.53	0.45	0.02	Labradorite
MB97-51 pl area B matrix	356	0.36	0.59	0.04	Andesine
MB97-51 pl area B mega	367	0.58	0.40	0.02	Labradorite
MB97-51 pl area B mega	368	0.52	0.46	0.03	Labradorite
MB97-51 pl area B mega	369	0.56	0.42	0.02	Labradorite
MB97-51 pl area B mega	370	0.52	0.46	0.03	Labradorite
MB97-74A pl area A	115	0.54	0.44	0.03	Labradorite
MB97-74A pl area A	116	0.65	0.33	0.02	Labradorite
MB97-74A pl area A	117	0.59	0.39	0.02	Labradorite
MB97-74A pl area A core matrix	134	0.56	0.41	0.02	Labradorite
MB97-74A pl area A core matrix	135	0.54	0.43	0.02	Labradorite
MB97-74A pl area A core matrix	136	0.54	0.43	0.02	Labradorite
MB97-74A pl area A core matrix	137	0.54	0.44	0.03	Labradorite
MB97-74A pl area A rim 5um matrix	138	0.15	0.66	0.17	Anorthoclase
MB97-74A pl area A rim 5um matrix	139	0.26	0.63	0.09	Oligoclase
MB97-74A pl area A rim 5um matrix	140	0.27	0.63	0.08	Oligoclase
MB97-74A pl area A rim 5um matrix	141	0.17	0.67	0.15	Anorthoclase
MB97-74A pl area B matrix 5um	146	0.03	0.65	0.31	Anorthoclase
MB97-74A pl area B matrix 5um	147	0.53	0.44	0.03	Labradorite
MB97-74A pl area B matrix 5um	148	0.54	0.43	0.02	Labradorite
MB97-74A pl area B matrix 5um	149	0.49	0.48	0.03	Andesine
MB97-74A pl area B mega	142	0.50	0.46	0.03	Labradorite
MB97-74A pl area B mega	143	0.52	0.44	0.03	Labradorite
MB97-74A pl area B mega	144	0.56	0.40	0.02	Labradorite
MB97-74A pl area B mega	145	0.59	0.38	0.02	Labradorite
MB97-75 pl area A matrix	171	0.22	0.65	0.11	Oligoclase
MB97-75 pl area A matrix	172	0.46	0.50	0.04	Andesine
MB97-75 pl area A matrix	173	0.35	0.59	0.05	Andesine

MB97-75 pl area A mega	167	0.58	0.39	0.02	Labradorite
MB97-75 pl area A mega	168	0.56	0.41	0.02	Labradorite
MB97-75 pl area A mega	169	0.54	0.43	0.02	Labradorite
MB97-75 pl area A mega	170	0.58	0.39	0.02	Labradorite
MB97-75 pl area B matrix	182	0.56	0.41	0.02	Labradorite
MB97-75 pl area B matrix	183	0.50	0.46	0.03	Labradorite
MB97-75 pl area B matrix	184	0.30	0.64	0.03	Andesine
MB97-75 pl area B mega	174	0.52	0.44	0.03	Labradorite
MB97-75 pl area B mega	175	0.57	0.39	0.02	Labradorite
MB97-75 pl area B mega	176	0.58	0.39	0.02	Labradorite
MB97-75 pl area B mega	177	0.53	0.43	0.03	Labradorite
MB97-75 pl area B mega	178	0.51	0.45	0.03	Labradorite
MB97-75 pl area B mega	179	0.54	0.42	0.02	Labradorite
MB97-75 pl area B mega	180	0.54	0.42	0.02	Labradorite
MB97-75 pl area B mega	181	0.59	0.38	0.02	Labradorite
MB97-76A pl area A matrix	265	0.60	0.39	0.02	Labradorite
MB97-76A pl area A matrix	266	0.36	0.59	0.05	Andesine
MB97-76A pl area A matrix	267	0.52	0.46	0.03	Labradorite
MB97-76A pl area A matrix	268	0.14	0.68	0.18	Anorthoclase
MB97-76A pl area A mega rim-core	259	0.53	0.44	0.03	Labradorite
MB97-76A pl area A mega rim-core	255	0.60	0.38	0.02	Labradorite
MB97-76A pl area A mega rim-core	256	0.56	0.42	0.02	Labradorite
MB97-76A pl area A mega rim-core	257	0.55	0.43	0.02	Labradorite
MB97-76A pl area A mega rim-core	258	0.53	0.45	0.03	Labradorite
MB97-76A pl area A mega rim-core	260	0.54	0.44	0.03	Labradorite
MB97-76A pl area A mega rim-core	261	0.55	0.43	0.02	Labradorite
MB97-76A pl area A mega rim-core	262	0.57	0.42	0.02	Labradorite
MB97-76A pl area A mega rim-core	263	0.52	0.46	0.03	Labradorite
MB97-76A pl area A mega rim-core	264	0.53	0.44	0.03	Labradorite
MB97-76A pl area A mega zoning points	397	0.49	0.41	0.03	Labradorite
MB97-76A pl area A mega zoning points	387	0.59	0.39	0.02	Labradorite
MB97-76A pl area A mega zoning points	388	0.56	0.42	0.02	Labradorite
MB97-76A pl area A mega zoning points	389	0.55	0.43	0.03	Labradorite
MB97-76A pl area A mega zoning points	390	0.59	0.39	0.02	Labradorite
MB97-76A pl area A mega zoning points	391	0.53	0.44	0.03	Labradorite
MB97-76A pl area A mega zoning points	392	0.55	0.43	0.02	Labradorite
MB97-76A pl area A mega zoning points	393	0.55	0.42	0.03	Labradorite
MB97-76A pl area A mega zoning points	394	0.58	0.39	0.03	Labradorite
MB97-76A pl area A mega zoning points	395	0.53	0.45	0.03	Labradorite
MB97-76A pl area A mega zoning points	396	0.52	0.46	0.03	Labradorite
MB97-76A pl area A mega zoning points	398	0.54	0.43	0.02	Labradorite

MB97-76A pl area A mega zoning points	399	0.56	0.42	0.02	Labradorite
MB97-76A pl area A mega zoning points	400	0.55	0.43	0.03	Labradorite
MB97-76A pl area A mega zoning points	401	0.56	0.42	0.02	Labradorite
MB97-76A pl area A mega zoning points	402	0.57	0.40	0.02	Labradorite
MB97-76A pl area A mega zoning points	403	0.58	0.40	0.02	Labradorite
MB97-76A pl area A mega zoning points	404	0.58	0.40	0.02	Labradorite
MB97-76A pl area A mega zoning points	405	0.58	0.40	0.02	Labradorite
MB97-76A pl area A mega zoning points	406	0.55	0.43	0.02	Labradorite
MB97-76A pl area A mega zoning points	408	0.56	0.42	0.02	Labradorite
MB97-76A pl area A mega zoning points	409	0.58	0.40	0.02	Labradorite
MB97-76A pl area A mega zoning points	410	0.60	0.38	0.02	Labradorite
MB97-76A pl area A mega zoning points	411	0.56	0.42	0.02	Labradorite
MB97-76A pl area A mega zoning points	412	0.56	0.42	0.02	Labradorite
MB97-76A pl area A mega zoning points	413	0.55	0.43	0.02	Labradorite
MB97-76A pl area A mega zoning points	414	0.55	0.43	0.02	Labradorite
MB97-76A pl area A mega zoning points	415	0.54	0.44	0.03	Labradorite
MB97-76A pl area B matrix	282	0.31	0.62	0.07	Andesine
MB97-76A pl area B matrix	283	0.59	0.39	0.02	Labradorite
MB97-76A pl area B matrix	284	0.46	0.51	0.04	Andesine
MB97-76A pl area B matrix	285	0.04	0.60	0.35	Anorthoclase
MB97-76A pl area B mega	278	0.60	0.38	0.02	Labradorite
MB97-76A pl area B mega	279	0.54	0.44	0.02	Labradorite
MB97-76A pl area B mega	280	0.56	0.42	0.02	Labradorite
MB97-76A pl area B mega	281	0.57	0.41	0.02	Labradorite
MB97-76A pl area B mega zoning points	416	0.56	0.43	0.02	Labradorite
MB97-76A pl area B mega zoning points	417	0.58	0.41	0.02	Labradorite
MB97-76A pl area B mega zoning points	418	0.54	0.44	0.02	Labradorite
MB97-76A pl area B mega zoning points	419	0.58	0.41	0.02	Labradorite
MB97-76A pl area B mega zoning points	420	0.54	0.44	0.02	Labradorite
MB97-76A pl area B mega zoning points	421	0.58	0.41	0.02	Labradorite
MB97-76A pl area B mega zoning points	422	0.56	0.43	0.02	Labradorite
MB97-76A pl area B mega zoning points	423	0.59	0.39	0.02	Labradorite
MB97-76A pl area B mega zoning points	424	0.59	0.39	0.02	Labradorite
MB97-76A pl area B mega zoning points	425	0.60	0.38	0.02	Labradorite
MB97-76A pl area B mega zoning points	426	0.56	0.42	0.02	Labradorite
MB97-76A pl area B mega zoning points	427	0.61	0.38	0.02	Labradorite
MB97-76A pl area B mega zoning points	428	0.56	0.42	0.02	Labradorite
MB97-76A pl area B mega zoning points	429	0.56	0.42	0.02	Labradorite
MB97-76A pl area B mega zoning points	430	0.58	0.40	0.02	Labradorite
MB97-76A pl area B mega zoning points	431	0.58	0.41	0.02	Labradorite
MB97-76A pl area B mega zoning points	432	0.60	0.39	0.02	Labradorite

MB97-76A pl area B mega zoning points	433	0.59	0.40	0.02	Labradorite
MB97-76A pl area B mega zoning points	434	0.57	0.42	0.02	Labradorite
MB97-76A pl area B mega zoning points	435	0.59	0.39	0.02	Labradorite
MB97-76A pl area B mega zoning points	436	0.58	0.40	0.02	Labradorite
MB97-76A pl area B mega zoning points	437	0.60	0.38	0.02	Labradorite
MB97-76A pl area B mega zoning points	438	0.59	0.39	0.02	Labradorite
MB97-76A pl area B mega zoning points	439	0.56	0.42	0.02	Labradorite
MB97-76A pl area B mega zoning points	440	0.59	0.39	0.02	Labradorite
MB97-76A pl area B mega zoning points	441	0.56	0.42	0.02	Labradorite
MB97-76A pl area B mega zoning points	442	0.55	0.43	0.02	Labradorite
MB97-76A pl area B mega zoning points	443	0.54	0.44	0.02	Labradorite
MB97-76A pl area B mega zoning points	444	0.57	0.41	0.02	Labradorite
MB97-76A pl area B mega zoning points	445	0.55	0.43	0.02	Labradorite
MB97-76B pl area A matrix	781	0.46	0.51	0.03	Andesine
MB97-76B pl area A matrix	779	0.45	0.52	0.04	Andesine
MB97-76B pl area B	737	0.47	0.48	0.03	Andesine
MB97-76C pl area A	319	0.52	0.45	0.02	Labradorite
MB97-76C pl area A	320	0.52	0.45	0.03	Labradorite
MB97-76C pl area A	321	0.52	0.46	0.03	Labradorite
MB97-76C pl area A	322	0.35	0.60	0.04	Andesine
MB97-76C pl area B	304	0.53	0.45	0.02	Labradorite
MB97-76C pl area B	305	0.45	0.52	0.04	Andesine
MB97-76C pl area B	306	0.52	0.46	0.03	Labradorite
MB97-76C pl area B	307	0.56	0.42	0.02	Labradorite
MB97-76C pl area B transect	453	0.52	0.46	0.02	Labradorite
MB97-76C pl area B transect	454	0.17	0.67	0.17	Anorthoclase
MB97-76C pl area B transect	455	0.46	0.52	0.03	Andesine
MB97-76C pl area B transect	456	0.51	0.47	0.02	Labradorite
MB97-76C pl area B transect	457	0.48	0.50	0.03	Andesine
MB97-76C pl area B transect	458	0.37	0.60	0.05	Andesine
MB97-76C pl area B transect	459	0.39	0.57	0.04	Andesine
MB97-76C pl area B transect	460	0.57	0.42	0.02	Labradorite
MB97-76C pl area B transect	461	0.55	0.43	0.02	Labradorite
MB97-76C pl area B transect	462	0.52	0.46	0.02	Labradorite

Cu constraints

Table 14: Plagioclase Cu constraints

Sample	Line	Cu WT%	CuO	Cu CDL99	calc Cu ppm DL	Cu %ERR
MB97-15 pl area A matrix	327	-0.00333	-0.00417	0.01380	172.75	-194.55
MB97-15 pl area A matrix	328	-0.00548	-0.00686	0.01374	171.96	-117.47

MB97-15 pl area A matrix	329	0.00279	0.00349	0.01377	172.29	233.48
MB97-15 pl area A matrix	330	-0.00318	-0.00398	0.01370	171.44	-202.63
MB97-15 pl area B matrix	341	0.00037	0.00047	0.01382	172.97	1744.94
MB97-15 pl area B matrix	342	0.00175	0.00219	0.01387	173.57	373.82
MB97-15 pl area B matrix	343	0.00423	0.00529	0.01348	168.77	150.95
MB97-15 pl area B matrix	344	-0.00744	-0.00932	0.01394	174.62	-87.63
MB97-19 pl area A matrix rim-core	154	0.00784	0.00981	0.01376	172.24	83.41
MB97-19 pl area A matrix rim-core	155	0.00433	0.00542	0.01365	170.80	149.29
MB97-19 pl area A matrix rim-core	156	0.00595	0.00744	0.01386	173.50	110.56
MB97-19 pl area A matrix rim-core	157	0.00637	0.00798	0.01368	171.18	101.80
MB97-19 pl area A mega	150	-0.00779	-0.00975	0.01391	174.15	-83.56
MB97-19 pl area A mega	151	0.00050	0.00063	0.01373	171.94	1296.58
MB97-19 pl area A mega	152	0.00648	0.00812	0.01364	170.69	99.79
MB97-19 pl area A mega	153	0.00157	0.00197	0.01382	172.91	414.49
MB97-19 pl area B matrix	163	-0.00089	-0.00111	0.01391	173.48	-737.75
MB97-19 pl area B matrix	164	-0.00274	-0.00343	0.01373	171.91	-235.28
MB97-19 pl area B matrix	165	0.00082	0.00102	0.01371	171.62	791.39
MB97-19 pl area B matrix	166	-0.01525	-0.01909	0.01406	176.00	-42.80
MB97-19 pl area B mega	159	0.01583	0.00313	0.01361	173.52	41.18
MB97-19 pl area B mega	158	0.00250	0.01981	0.01386	170.30	261.80
MB97-19 pl area B mega	160	0.00238	0.00297	0.01389	173.88	276.27
MB97-19 pl area B mega	161	-0.00082	-0.00103	0.01377	172.91	-788.61
MB97-19 pl area B mega	162	-0.00497	-0.00622	0.01383	173.02	-130.47
MB97-19 pl area B multi	796	0.01794	0.02246	0.01342	168.01	35.94
MB97-19 pl area B multi	797	-0.00043	-0.00054	0.01378	172.99	-1493.90
MB97-19 pl area B multi	798	-0.00181	-0.00227	0.01382	173.31	-358.94
MB97-37 pl area A matrix	725	-0.00555	-0.00695	0.01384	173.25	-116.80
MB97-37 pl area A matrix	726	-0.00718	-0.00899	0.01395	174.70	-90.98
MB97-37 pl area A matrix	727	0.00707	0.00885	0.01366	171.00	91.71
MB97-37 pl area A mega	705	-0.00229	-0.00286	0.01378	172.12	-283.40
MB97-37 pl area A mega	706	0.00024	0.00030	0.01379	172.67	2686.05
MB97-37 pl area A mega	707	0.00275	0.00344	0.01387	173.59	238.24
MB97-37 pl area B matrix	703	0.00655	0.00820	0.01363	170.61	98.72
MB97-37 pl area B matrix	704	-0.00547	-0.00685	0.01388	173.75	-118.92
MB97-37 pl area B mega	693	-0.00759	-0.00950	0.01376	172.23	-84.84
MB97-37 pl area B mega	694	0.00417	0.00522	0.01357	169.92	154.27
MB97-37 pl area B mega	695	-0.00332	-0.00415	0.01392	174.01	-197.26
MB97-37 pl area B mega	696	0.00229	0.00286	0.01391	174.10	287.26
MB97-37 pl area B mega	697	0.00959	0.01200	0.01380	172.69	68.49
MB97-38 pl area A matrix	200	-0.00303	-0.00379	0.01393	174.20	-216.29
MB97-38 pl area A matrix	201	0.00051	0.00064	0.01398	175.17	1292.56

MB97-38 pl area A matrix	202	0.00014	0.00018	0.01386	173.92	4621.38
MB97-38 pl area A mega rim-core	196	0.00050	0.00062	0.01376	172.07	1311.45
MB97-38 pl area A mega rim-core	197	-0.01598	-0.02001	0.01410	176.51	-40.92
MB97-38 pl area A mega rim-core	198	0.00514	0.00643	0.01364	170.73	125.82
MB97-38 pl area A mega rim-core	199	0.00944	0.01182	0.01369	171.37	69.00
MB97-38 pl area B matrix	209	-0.00393	-0.00492	0.01399	175.10	-167.23
MB97-38 pl area B matrix	210	0.00360	0.00451	0.01362	170.51	178.93
MB97-38 pl area B matrix	211	-0.01017	-0.01273	0.01397	174.83	-64.11
MB97-38 pl area B mega	203	0.00519	0.00650	0.01387	173.70	126.64
MB97-38 pl area B mega	204	-0.00659	-0.00824	0.01392	174.07	-98.99
MB97-38 pl area B mega	205	0.00352	0.00441	0.01376	172.18	184.67
MB97-38 pl area B mega	206	-0.00613	-0.00767	0.01384	173.17	-105.84
MB97-38 pl area B mega	207	-0.00063	-0.00079	0.01371	171.86	-1021.10
MB97-38 pl area B mega	208	-0.00530	-0.00664	0.01385	173.55	-122.50
MB97-39 pl area A matrix	670	0.00202	0.00252	0.01389	173.91	325.39
MB97-39 pl area A matrix	671	-0.00043	-0.00053	0.01380	170.11	-1528.60
MB97-39 pl area A matrix	672	0.00492	0.00615	0.01356	169.78	130.76
MB97-39 pl area A matrix	673	-0.00882	-0.01104	0.01384	173.27	-73.31
MB97-39 pl area B matrix	680	-0.00780	-0.00976	0.01385	173.28	-83.06
MB97-39 pl area B matrix	681	0.00149	0.00186	0.01379	172.68	437.69
MB97-39 pl area B matrix	682	0.00644	0.00806	0.01362	170.50	100.35
MB97-39 pl area B matrix	683	-0.00125	-0.00157	0.01390	174.57	-522.91
MB97-39 pl area B mega	640	-0.00674	-0.00844	0.01388	173.81	-96.38
MB97-39 pl area B mega	641	-0.00283	-0.00354	0.01375	172.00	-228.65
MB97-39 pl area B mega	642	-0.00682	-0.00853	0.01389	173.75	-95.40
MB97-39 pl area B mega	643	-0.01032	-0.01292	0.01394	174.51	-63.00
MB97-39 pl area B mega	644	0.00670	0.00838	0.01382	172.95	97.91
MB97-39 pl area B mega	645	-0.00364	-0.00455	0.01395	174.38	-180.20
MB97-39 pl area B mega	646	-0.00035	-0.00044	0.01376	172.98	-1837.30
MB97-51 pl area A matrix	375	0.00374	0.00468	0.01351	169.07	171.02
MB97-51 pl area A matrix	376	-0.00758	-0.00949	0.01377	172.36	-84.92
MB97-51 pl area A matrix	377	-0.00514	-0.00644	0.01383	173.27	-126.11
MB97-51 pl area A matrix	378	-0.00054	-0.00067	0.01384	171.74	-1215.90
MB97-51 pl area A mega	371	0.00012	0.00015	0.01396	175.37	5433.39
MB97-51 pl area A mega	372	0.00452	0.00566	0.01386	173.45	145.07
MB97-51 pl area A mega	373	-0.00390	-0.00488	0.01407	176.03	-169.51
MB97-51 pl area A mega	374	0.00171	0.00214	0.01385	173.42	383.08
MB97-51 pl area B matrix	354	0.01361	0.00730	0.01359	173.62	47.72
MB97-51 pl area B matrix	353	0.00584	0.01704	0.01387	170.05	112.72
MB97-51 pl area B matrix	355	0.00574	0.00719	0.01378	172.49	113.77
MB97-51 pl area B matrix	356	0.00105	0.00131	0.01371	171.75	618.48

MB97-51 pl area B mega	367	-0.00340	-0.00426	0.01385	173.51	-191.11
MB97-51 pl area B mega	368	-0.00308	-0.00385	0.01394	174.20	-212.72
MB97-51 pl area B mega	369	0.00441	0.00552	0.01381	172.85	148.18
MB97-51 pl area B mega	370	-0.00649	-0.00812	0.01404	175.65	-101.37
MB97-74A pl area A	115	0.00312	0.00390	0.01367	171.17	207.42
MB97-74A pl area A	116	0.00911	0.01141	0.01366	170.98	71.33
MB97-74A pl area A	117	-0.01678	-0.02101	0.01402	175.55	-38.73
MB97-74A pl area A core matrix	134	-0.01678	-0.02101	0.01402	175.55	-38.73
MB97-74A pl area A core matrix	135	-0.01423	-0.01781	0.01404	175.68	-45.85
MB97-74A pl area A core matrix	136	0.00990	0.01240	0.01366	170.97	65.67
MB97-74A pl area A core matrix	137	-0.00542	-0.00678	0.01389	173.79	-120.24
MB97-74A pl area A rim 5um matrix	138	0.00426	0.00533	0.01362	170.51	151.45
MB97-74A pl area A rim 5um matrix	139	0.00085	0.00106	0.01364	170.74	757.51
MB97-74A pl area A rim 5um matrix	140	-0.00042	-0.00053	0.01365	172.26	-1513.50
MB97-74A pl area A rim 5um matrix	141	-0.00490	-0.00613	0.01375	172.07	-131.63
MB97-74A pl area B matrix 5um	146	-0.01471	-0.01841	0.01371	171.63	-43.29
MB97-74A pl area B matrix 5um	147	-0.00285	-0.00356	0.01386	173.17	-228.85
MB97-74A pl area B matrix 5um	148	0.00950	0.01189	0.01375	172.15	68.94
MB97-74A pl area B matrix 5um	149	-0.00510	-0.00639	0.01377	172.48	-126.46
MB97-74A pl area B mega	142	-0.00206	-0.00257	0.01382	172.41	-316.22
MB97-74A pl area B mega	143	-0.00992	-0.01242	0.01405	175.91	-66.09
MB97-74A pl area B mega	144	-0.00363	-0.00454	0.01376	172.06	-177.98
MB97-74A pl area B mega	145	0.00204	0.00255	0.01360	170.17	315.01
MB97-75 pl area A matrix	171	-0.00330	-0.00413	0.01369	171.36	-194.99
MB97-75 pl area A matrix	172	0.00429	0.00537	0.01362	170.45	150.30
MB97-75 pl area A matrix	173	0.01255	0.01571	0.01346	168.52	51.25
MB97-75 pl area A mega	167	0.00386	0.00483	0.01371	171.58	168.03
MB97-75 pl area A mega	168	-0.00112	-0.00140	0.01386	173.24	-584.77
MB97-75 pl area A mega	169	-0.00635	-0.00795	0.01378	172.53	-101.60
MB97-75 pl area A mega	170	-0.00939	-0.01176	0.01379	172.67	-68.54
MB97-75 pl area B matrix	182	0.00130	0.00163	0.01390	173.90	503.14
MB97-75 pl area B matrix	183	-0.00016	-0.00020	0.01382	172.71	-4023.00
MB97-75 pl area B matrix	184	0.00393	0.00492	0.01354	169.51	162.96
MB97-75 pl area B mega	174	-0.00280	-0.00351	0.01383	173.34	-231.76
MB97-75 pl area B mega	175	-0.00279	-0.00349	0.01383	172.96	-233.04
MB97-75 pl area B mega	176	0.01065	0.01334	0.01370	171.45	61.27
MB97-75 pl area B mega	177	0.00438	0.00548	0.01357	169.84	146.66
MB97-75 pl area B mega	178	-0.00552	-0.00691	0.01376	172.27	-116.86
MB97-75 pl area B mega	179	0.00085	0.00107	0.01370	171.54	757.17
MB97-75 pl area B mega	180	0.00333	0.00417	0.01376	172.27	195.42
MB97-75 pl area B mega	181	-0.00941	-0.01178	0.01389	173.86	-68.88

MB97-76A pl area A matrix	265	0.00079	0.00099	0.01376	172.12	819.44
MB97-76A pl area A matrix	266	-0.00421	-0.00527	0.01358	170.03	-151.44
MB97-76A pl area A matrix	267	-0.00004	-0.00004	0.01387	138.69	-18427.00
MB97-76A pl area A matrix	268	0.00455	0.00570	0.01346	168.44	140.07
MB97-76A pl area A mega rim-core	259	0.01704	0.00804	0.01343	172.58	37.82
MB97-76A pl area A mega rim-core	255	0.00643	0.00126	0.01379	172.67	101.79
MB97-76A pl area A mega rim-core	256	0.00101	0.00597	0.01380	170.46	644.71
MB97-76A pl area A mega rim-core	257	0.00477	-0.01160	0.01362	176.39	135.34
MB97-76A pl area A mega rim-core	258	-0.00927	0.02133	0.01410	168.06	-71.05
MB97-76A pl area A mega rim-core	260	-0.00294	-0.00369	0.01368	171.66	-218.34
MB97-76A pl area A mega rim-core	261	-0.00513	-0.00642	0.01378	172.40	-126.05
MB97-76A pl area A mega rim-core	262	-0.00663	-0.00830	0.01397	174.88	-98.63
MB97-76A pl area A mega rim-core	263	-0.00741	-0.00927	0.01397	174.82	-88.27
MB97-76A pl area A mega rim-core	264	0.00107	0.00133	0.01387	173.59	614.53
MB97-76A pl area A mega zoning points	397	0.04495	0.01231	0.01364	170.78	14.96
MB97-76A pl area A mega zoning points	387	0.00983	-0.00549	0.01364	175.98	66.08
MB97-76A pl area A mega zoning points	388	-0.00438	-0.00153	0.01404	173.48	-150.35
MB97-76A pl area A mega zoning points	389	-0.00122	-0.00109	0.01383	174.44	-532.21
MB97-76A pl area A mega zoning points	390	-0.00087	-0.01893	0.01392	177.32	-749.71
MB97-76A pl area A mega zoning points	391	-0.01512	-0.00206	0.01416	175.31	-43.51
MB97-76A pl area A mega zoning points	392	-0.00164	0.00444	0.01396	173.32	-399.70
MB97-76A pl area A mega zoning points	393	0.00355	0.00599	0.01385	174.69	184.61
MB97-76A pl area A mega zoning points	394	0.00478	0.00382	0.01396	174.82	138.22
MB97-76A pl area A mega zoning points	395	0.00305	0.00230	0.01397	171.13	216.60
MB97-76A pl area A mega zoning points	396	0.00184	0.05627	0.01367	170.76	350.87
MB97-76A pl area A mega zoning points	398	-0.01799	-0.02252	0.01396	174.71	-35.91
MB97-76A pl area A mega zoning points	399	-0.00428	-0.00535	0.01379	172.33	-151.30
MB97-76A pl area A mega zoning points	400	-0.00453	-0.00568	0.01401	175.72	-145.04
MB97-76A pl area A mega zoning points	401	-0.01060	-0.01327	0.01402	175.54	-61.68
MB97-76A pl area A mega zoning points	402	-0.00691	-0.00865	0.01384	173.21	-93.68
MB97-76A pl area A mega zoning points	403	-0.00932	-0.01167	0.01399	175.15	-70.09
MB97-76A pl area A mega zoning points	404	0.00688	0.00861	0.01358	169.93	93.66
MB97-76A pl area A mega zoning points	405	0.00189	0.00237	0.01384	173.30	346.03
MB97-76A pl area A mega zoning points	406	-0.01033	-0.01293	0.01411	176.60	-63.73
MB97-76A pl area A mega zoning points	408	-0.00742	-0.00929	0.01381	172.87	-87.07
MB97-76A pl area A mega zoning points	409	-0.00003	-0.00004	0.01359	181.17	-21027.00
MB97-76A pl area A mega zoning points	410	0.00263	0.00329	0.01390	173.96	250.02
MB97-76A pl area A mega zoning points	411	-0.00222	-0.00278	0.01378	172.51	-291.30
MB97-76A pl area A mega zoning points	412	-0.00548	-0.00686	0.01385	173.32	-118.42
MB97-76A pl area A mega zoning points	413	-0.00604	-0.00756	0.01392	174.26	-108.03
MB97-76A pl area A mega zoning points	414	-0.00676	-0.00846	0.01393	174.33	-96.46

MB97-76A pl area A mega zoning points	415	-0.00928	-0.01162	0.01391	174.15	-69.97
MB97-76A pl area B matrix	282	-0.00538	-0.00673	0.01394	174.43	-121.57
MB97-76A pl area B matrix	283	-0.01300	-0.01627	0.01396	174.71	-49.99
MB97-76A pl area B matrix	284	0.01075	0.01346	0.01345	168.35	59.66
MB97-76A pl area B matrix	285	-0.00646	-0.00809	0.01388	173.85	-100.61
MB97-76A pl area B mega	278	0.00083	0.00104	0.01369	171.32	780.60
MB97-76A pl area B mega	279	-0.00099	-0.00123	0.01385	172.01	-661.67
MB97-76A pl area B mega	280	-0.01207	-0.01511	0.01392	174.28	-53.73
MB97-76A pl area B mega	281	-0.01133	-0.01418	0.01386	173.46	-57.00
MB97-76A pl area B mega zoning points	416	0.00465	0.00582	0.01381	172.88	140.68
MB97-76A pl area B mega zoning points	417	0.00691	0.00865	0.01379	172.62	94.75
MB97-76A pl area B mega zoning points	418	0.00114	0.00143	0.01377	172.45	571.14
MB97-76A pl area B mega zoning points	419	0.00406	0.00508	0.01365	170.84	159.08
MB97-76A pl area B mega zoning points	420	-0.01234	-0.01545	0.01392	174.24	-52.50
MB97-76A pl area B mega zoning points	421	0.00157	0.00197	0.01377	172.32	413.24
MB97-76A pl area B mega zoning points	422	0.00161	0.00202	0.01368	171.26	400.47
MB97-76A pl area B mega zoning points	423	0.01016	0.01272	0.01356	169.69	63.55
MB97-76A pl area B mega zoning points	424	0.01013	0.01267	0.01365	170.85	64.22
MB97-76A pl area B mega zoning points	425	-0.00294	-0.00368	0.01399	175.05	-223.80
MB97-76A pl area B mega zoning points	426	-0.00257	-0.00322	0.01391	174.33	-254.71
MB97-76A pl area B mega zoning points	427	-0.01145	-0.01434	0.01391	174.22	-56.60
MB97-76A pl area B mega zoning points	428	0.00184	0.00230	0.01378	172.52	353.81
MB97-76A pl area B mega zoning points	429	-0.01209	-0.01513	0.01406	175.94	-54.17
MB97-76A pl area B mega zoning points	430	0.00388	0.00486	0.01384	173.26	168.74
MB97-76A pl area B mega zoning points	431	0.00482	0.00604	0.01378	172.52	135.38
MB97-76A pl area B mega zoning points	432	0.00211	0.00265	0.01380	172.71	308.45
MB97-76A pl area B mega zoning points	433	0.00948	0.01187	0.01371	171.63	68.83
MB97-76A pl area B mega zoning points	434	0.00485	0.00607	0.01360	170.24	132.97
MB97-76A pl area B mega zoning points	435	0.00716	0.00896	0.01372	171.77	91.04
MB97-76A pl area B mega zoning points	436	-0.00252	-0.00315	0.01394	174.24	-260.61
MB97-76A pl area B mega zoning points	437	0.00141	0.00176	0.01391	174.07	466.85
MB97-76A pl area B mega zoning points	438	0.00740	0.00927	0.01368	171.26	87.81
MB97-76A pl area B mega zoning points	439	-0.00029	-0.00037	0.01377	175.71	-2208.30
MB97-76A pl area B mega zoning points	440	-0.00290	-0.00363	0.01386	173.45	-224.85
MB97-76A pl area B mega zoning points	441	-0.00133	-0.00167	0.01391	174.70	-491.53
MB97-76A pl area B mega zoning points	442	-0.00099	-0.00124	0.01386	173.54	-656.68
MB97-76A pl area B mega zoning points	443	0.00612	0.00766	0.01378	172.55	106.84
MB97-76A pl area B mega zoning points	444	0.00127	0.00159	0.01392	174.27	516.20
MB97-76A pl area B mega zoning points	445	-0.01052	-0.01316	0.01403	175.52	-62.24
MB97-76B pl area A matrix	781	0.01528	0.00521	0.01371	172.85	42.95
MB97-76B pl area A matrix	779	0.00416	0.01913	0.01381	171.56	157.21

MB97-76B pl area B	737	-0.00747	-0.00936	0.01397	174.98	-87.44
MB97-76C pl area A	319	0.00647	0.00810	0.01380	172.76	101.25
MB97-76C pl area A	320	-0.00812	-0.01017	0.01388	173.83	-79.91
MB97-76C pl area A	321	0.00377	0.00472	0.01374	172.02	172.37
MB97-76C pl area A	322	0.00337	0.00422	0.01366	171.05	191.85
MB97-76C pl area B	304	0.01172	0.01467	0.01363	170.65	55.50
MB97-76C pl area B	305	0.00563	0.00704	0.01363	170.57	114.83
MB97-76C pl area B	306	-0.00474	-0.00593	0.01391	174.01	-137.67
MB97-76C pl area B	307	-0.00667	-0.00835	0.01406	176.06	-98.76
MB97-76C pl area B transect	453	-0.00142	-0.00178	0.01382	173.17	-458.08
MB97-76C pl area B transect	454	0.00964	0.01207	0.01355	169.63	66.91
MB97-76C pl area B transect	455	-0.01244	-0.01557	0.01380	172.67	-51.62
MB97-76C pl area B transect	456	-0.00767	-0.00960	0.01387	173.61	-84.57
MB97-76C pl area B transect	457	0.01112	0.01392	0.01373	171.92	58.90
MB97-76C pl area B transect	458	-0.00375	-0.00469	0.01389	173.73	-174.12
MB97-76C pl area B transect	459	-0.00369	-0.00461	0.01367	170.77	-174.18
MB97-76C pl area B transect	460	0.00267	0.00334	0.01388	173.70	246.07
MB97-76C pl area B transect	461	0.00300	0.00376	0.01365	170.96	215.26
MB97-76C pl area B transect	462	-0.01028	-0.01287	0.01402	175.52	-63.65

Olivine

Oxide concentrations

Table 15: Olivine chemical data (oxide concentrations)

Sample	Line	wt% SiO2	wt% TiO2	wt% Al2O3	wt% Cr2O3	wt% FeO	wt% MnO	wt% MgO	wt% CaO	Cu (ppm)	Total
MB97-15 area A	333	36.93	0.03	0.02	0.00	33.20	0.51	29.37	0.34	BDL	100.41
MB97-15 area A	335	36.48	0.03	0.02	0.00	33.46	0.52	29.23	0.31	BDL	100.04
MB97-15 area A	332	36.71	0.03	0.03	0.00	33.47	0.53	29.13	0.32	BDL	100.21
MB97-15 area A	331	35.96	0.06	0.01	-0.01	36.80	0.62	25.81	0.36	69.92	99.63
MB97-15 area B	346	37.13	0.03	0.08	0.00	30.53	0.43	30.01	0.37	67.29	98.58
MB97-15 area B	348	36.88	0.03	0.03	0.00	31.85	0.49	30.87	0.32	BDL	100.47
MB97-15 area B	347	33.42	0.26	0.08	-0.01	45.54	0.73	18.87	0.36	429.74	99.31
MB97-15 area B rim-core 1	479	36.69	0.03	0.03	0.00	31.91	0.50	30.59	0.33	BDL	100.07
MB97-15 area B rim-core 1	478	36.90	0.03	0.03	0.00	32.85	0.52	29.88	0.35	BDL	100.57
MB97-15 area B rim-core 1	477	36.37	0.04	0.03	0.00	35.18	0.57	27.83	0.35	BDL	100.36
MB97-15 area B rim-core 1	476	35.58	0.04	0.02	-0.01	38.13	0.66	25.34	0.30	BDL	100.05
MB97-15 area B rim-core 1	475	34.84	0.07	0.00	-0.01	42.42	0.77	21.44	0.27	108.87	99.81
MB97-15 area B rim-core 2	484	36.34	0.03	0.02	0.00	31.69	0.50	30.61	0.32	80.22	99.53

MB97-15 area B rim-core 2	483	36.28	0.04	0.02	0.00	33.66	0.54	29.10	0.33	BDL	99.98
MB97-15 area B rim-core 2	482	35.35	0.08	0.02	-0.01	38.70	0.64	24.83	0.34	BDL	99.95
MB97-15 area B rim-core 2	481	34.30	0.27	0.01	-0.01	43.78	0.77	20.54	0.32	83.68	100.00
MB97-15 area B rim-core 2	480	34.32	0.30	0.01	-0.01	44.21	0.76	20.29	0.33	BDL	100.21
MB97-19 2 area B rim-core	247	37.20	0.05	0.02	0.00	32.25	0.50	30.13	0.34	BDL	100.50
MB97-19 2 area B rim-core	246	37.19	0.04	0.02	0.00	32.34	0.51	30.15	0.35	BDL	100.60
MB97-19 2 area B rim-core	245	36.71	0.06	0.02	0.00	34.31	0.54	28.55	0.35	96.20	100.54
MB97-19 2 area B rim-core	244	36.20	0.08	0.02	-0.01	38.21	0.67	25.12	0.33	BDL	100.60
MB97-19 area B rim-core	243	36.57	0.06	0.01	-0.01	35.40	0.56	27.61	0.34	BDL	100.54
MB97-19 area B rim-core	242	36.57	0.06	0.01	-0.01	35.54	0.54	27.44	0.36	BDL	100.51
MB97-19 area B rim-core	241	36.13	0.07	0.01	-0.01	36.88	0.62	26.24	0.33	BDL	100.29
MB97-19 area B rim-core	240	35.56	0.10	0.02	-0.01	39.93	0.68	23.73	0.24	BDL	100.24
MB97-37 area A	709	36.34	0.04	0.02	0.00	34.38	0.48	28.65	0.29	BDL	100.20
MB97-37 area A	708	35.96	0.05	0.01	0.00	36.11	0.53	26.79	0.37	BDL	99.82
MB97-37 area A	713	35.83	0.07	0.02	0.00	37.07	0.53	26.38	0.28	BDL	100.18
MB97-37 area A	712	35.41	0.06	0.01	0.00	38.90	0.56	24.80	0.28	88.64	100.04
MB97-37 area B	701	37.20	0.03	0.02	0.00	30.18	0.38	32.09	0.25	BDL	100.16
MB97-37 area B	699	36.57	0.04	0.02	0.00	33.82	0.45	29.01	0.27	BDL	100.19
MB97-37 area B	700	36.00	0.04	0.02	-0.01	36.97	0.51	26.43	0.29	BDL	100.24
MB97-37 area B	702	35.13	0.05	0.01	-0.01	41.66	0.64	22.46	0.32	BDL	100.26
MB97-37 area B	698	35.10	0.06	0.01	-0.01	41.55	0.64	22.09	0.33	BDL	99.76
MB97-38 area A rim-core	225	37.17	0.05	0.03	0.00	31.98	0.39	30.72	0.26	BDL	100.61
MB97-38 area A rim-core	224	34.60	0.07	0.01	-0.01	45.60	0.70	19.17	0.33	BDL	100.48
MB97-38 area B	213	37.99	0.04	0.02	0.00	27.44	0.34	34.31	0.25	BDL	100.38
MB97-38 area B	216	37.96	0.04	0.03	0.01	29.03	0.38	33.16	0.27	BDL	100.88
MB97-38 area B	215	34.20	0.10	0.02	-0.01	46.92	0.72	17.96	0.38	BDL	100.30
MB97-38 area B rim-core	220	36.73	0.05	0.03	0.01	32.07	0.43	30.54	0.27	BDL	100.12
MB97-38 area B rim-core	219	36.94	0.06	0.04	0.01	32.43	0.42	30.25	0.28	BDL	100.40
MB97-38 area B rim-core	218	36.35	0.07	0.07	0.00	35.57	0.48	27.40	0.29	75.10	100.25
MB97-38 area B rim-core	217	35.16	0.10	0.03	0.00	42.57	0.61	21.76	0.31	BDL	100.55
MB97-39 area A	663	38.56	0.03	0.05	0.00	23.55	0.34	37.43	0.22	BDL	100.18
MB97-39 area A	659	37.56	0.06	0.02	0.00	29.60	0.49	32.27	0.29	BDL	100.28
MB97-39 area A	664	37.25	0.04	0.04	0.00	29.89	0.47	32.11	0.26	BDL	100.07
MB97-39 area A	662	37.07	0.04	0.03	0.00	30.02	0.49	31.82	0.31	BDL	99.78
MB97-39 area A	660	37.16	0.04	0.04	0.00	30.20	0.49	31.96	0.29	BDL	100.18
MB97-39 area A	661	36.87	0.05	0.02	0.00	31.63	0.51	30.76	0.34	BDL	100.18
MB97-39 area B	676	37.76	0.02	0.04	0.01	26.52	0.40	35.37	0.22	BDL	100.35

MB97-39 area B	675	37.25	0.03	0.04	0.00	30.17	0.48	32.36	0.24	BDL	100.57
MB97-39 area B	674	37.24	0.03	0.03	0.00	31.09	0.49	31.35	0.26	63.68	100.51
MB97-51 area A	385	36.42	0.04	0.03	-0.01	34.16	0.54	28.70	0.26	BDL	100.12
MB97-51 area A	386	35.75	0.05	0.03	-0.01	36.57	0.57	26.47	0.25	BDL	99.69
MB97-51 area B	359	35.40	0.07	0.03	-0.01	37.97	0.64	25.29	0.29	BDL	99.68
MB97-51 area B	357	35.39	0.19	0.02	-0.01	39.54	0.62	23.94	0.24	BDL	99.92
MB97-51 area B	358	35.09	0.09	0.02	-0.01	40.18	0.69	23.68	0.28	BDL	100.02
MB97-51 area B	360	35.33	0.07	0.02	-0.01	40.43	0.67	23.60	0.26	BDL	100.37
MB97-74A area A	120	35.93	0.08	0.02	-0.01	35.64	0.61	26.98	0.37	176.43	99.64
MB97-74A area A	125	35.85	0.08	0.03	-0.01	36.46	0.60	26.44	0.37	135.38	99.82
MB97-74A area A	119	34.72	0.08	0.02	-0.01	40.74	0.74	22.75	0.36	154.10	99.41
MB97-74A area A	118	34.30	0.12	0.01	-0.01	44.23	0.99	18.66	0.41	241.14	98.74
MB97-74A area A	124	34.20	0.20	0.01	-0.01	46.51	1.03	17.96	0.42	BDL	100.33
MB97-74A area A rim-core	129	36.73	0.06	0.03	-0.01	31.60	0.50	30.55	0.32	BDL	99.78
MB97-74A area A rim-core	128	36.59	0.07	0.03	-0.01	33.79	0.55	28.84	0.33	93.79	100.19
MB97-74A area A rim-core	127	35.35	0.07	0.02	-0.01	40.68	0.77	22.91	0.37	BDL	100.17
MB97-74A area A rim-core	126	34.90	0.10	0.01	-0.01	44.39	0.93	19.30	0.44	75.95	100.07
MB97-75 area B rim-core	239	36.96	0.04	0.03	-0.01	33.02	0.52	29.62	0.29	BDL	100.47
MB97-75 area B rim-core	238	36.94	0.04	0.03	-0.01	33.07	0.55	29.53	0.29	BDL	100.46
MB97-75 area B rim-core	237	36.86	0.05	0.05	-0.01	34.60	0.59	28.21	0.32	BDL	100.68
MB97-75 area B rim-core	236	35.31	0.07	0.02	-0.01	41.66	0.85	22.01	0.33	BDL	100.23
MB97-75 area B rim-core	235	35.24	0.06	0.01	-0.01	42.97	0.89	20.87	0.35	BDL	100.38
MB97-75 area C	231	35.57	0.13	0.02	-0.01	40.86	1.13	22.53	0.29	BDL	100.51
MB97-75 area C	232	34.59	0.11	0.01	-0.01	44.10	0.91	19.85	0.30	75.07	99.88
MB97-75 area C	233	34.66	0.19	0.01	-0.01	45.75	1.06	18.63	0.36	BDL	100.64
MB97-75 area C	234	34.00	0.15	0.01	-0.01	48.55	1.16	16.29	0.32	BDL	100.48
MB97-76A area A	273	37.00	0.04	0.03	-0.01	27.59	0.41	33.36	0.27	78.07	98.70
MB97-76A area A	271	36.52	0.06	0.03	-0.01	33.20	0.57	29.27	0.32	92.29	99.98
MB97-76A area A	269	36.41	0.05	0.03	-0.01	33.69	0.62	28.73	0.34	73.51	99.87
MB97-76A area A	270	36.08	0.08	0.03	-0.01	34.77	0.61	28.16	0.38	BDL	100.10
MB97-76A area A	272	35.88	0.12	0.02	-0.01	36.18	0.67	26.87	0.37	BDL	100.09
MB97-76A area B	290	36.66	0.06	0.04	-0.01	33.24	0.56	29.59	0.27	BDL	100.39
MB97-76A area B	291	34.46	0.08	0.01	-0.01	44.17	0.93	19.91	0.39	BDL	99.93
MB97-76A area B rim-core	289	36.37	0.05	0.03	-0.01	33.76	0.57	28.74	0.29	BDL	99.80
MB97-76A area B rim-core	288	36.25	0.06	0.03	-0.01	35.00	0.64	27.64	0.32	BDL	99.93
MB97-76A area B rim-core	287	35.41	0.14	0.02	-0.01	38.82	0.76	24.54	0.34	BDL	100.01

MB97-76C area A	308	37.31	0.04	0.03	-0.01	28.77	0.43	33.11	0.28	BDL	99.96
MB97-76C area A	310	37.17	0.04	0.02	-0.01	30.54	0.51	31.85	0.24	BDL	100.37
MB97-76C area A	309	35.79	0.05	0.02	-0.01	37.45	0.65	26.18	0.29	BDL	100.42
MB97-76C area A	312	35.24	0.09	0.00	-0.01	41.59	0.91	21.85	0.31	64.00	99.99
MB97-76C area A	311	35.49	0.06	0.01	-0.01	44.67	0.71	17.24	0.21	BDL	98.37
MB97-76C area A rim-core	250	36.45	0.04	0.02	-0.01	31.78	0.53	30.73	0.23	BDL	99.76
MB97-76C area A rim-core	315	36.98	0.03	0.03	-0.01	31.87	0.53	30.79	0.22	BDL	100.45
MB97-76C area A rim-core	314	36.60	0.04	0.02	-0.01	33.73	0.57	29.20	0.25	58.39	100.40
MB97-76C area A rim-core	249	36.04	0.04	0.02	-0.01	33.68	0.57	29.11	0.25	BDL	99.69
MB97-76C area A rim-core	313	36.33	0.06	0.02	-0.01	35.99	0.64	27.26	0.29	BDL	100.59
MB97-76C area A rim-core	248	35.92	0.06	0.01	-0.01	35.91	0.63	27.15	0.28	BDL	99.95
MB97-76C area A rim-core 2	326	37.18	0.04	0.02	-0.01	30.36	0.52	31.90	0.24	122.39	100.25
MB97-76C area A rim-core 2	254	36.69	0.04	0.01	-0.01	30.43	0.50	31.90	0.24	108.62	99.81
MB97-76C area A rim-core 2	325	36.97	0.04	0.02	-0.01	30.67	0.51	31.64	0.24	BDL	100.09
MB97-76C area A rim-core 2	253	36.89	0.04	0.01	-0.01	30.73	0.51	31.64	0.24	BDL	100.05
MB97-76C area A rim-core 2	252	36.33	0.04	0.01	-0.01	32.58	0.55	29.92	0.26	BDL	99.66
MB97-76C area A rim-core 2	324	36.85	0.04	0.01	-0.01	32.63	0.55	29.93	0.25	BDL	100.25
MB97-76C area A rim-core 2	323	35.86	0.05	0.02	-0.01	37.29	0.67	25.61	0.26	78.66	99.74
MB97-76C area A rim-core 2	251	35.67	0.04	0.02	-0.01	37.59	0.66	25.77	0.25	BDL	100.02
MB97-76C area A zoning rim-core	452	36.75	0.04	0.01	-0.01	30.35	0.52	31.88	0.24	BDL	99.79
MB97-76C area A zoning rim-core	451	36.41	0.04	0.02	-0.01	33.01	0.56	29.71	0.25	BDL	99.98
MB97-76C area A zoning rim-core	450	36.09	0.04	0.01	-0.01	35.19	0.61	27.89	0.26	BDL	100.08
MB97-76C area A zoning rim-core	449	35.76	0.03	0.02	-0.01	37.99	0.67	25.56	0.27	59.93	100.31
MB97-76C area A zoning rim-core	448	35.40	0.05	0.02	-0.01	39.31	0.67	24.41	0.28	67.87	100.14
MB97-76C area A zoning rim-core	447	34.99	0.06	0.01	-0.01	42.32	0.82	20.71	0.28	85.99	99.19
MB97-76C area A zoning rim-core	446	35.43	0.06	0.01	-0.01	43.86	0.71	17.19	0.20	75.28	97.46
MB97-76C area B	303	36.60	0.05	0.03	-0.01	31.40	0.49	31.10	0.28	83.28	99.95
MB97-76C area B	301	36.09	0.05	0.02	-0.01	36.32	0.64	27.01	0.31	BDL	100.43
MB97-76C area B	300	34.88	0.07	0.01	-0.01	43.25	0.78	21.10	0.27	BDL	100.35

Formula weights and minerals

Table 16: Olivine formula weights and mineral determination

SAMPLE	LINE	Fe FORMULA	Mn FORMULA	Mg FORMULA	Fo	Fa	Tp	Mineral
MB97-15 area A	333	0.76	0.01	1.20	60.82	38.58	0.60	Forsterite
MB97-15 area A	335	0.77	0.01	1.20	60.52	38.87	0.61	Forsterite
MB97-15 area A	332	0.77	0.01	1.20	60.43	38.94	0.62	Forsterite
MB97-15 area A	331	0.87	0.01	1.09	55.14	44.11	0.75	Forsterite
MB97-15 area B	346	0.71	0.01	1.24	63.34	36.14	0.52	Forsterite
MB97-15 area B	348	0.72	0.01	1.25	62.98	36.45	0.57	Forsterite
MB97-15 area B	347	1.13	0.02	0.84	42.10	56.98	0.92	Fayalite
MB97-15 area B rim-core 1	479	0.73	0.01	1.25	62.72	36.70	0.58	Forsterite
MB97-15 area B rim-core 1	478	0.75	0.01	1.22	61.47	37.92	0.61	Forsterite
MB97-15 area B rim-core 1	477	0.82	0.01	1.15	58.11	41.21	0.68	Forsterite
MB97-15 area B rim-core 1	476	0.90	0.02	1.07	53.80	45.40	0.79	Forsterite
MB97-15 area B rim-core 1	475	1.03	0.02	0.93	46.94	52.10	0.96	Fayalite
MB97-15 area B rim-core 2	484	0.73	0.01	1.25	62.89	36.52	0.58	Forsterite
MB97-15 area B rim-core 2	483	0.78	0.01	1.20	60.27	39.10	0.64	Forsterite
MB97-15 area B rim-core 2	482	0.92	0.02	1.05	52.94	46.28	0.77	Forsterite
MB97-15 area B rim-core 2	481	1.07	0.02	0.89	45.11	53.93	0.96	Fayalite
MB97-15 area B rim-core 2	480	1.08	0.02	0.88	44.57	54.48	0.95	Fayalite
MB97-19 2 area B rim-core	247	0.74	0.01	1.23	62.12	37.30	0.58	Forsterite
MB97-19 2 area B rim-core	246	0.74	0.01	1.23	62.06	37.34	0.60	Forsterite
MB97-19 2 area B rim-core	245	0.79	0.01	1.17	59.35	40.01	0.64	Forsterite
MB97-19 2 area B rim-core	244	0.90	0.02	1.05	53.52	45.67	0.81	Forsterite
MB97-19 area B rim-core	243	0.82	0.01	1.14	57.77	41.56	0.67	Forsterite
MB97-19 area B rim-core	242	0.82	0.01	1.14	57.55	41.81	0.64	Forsterite
MB97-19 area B rim-core	241	0.86	0.01	1.10	55.49	43.76	0.75	Forsterite
MB97-19 area B rim-core	240	0.95	0.02	1.01	51.02	48.16	0.83	Forsterite
MB97-37 area A	709	0.79	0.01	1.18	59.43	40.01	0.57	Forsterite
MB97-37 area A	708	0.85	0.01	1.12	56.57	42.79	0.64	Forsterite
MB97-37 area A	713	0.87	0.01	1.10	55.56	43.80	0.64	Forsterite
MB97-37 area A	712	0.92	0.01	1.05	52.84	46.48	0.68	Forsterite
MB97-37 area B	701	0.68	0.01	1.29	65.18	34.38	0.44	Forsterite
MB97-37 area B	699	0.78	0.01	1.19	60.14	39.33	0.53	Forsterite

MB97-37 area B	700	0.87	0.01	1.10	55.69	43.70	0.61	Forsterite
MB97-37 area B	702	1.00	0.02	0.96	48.62	50.60	0.78	Fayalite
MB97-37 area B	698	1.01	0.02	0.95	48.27	50.93	0.79	Fayalite
MB97-38 area A rim-core	225	0.73	0.01	1.24	62.85	36.70	0.45	Forsterite
MB97-38 area A rim-core	224	1.12	0.02	0.84	42.46	56.66	0.88	Fayalite
MB97-38 area B	213	0.61	0.01	1.36	68.76	30.85	0.39	Forsterite
MB97-38 area B	216	0.65	0.01	1.32	66.78	32.79	0.43	Forsterite
MB97-38 area B	215	1.16	0.02	0.79	40.19	58.90	0.92	Fayalite
MB97-38 area B rim-core	220	0.73	0.01	1.24	62.61	36.89	0.50	Forsterite
MB97-38 area B rim-core	219	0.74	0.01	1.23	62.13	37.37	0.50	Forsterite
MB97-38 area B rim-core	218	0.83	0.01	1.14	57.53	41.90	0.57	Forsterite
MB97-38 area B rim-core	217	1.03	0.01	0.93	47.31	51.93	0.76	Fayalite
MB97-39 area A	663	0.52	0.01	1.46	73.63	25.99	0.38	Forsterite
MB97-39 area A	659	0.67	0.01	1.30	65.65	33.77	0.57	Forsterite
MB97-39 area A	664	0.68	0.01	1.30	65.33	34.13	0.55	Forsterite
MB97-39 area A	662	0.68	0.01	1.29	65.02	34.41	0.57	Forsterite
MB97-39 area A	660	0.68	0.01	1.29	64.98	34.45	0.57	Forsterite
MB97-39 area A	661	0.72	0.01	1.25	63.05	36.36	0.59	Forsterite
MB97-39 area B	676	0.59	0.01	1.40	70.07	29.48	0.45	Forsterite
MB97-39 area B	675	0.68	0.01	1.30	65.30	34.15	0.55	Forsterite
MB97-39 area B	674	0.70	0.01	1.27	63.89	35.54	0.57	Forsterite
MB97-51 area A	385	0.79	0.01	1.18	59.58	39.78	0.63	Forsterite
MB97-51 area A	386	0.86	0.01	1.11	55.95	43.36	0.69	Forsterite
MB97-51 area B	359	0.90	0.02	1.07	53.86	45.36	0.78	Forsterite
MB97-51 area B	357	0.94	0.01	1.02	51.52	47.72	0.76	Forsterite
MB97-51 area B	358	0.96	0.02	1.01	50.80	48.36	0.84	Forsterite
MB97-51 area B	360	0.96	0.02	1.00	50.57	48.61	0.82	Forsterite
MB97-74A area A	120	0.84	0.01	1.13	57.02	42.25	0.73	Forsterite
MB97-74A area A	125	0.86	0.01	1.11	55.97	43.30	0.73	Forsterite
MB97-74A area A	119	0.98	0.02	0.98	49.43	49.65	0.91	Fayalite
MB97-74A area A	118	1.10	0.03	0.83	42.37	56.34	1.28	Fayalite
MB97-74A area A	124	1.15	0.03	0.79	40.24	58.45	1.31	Fayalite
MB97-74A area A rim-core	129	0.72	0.01	1.25	62.91	36.50	0.58	Forsterite
MB97-74A area A rim-core	128	0.78	0.01	1.19	59.95	39.40	0.65	Forsterite
MB97-74A area A rim-core	127	0.98	0.02	0.98	49.62	49.43	0.95	Forsterite

MB97-74A area A rim-core	126	1.09	0.02	0.85	43.16	55.67	1.18	Fayalite
MB97-75 area B rim-core	239	0.76	0.01	1.21	61.15	38.24	0.61	Forsterite
MB97-75 area B rim-core	238	0.76	0.01	1.21	61.02	38.33	0.65	Forsterite
MB97-75 area B rim-core	237	0.80	0.01	1.16	58.82	40.48	0.70	Forsterite
MB97-75 area B rim-core	236	1.00	0.02	0.95	47.99	50.96	1.05	Fayalite
MB97-75 area B rim-core	235	1.04	0.02	0.90	45.89	53.00	1.11	Fayalite
MB97-75 area C	231	0.98	0.03	0.96	48.88	49.73	1.39	Fayalite
MB97-75 area C	232	1.08	0.02	0.87	44.01	54.84	1.15	Fayalite
MB97-75 area C	233	1.12	0.03	0.82	41.50	57.16	1.34	Fayalite
MB97-75 area C	234	1.21	0.03	0.73	36.86	61.65	1.49	Fayalite
MB97-76A area A	273	0.63	0.01	1.35	67.98	31.54	0.48	Forsterite
MB97-76A area A	271	0.77	0.01	1.20	60.71	38.62	0.67	Forsterite
MB97-76A area A	269	0.78	0.01	1.19	59.88	39.39	0.73	Forsterite
MB97-76A area A	270	0.81	0.01	1.16	58.65	40.62	0.72	Forsterite
MB97-76A area A	272	0.85	0.02	1.12	56.51	42.69	0.80	Forsterite
MB97-76A area B	290	0.76	0.01	1.21	60.94	38.41	0.65	Forsterite
MB97-76A area B	291	1.08	0.02	0.87	44.03	54.81	1.17	Fayalite
MB97-76A area B rim-core	289	0.78	0.01	1.19	59.87	39.45	0.68	Forsterite
MB97-76A area B rim-core	288	0.82	0.02	1.15	58.02	41.21	0.76	Forsterite
MB97-76A area B rim-core	287	0.92	0.02	1.04	52.49	46.59	0.92	Forsterite
MB97-76C area A	308	0.65	0.01	1.33	66.90	32.61	0.49	Forsterite
MB97-76C area A	310	0.69	0.01	1.28	64.64	34.77	0.59	Forsterite
MB97-76C area A	309	0.88	0.02	1.09	55.04	44.18	0.78	Forsterite
MB97-76C area A	312	1.01	0.02	0.94	47.82	51.05	1.13	Fayalite
MB97-76C area A	311	1.13	0.02	0.78	40.38	58.68	0.94	Fayalite
MB97-76C area A rim-core	250	0.73	0.01	1.25	62.90	36.49	0.62	Forsterite
MB97-76C area A rim-core	315	0.73	0.01	1.25	62.88	36.51	0.61	Forsterite
MB97-76C area A rim-core	314	0.78	0.01	1.20	60.27	39.06	0.67	Forsterite
MB97-76C area A rim-core	249	0.78	0.01	1.20	60.23	39.10	0.67	Forsterite
MB97-76C area A rim-core	313	0.84	0.02	1.13	57.01	42.22	0.76	Forsterite
MB97-76C area A rim-core	248	0.84	0.02	1.13	56.97	42.27	0.76	Forsterite
MB97-76C area A rim-core 2	326	0.69	0.01	1.29	64.81	34.60	0.60	Forsterite
MB97-76C area A rim-core 2	254	0.69	0.01	1.29	64.77	34.65	0.57	Forsterite
MB97-76C area A rim-core 2	325	0.70	0.01	1.28	64.39	35.02	0.59	Forsterite
MB97-76C area A rim-core 2	253	0.70	0.01	1.28	64.35	35.06	0.59	Forsterite
MB97-76C area A rim-core 2	252	0.75	0.01	1.23	61.68	37.68	0.64	Forsterite

MB97-76C area A rim-core 2	324	0.75	0.01	1.22	61.65	37.70	0.64	Forsterite
MB97-76C area A rim-core 2	323	0.88	0.02	1.08	54.59	44.60	0.81	Forsterite
MB97-76C area A rim-core 2	251	0.89	0.02	1.08	54.56	44.64	0.80	Forsterite
MB97-76C area A zoning rim-core	452	0.69	0.01	1.29	64.80	34.61	0.60	Forsterite
MB97-76C area A zoning rim-core	451	0.76	0.01	1.22	61.20	38.15	0.65	Forsterite
MB97-76C area A zoning rim-core	450	0.82	0.01	1.16	58.13	41.15	0.72	Forsterite
MB97-76C area A zoning rim-core	449	0.89	0.02	1.07	54.10	45.10	0.81	Forsterite
MB97-76C area A zoning rim-core	448	0.93	0.02	1.03	52.11	47.08	0.81	Forsterite
MB97-76C area A zoning rim-core	447	1.04	0.02	0.91	46.11	52.85	1.04	Fayalite
MB97-76C area A zoning rim-core	446	1.12	0.02	0.78	40.73	58.31	0.96	Fayalite
MB97-76C area B	303	0.72	0.01	1.26	63.47	35.96	0.57	Forsterite
MB97-76C area B	301	0.85	0.02	1.12	56.57	42.67	0.76	Forsterite
MB97-76C area B	300	1.05	0.02	0.91	46.07	52.97	0.96	Fayalite

Cu constraints

Table 17: Olivine Cu constraints

SAMPLE	LINE	Cu WT%	CuO	Cu CDL99	Calc Cu ppm DL	Cu %ERR
MB97-15 area A	333	0.000687	0.00086	0.008651	108.29	593.66
MB97-15 area A	335	-0.00996	-0.01247	0.008722	109.20	-40.93
MB97-15 area A	332	0.000856	0.001071	0.008682	108.63	478.72
MB97-15 area A	331	0.005586	0.006992	0.008729	109.26	74.00
MB97-15 area B	346	0.005376	0.006729	0.008548	106.99	75.31
MB97-15 area B	348	-0.00244	-0.00305	0.008633	107.91	-166.69
MB97-15 area B	347	0.03433	0.042974	0.009057	113.37	12.75
MB97-15 area B rim-core 1	479	-0.00214	-0.00268	0.008685	108.77	-191.14
MB97-15 area B rim-core 1	478	0.001745	0.002185	0.00864	108.19	233.69
MB97-15 area B rim-core 1	477	0.004257	0.005328	0.008724	109.19	96.96
MB97-15 area B rim-core 1	476	-0.00448	-0.0056	0.008829	110.36	-92.64
MB97-15 area B rim-core 1	475	0.008697	0.010887	0.008919	111.65	48.67
MB97-15 area B rim-core 2	484	0.006409	0.008022	0.008599	107.63	63.59
MB97-15 area B rim-core 2	483	0.001954	0.002446	0.008665	108.47	209.40
MB97-15 area B rim-core 2	482	-0.00444	-0.00556	0.008891	111.34	-94.05
MB97-15 area B rim-core 2	481	0.006685	0.008368	0.009014	112.83	63.89
MB97-15 area B rim-core 2	480	-0.0018	-0.00225	0.009005	112.56	-235.68
MB97-19 2 area B rim-core	247	-0.00151	-0.00189	0.008662	108.42	-270.12
MB97-19 2 area B rim-core	246	-0.00132	-0.00165	0.008663	108.29	-309.61
MB97-19 2 area B rim-core	245	0.007685	0.00962	0.008689	108.77	53.64

MB97-19 2 area B rim-core	244	-0.00299	-0.00375	0.008901	111.63	-139.92
MB97-19 area B rim-core	243	0.000354	0.000444	0.008765	109.93	1165.92
MB97-19 area B rim-core	242	-0.00347	-0.00434	0.008799	110.05	-119.26
MB97-19 area B rim-core	241	0.003876	0.004852	0.008811	110.30	107.49
MB97-19 area B rim-core	240	-0.00442	-0.00554	0.008891	111.44	-94.44
MB97-37 area A	709	-0.00266	-0.00333	0.008739	109.40	-154.64
MB97-37 area A	708	-0.00158	-0.00198	0.008741	109.54	-260.38
MB97-37 area A	713	0.003323	0.004159	0.008803	110.18	125.23
MB97-37 area A	712	0.007081	0.008864	0.008836	110.61	59.16
MB97-37 area B	701	-0.00036	-0.00046	0.008598	109.86	-1110.90
MB97-37 area B	699	0.003929	0.004918	0.008672	108.55	104.39
MB97-37 area B	700	-0.01148	-0.01437	0.008856	110.85	-36.04
MB97-37 area B	702	0.003556	0.004452	0.008943	111.96	118.87
MB97-37 area B	698	-0.00403	-0.00505	0.009015	112.97	-105.03
MB97-38 area A rim-core	225	0.002602	0.003258	0.008594	107.61	156.01
MB97-38 area A rim-core	224	0.003608	0.004517	0.009012	112.82	118.06
MB97-38 area B	213	-0.00236	-0.00295	0.008557	106.96	-170.77
MB97-38 area B	216	0.002369	0.002966	0.00855	107.05	170.49
MB97-38 area B	215	0.003315	0.00415	0.009055	113.36	129.09
MB97-38 area B rim-core	220	-0.0059	-0.00739	0.008683	108.76	-69.01
MB97-38 area B rim-core	219	-0.00972	-0.01216	0.008708	108.94	-41.90
MB97-38 area B rim-core	218	0.006	0.00751	0.008717	109.11	68.83
MB97-38 area B rim-core	217	0.003749	0.004693	0.008914	111.59	112.42
MB97-39 area A	663	-0.00018	-0.00022	0.008347	102.02	-2209.10
MB97-39 area A	659	-0.00441	-0.00552	0.008554	107.07	-91.03
MB97-39 area A	664	0.004372	0.005473	0.008526	106.73	92.26
MB97-39 area A	662	0.00194	0.002428	0.008584	107.43	208.94
MB97-39 area A	660	-0.00159	-0.00199	0.008619	107.87	-255.34
MB97-39 area A	661	-0.00317	-0.00397	0.008603	107.74	-127.44
MB97-39 area B	676	-0.00164	-0.00206	0.008513	106.93	-243.62
MB97-39 area B	675	-0.00404	-0.00506	0.008641	108.23	-100.44
MB97-39 area B	674	0.005087	0.006368	0.008648	108.26	80.48
MB97-51 area A	385	-0.00721	-0.00903	0.008795	110.15	-57.14
MB97-51 area A	386	0.000393	0.000492	0.008781	109.93	1053.67
MB97-51 area B	359	0.000381	0.000476	0.008879	110.93	1100.03
MB97-51 area B	357	-0.00707	-0.00885	0.008952	112.06	-59.36
MB97-51 area B	358	-0.00225	-0.00282	0.008984	112.60	-187.84
MB97-51 area B	360	0.001466	0.001835	0.008927	111.74	287.33
MB97-74A area A	120	0.014094	0.017643	0.015023	188.06	50.83
MB97-74A area A	125	0.010815	0.013538	0.008694	108.83	38.23
MB97-74A area A	119	0.012311	0.01541	0.015275	191.20	59.07

MB97-74A area A	118	0.019263	0.024114	0.015412	192.93	38.28
MB97-74A area A	124	0.000722	0.000904	0.009077	113.65	593.03
MB97-74A area A rim-core	129	-0.00093	-0.00116	0.008596	107.22	-437.38
MB97-74A area A rim-core	128	0.007493	0.009379	0.008687	108.74	54.99
MB97-74A area A rim-core	127	-0.00201	-0.00252	0.008943	112.12	-209.23
MB97-74A area A rim-core	126	0.006067	0.007595	0.009026	112.99	70.45
MB97-75 area B rim-core	239	0.00005	0.000063	0.008674	109.29	8153.63
MB97-75 area B rim-core	238	0.002767	0.003464	0.008639	108.15	147.53
MB97-75 area B rim-core	237	0.004306	0.005391	0.008712	109.07	95.70
MB97-75 area B rim-core	236	0.000321	0.000402	0.008946	112.03	1314.04
MB97-75 area B rim-core	235	0.001236	0.001547	0.008997	112.61	343.49
MB97-75 area C	231	-0.00418	-0.00523	0.008897	111.32	-100.11
MB97-75 area C	232	0.005997	0.007507	0.008943	111.95	70.62
MB97-75 area C	233	-0.00308	-0.00385	0.009101	113.76	-139.05
MB97-75 area C	234	0.003499	0.00438	0.009118	114.14	123.16
MB97-76A area A	273	0.006236	0.007807	0.008433	105.57	64.09
MB97-76A area A	271	0.007372	0.009229	0.008649	108.28	55.64
MB97-76A area A	269	0.005872	0.007351	0.008664	108.46	69.89
MB97-76A area A	270	-0.00407	-0.0051	0.008756	109.72	-101.02
MB97-76A area A	272	-0.00039	-0.00049	0.008749	109.92	-1048.50
MB97-76A area B	290	0.002512	0.003144	0.008729	109.25	164.18
MB97-76A area B	291	-0.00851	-0.01065	0.009071	113.52	-49.94
MB97-76A area B rim-core	289	0.001542	0.001931	0.008752	109.60	267.84
MB97-76A area B rim-core	288	0.000519	0.000649	0.008732	109.19	794.15
MB97-76A area B rim-core	287	0.003752	0.004697	0.008876	111.12	111.85
MB97-76C area A	308	0.000736	0.000922	0.008586	107.56	549.98
MB97-76C area A	310	0.003122	0.003908	0.008569	107.26	129.74
MB97-76C area A	309	-0.0002	-0.00025	0.008787	109.84	-2060.90
MB97-76C area A	312	0.005113	0.0064	0.008916	111.60	82.53
MB97-76C area A	311	0.003402	0.004258	0.008966	112.22	124.57
MB97-76C area A rim-core	250	-0.00256	-0.00321	0.008706	109.17	-159.92
MB97-76C area A rim-core	315	0.000212	0.000266	0.008672	108.81	1926.08
MB97-76C area A rim-core	314	0.004664	0.005839	0.008628	108.02	87.54
MB97-76C area A rim-core	249	-0.00157	-0.00196	0.008711	108.75	-261.91
MB97-76C area A rim-core	313	0.003304	0.004136	0.008694	108.83	124.37
MB97-76C area A rim-core	248	-0.00587	-0.00735	0.008829	110.55	-70.59
MB97-76C area A rim-core 2	326	0.009778	0.012239	0.008535	106.83	41.49
MB97-76C area A rim-core 2	254	0.008677	0.010862	0.008516	106.60	46.61
MB97-76C area A rim-core 2	325	-0.00029	-0.00036	0.008561	106.27	-1400.70
MB97-76C area A rim-core 2	253	0.00175	0.002191	0.008618	107.90	232.50
MB97-76C area A rim-core 2	252	-0.00117	-0.00146	0.008665	108.13	-349.23

MB97-76C area A rim-core 2	324	-0.00154	-0.00193	0.008707	109.12	-266.09
MB97-76C area A rim-core 2	323	0.006284	0.007866	0.008763	109.69	66.07
MB97-76C area A rim-core 2	251	0.002164	0.002708	0.008752	109.52	191.02
MB97-76C area A zoning rim-core	452	0.001239	0.001551	0.008643	108.19	329.18
MB97-76C area A zoning rim-core	451	0.001571	0.001967	0.008691	108.82	261.04
MB97-76C area A zoning rim-core	450	-0.00367	-0.00459	0.008753	109.47	-112.10
MB97-76C area A zoning rim-core	449	0.004788	0.005993	0.008854	110.82	87.51
MB97-76C area A zoning rim-core	448	0.005422	0.006787	0.008844	110.70	77.22
MB97-76C area A zoning rim-core	447	0.006869	0.008599	0.008928	111.77	61.59
MB97-76C area A zoning rim-core	446	0.006014	0.007528	0.008911	111.54	70.18
MB97-76C area B	303	0.006653	0.008328	0.008552	107.05	60.94
MB97-76C area B	301	0.003867	0.004841	0.008762	109.69	107.14
MB97-76C area B	300	0.003679	0.004606	0.008916	111.63	114.56

Pyroxene

Oxide concentrations

Table 18: Pyroxene chemical data (oxide concentrations)

Sample	Line	wt% SiO2	wt% TiO2	wt% Al2O3	wt% Cr2O3	wt% FeO	wt% MnO	wt% MgO	wt% CaO	wt% Na2O	wt% K2O	Cu (ppm)	Total
MB97-15 area A	337	49.51	1.71	2.40	0.00	12.49	0.31	12.90	18.96	0.46	0.00	86.63	98.75
MB97-15 area A	338	49.13	2.07	2.57	0.00	12.36	0.30	12.52	19.12	0.48	0.00	BDL	98.54
MB97-15 area A	339	49.74	1.82	2.42	0.00	11.51	0.28	12.75	19.75	0.44	0.00	BDL	98.71
MB97-15 area A	340	49.10	1.82	3.47	0.17	10.15	0.20	13.35	20.06	0.43	0.00	BDL	98.74
MB97-15 area B	349	49.04	2.00	3.29	0.02	11.12	0.24	13.30	19.38	0.47	0.00	BDL	98.86
MB97-15 area B	350	49.12	1.80	3.18	0.07	10.61	0.22	13.36	19.92	0.43	0.00	BDL	98.70
MB97-15 area B	351	48.98	1.86	3.24	0.06	10.45	0.21	13.20	20.08	0.44	0.00	BDL	98.52
MB97-15 area B	352	49.28	1.93	2.40	0.00	12.52	0.32	12.66	19.20	0.47	0.00	BDL	98.77
MB97-19 area B	193	50.27	1.88	2.98	0.32	10.32	0.25	14.66	18.12	0.35	0.00	149.30	99.17
MB97-19 area B	194	36.42	0.04	0.02	0.00	31.55	0.46	30.89	0.26	0.01	0.00	BDL	99.65
MB97-19 area B	195	36.85	0.03	0.03	0.01	27.91	0.37	34.00	0.24	0.01	0.00	BDL	99.45
MB97-19 area B multi	793	49.98	1.68	2.17	0.09	10.09	0.23	14.68	18.94	0.34	0.00	BDL	98.19
MB97-19 area B multi	794	49.53	1.90	2.91	0.31	10.36	0.26	14.70	18.12	0.35	0.00	BDL	98.42
MB97-19 area B multi	795	49.80	1.69	2.58	0.27	9.85	0.23	14.67	18.83	0.33	0.00	BDL	98.25
MB97-37 area A	717	49.90	1.32	1.94	0.00	12.61	0.27	13.06	18.76	0.36	0.00	271.09	98.26
MB97-37 area A	715	34.28	0.05	0.02	-0.01	40.00	0.59	24.04	0.33	0.02	0.00	107.79	99.32

MB97-37 area A	716	48.78	1.98	2.83	0.02	11.69	0.30	13.50	18.52	0.38	0.00	BDL	98.01
MB97-37 area A	718	34.13	0.06	0.01	-0.01	40.66	0.62	22.97	0.36	0.01	0.00	BDL	98.80
MB97-37 area A	719	33.57	0.06	0.01	-0.01	43.15	0.66	21.01	0.34	0.01	0.00	BDL	98.80
MB97-37 area B	691	33.97	0.06	0.01	-0.01	42.49	0.65	21.94	0.33	0.01	0.00	BDL	99.45
MB97-37 area B	692	33.68	0.06	0.01	-0.01	43.51	0.69	20.87	0.33	0.01	0.00	BDL	99.16
MB97-38 area A	228	47.95	2.74	3.38	0.05	13.01	0.25	11.46	19.37	0.46	0.00	141.50	98.69
MB97-38 area A	230	49.82	1.47	2.00	0.01	15.06	0.31	10.88	19.06	0.36	0.00	145.21	98.97
MB97-38 area A	229	49.46	1.89	2.44	0.03	14.11	0.30	11.47	18.86	0.37	0.00	BDL	98.92
MB97-38 area B	222	48.71	2.53	3.41	0.03	11.97	0.24	12.05	19.76	0.38	0.00	203.24	99.09
MB97-38 area B	221	49.55	1.83	2.61	0.03	12.46	0.25	12.14	19.65	0.36	0.00	117.46	98.88
MB97-38 area B	223	49.36	1.81	2.49	0.01	13.65	0.27	11.31	19.50	0.36	0.00	BDL	98.77
MB97-39 area A	666	48.56	1.90	3.56	0.04	11.62	0.27	13.58	18.54	0.40	0.00	158.93	98.50
MB97-39 area A	667	51.31	0.94	1.34	0.00	12.45	0.37	16.11	16.08	0.24	0.00	159.80	98.86
MB97-39 area A	665	50.66	1.14	1.88	0.03	11.19	0.30	14.71	18.35	0.31	0.00	BDL	98.58
MB97-39 area A	668	50.70	1.05	1.48	0.01	11.93	0.33	14.94	17.56	0.29	0.00	BDL	98.30
MB97-39 area A	669	49.24	1.78	2.63	0.00	13.00	0.36	13.80	17.15	0.38	0.01	BDL	98.35
MB97-39 area B	677	49.49	1.53	2.92	0.05	10.66	0.25	13.95	19.26	0.36	0.00	BDL	98.48
MB97-39 area B	678	48.81	1.95	2.97	0.02	11.35	0.26	13.43	19.15	0.38	0.00	BDL	98.31
MB97-39 area B	679	48.95	1.78	2.93	0.02	11.68	0.30	13.82	18.61	0.37	0.00	BDL	98.44
MB97-51 area A	380	50.77	1.14	1.86	0.02	9.99	0.23	14.93	19.37	0.35	0.01	180.19	98.68
MB97-51 area A	379	50.53	1.11	1.42	0.00	11.41	0.29	14.57	18.63	0.34	0.00	BDL	98.30
MB97-51 area A	381	49.84	1.36	2.57	0.06	9.80	0.21	14.71	19.61	0.36	0.00	BDL	98.53
MB97-51 area A	382	50.41	1.33	2.34	0.07	9.96	0.22	14.81	19.46	0.35	0.00	BDL	98.95
MB97-51 area B	361	47.98	2.22	4.13	0.32	10.58	0.22	13.56	19.12	0.42	0.01	84.32	98.56
MB97-51 area B	362	51.08	1.03	1.68	0.15	10.48	0.25	15.84	17.86	0.28	0.00	BDL	98.67
MB97-51 area B	363	50.49	1.37	2.25	0.04	10.06	0.23	14.52	19.82	0.38	0.01	BDL	99.15
MB97-51 area B	364	45.98	3.46	4.34	0.02	12.75	0.26	11.78	19.44	0.51	0.00	BDL	98.56
MB97-51 area B	365	49.71	1.40	2.69	0.06	9.73	0.21	14.50	19.69	0.37	0.00	BDL	98.37
MB97-51 area B	366	45.96	3.49	4.49	0.03	11.60	0.22	11.78	19.90	0.47	0.00	BDL	97.94
MB97-74A area A	131	48.56	2.35	2.69	-0.01	13.58	0.35	11.24	19.41	0.46	0.00	260.40	98.66
MB97-74A area A	132	48.02	2.68	2.09	-0.01	15.97	0.46	9.58	19.19	0.53	0.01	123.00	98.52
MB97-74A area A	121	48.27	2.50	2.89	0.00	12.90	0.31	11.21	20.03	0.46	0.00	BDL	98.57
MB97-74A area A	122	49.75	1.64	1.84	-0.01	13.02	0.35	12.10	19.54	0.37	0.01	BDL	98.61
MB97-74A area A	123	48.53	2.28	2.66	-0.01	13.00	0.32	11.31	19.96	0.44	0.00	BDL	98.50

MB97-74A area A	130	48.48	2.27	2.84	-0.01	13.32	0.33	11.44	19.51	0.46	0.00	BDL	98.64
MB97-74A area A	133	48.04	2.69	2.05	-0.01	15.90	0.44	9.19	19.67	0.55	0.01	BDL	98.53
MB97-75 area B	191	51.55	1.15	1.53	0.00	10.97	0.29	14.23	19.36	0.32	0.00	BDL	99.39
MB97-76A area A	274	49.37	1.74	2.83	0.00	10.59	0.26	13.32	20.09	0.41	0.00	126.16	98.62
MB97-76A area A	277	48.53	2.06	3.29	0.00	10.55	0.25	13.07	20.12	0.42	0.00	106.23	98.30
MB97-76A area A	275	50.66	1.26	1.73	0.00	10.44	0.28	14.30	19.70	0.32	0.00	BDL	98.67
MB97-76A area A	276	49.02	1.83	2.93	0.00	10.63	0.27	13.27	19.91	0.43	0.00	BDL	98.30
MB97-76A area B	292	47.83	2.43	3.83	0.00	11.15	0.25	12.73	19.69	0.47	0.00	BDL	98.37
MB97-76A area B	293	50.69	1.25	1.65	-0.01	10.64	0.30	14.24	19.53	0.32	0.00	BDL	98.63
MB97-76A area B	294	47.89	2.39	3.76	0.00	11.16	0.26	12.85	19.51	0.47	0.00	BDL	98.28
MB97-76A area B	295	49.82	1.71	2.33	0.00	11.88	0.32	12.71	19.78	0.43	0.00	BDL	98.99
MB97-76B area A	769	48.47	1.16	3.67	-0.01	7.66	0.55	14.39	21.69	0.82	0.03	BDL	98.45
MB97-76B area B	760	45.05	0.73	4.85	-0.01	11.96	1.01	11.63	22.00	0.47	0.01	128.91	97.71
MB97-76B area B	761	50.81	0.77	2.58	-0.01	6.28	0.56	15.97	21.27	0.61	0.03	BDL	98.87
MB97-76B area B	763	45.93	1.41	4.08	-0.02	10.48	0.77	12.29	21.59	0.87	0.03	BDL	97.44
MB97-76C area A	316	49.89	1.52	2.27	0.00	11.14	0.29	13.44	19.86	0.39	0.00	103.49	98.82
MB97-76C area A	317	49.79	1.60	2.40	0.00	11.01	0.29	13.39	19.84	0.39	0.00	BDL	98.70
MB97-76C area A	318	47.82	2.43	3.94	0.00	11.14	0.26	12.96	19.50	0.44	0.00	BDL	98.48
MB97-76C area B	297	49.73	1.56	2.48	0.00	10.98	0.28	13.61	19.38	0.39	0.00	140.81	98.44
MB97-76C area B	298	48.61	2.02	3.30	0.00	10.57	0.24	13.09	19.89	0.41	0.00	84.55	98.15
MB97-76C area B	299	49.43	1.70	2.69	0.00	10.69	0.25	13.31	20.00	0.40	0.00	67.99	98.48
MB97-76C area B	296	49.48	1.70	2.86	-0.01	10.70	0.26	13.29	19.91	0.39	0.00	BDL	98.59
MB97-76C orng area A	474	34.70	0.05	0.01	-0.02	36.59	0.67	26.25	0.27	0.01	0.00	190.61	98.55

Formula weights and minerals

Table 19: Pyroxene formula weights and mineral determination

SAMPLE	LINE	Fe FORMULA	Mg FORMULA	Ca FORMULA	Na FORMULA	Min
MB97-15 area A	337	0.398855	0.733989	0.7757	0.033765	Augite
MB97-15 area A	338	0.395971	0.715252	0.785041	0.036029	Augite
MB97-15 area A	339	0.367143	0.725034	0.807278	0.032825	Augite
MB97-15 area A	340	0.321705	0.754105	0.814284	0.031305	Augite
MB97-15 area B	349	0.352751	0.752064	0.787723	0.034403	Augite
MB97-15 area B	350	0.336573	0.755743	0.809867	0.031934	Augite
MB97-15 area B	351	0.332106	0.748341	0.817865	0.032636	Augite
MB97-15 area B	352	0.400279	0.721137	0.786311	0.035182	Augite

MB97-19 area B	193	0.324918	0.822835	0.730838	0.0256	Augite
MB97-19 area B	194	0.962999	1.6807	0.010275	0.000789	Enstatite
MB97-19 area B	195	0.837071	1.81792	0.009142	0.000872	Enstatite
MB97-19 area B multi	793	0.320582	0.831084	0.770509	0.024821	Augite
MB97-19 area B multi	794	0.328446	0.830601	0.736194	0.025703	Augite
MB97-19 area B multi	795	0.312529	0.829897	0.765374	0.024151	Augite
MB97-37 area A	717	0.404759	0.746958	0.771198	0.027123	Augite
MB97-37 area A	715	1.28049	1.37177	0.013337	0.001127	Enstatite
MB97-37 area A	716	0.374813	0.771176	0.760548	0.02853	Augite
MB97-37 area A	718	1.31614	1.32529	0.015011	0.000893	Augite
MB97-37 area A	719	1.41574	1.22889	0.014343	0.0009	Ferrosilite
MB97-37 area B	691	1.37745	1.26797	0.013598	0.000994	Ferrosilite
MB97-37 area B	692	1.42428	1.21786	0.013776	0.000822	Ferrosilite
MB97-38 area A	228	0.418944	0.657687	0.799054	0.03432	Augite
MB97-38 area A	230	0.486937	0.626719	0.789277	0.026845	Augite
MB97-38 area A	229	0.454593	0.65874	0.778208	0.027426	Augite
MB97-38 area B	222	0.38218	0.685794	0.80853	0.027995	Augite
MB97-38 area B	221	0.398807	0.692835	0.80585	0.026701	Augite
MB97-38 area B	223	0.439962	0.650141	0.805462	0.027096	Augite
MB97-39 area A	666	0.369999	0.770772	0.755991	0.02984	Augite
MB97-39 area A	667	0.392817	0.905753	0.64992	0.017679	Augite
MB97-39 area A	665	0.354504	0.831083	0.744972	0.022838	Augite
MB97-39 area A	668	0.379653	0.847418	0.715805	0.021073	Augite
MB97-39 area A	669	0.41593	0.786952	0.702867	0.028409	Augite
MB97-39 area B	677	0.338264	0.7894	0.783251	0.026676	Augite
MB97-39 area B	678	0.362337	0.764049	0.783428	0.028351	Augite
MB97-39 area B	679	0.372027	0.784423	0.759463	0.027205	Augite
MB97-51 area A	380	0.314889	0.83922	0.782692	0.025415	Augite
MB97-51 area A	379	0.362803	0.8263	0.759281	0.025251	Augite
MB97-51 area A	381	0.309332	0.82792	0.793054	0.026636	Augite
MB97-51 area A	382	0.313202	0.830406	0.784115	0.025741	Augite
MB97-51 area B	361	0.335903	0.767923	0.777792	0.030989	Augite
MB97-51 area B	362	0.330123	0.888851	0.720424	0.020488	Augite
MB97-51 area B	363	0.316243	0.813693	0.798015	0.027331	Augite
MB97-51 area B	364	0.410189	0.675587	0.801075	0.038128	Augite
MB97-51 area B	365	0.307805	0.817828	0.79819	0.026968	Augite
MB97-51 area B	366	0.374503	0.678385	0.823426	0.035155	Augite
MB97-74A area A	131	0.438369	0.646786	0.802886	0.034522	Augite
MB97-74A area A	132	0.523026	0.559354	0.805207	0.040284	Augite
MB97-74A area A	121	0.416306	0.64457	0.828153	0.034255	Augite
MB97-74A area A	122	0.418645	0.693831	0.805079	0.027513	Augite

MB97-74A area A	123	0.41961	0.650619	0.825473	0.033018	Augite
MB97-74A area A	130	0.429121	0.657294	0.805604	0.034164	Augite
MB97-74A area A	133	0.521336	0.537541	0.826524	0.041454	Augite
MB97-75 area B	191	0.345516	0.798912	0.781279	0.023126	Augite
MB97-76A area A	274	0.336395	0.754661	0.817871	0.030351	Augite
MB97-76A area A	277	0.33658	0.743439	0.822591	0.030772	Augite
MB97-76A area A	275	0.330533	0.806953	0.799101	0.023721	Augite
MB97-76A area A	276	0.339016	0.754413	0.813028	0.031699	Augite
MB97-76A area B	292	0.356323	0.725097	0.806015	0.034451	Augite
MB97-76A area B	293	0.337421	0.804902	0.793438	0.023609	Augite
MB97-76A area B	294	0.356825	0.732183	0.799044	0.034695	Augite
MB97-76A area B	295	0.378258	0.721278	0.807239	0.031701	Augite
MB97-76B area A	769	0.239701	0.802891	0.869753	0.059569	Diopside
MB97-76B area B	760	0.384613	0.666792	0.906657	0.03483	Diopside
MB97-76B area B	761	0.194686	0.882158	0.844273	0.043725	Augite
MB97-76B area B	763	0.335918	0.70188	0.886461	0.0644	Diopside
MB97-76C area A	316	0.353526	0.760756	0.807705	0.028952	Augite
MB97-76C area A	317	0.349815	0.758801	0.807841	0.028815	Augite
MB97-76C area A	318	0.355158	0.736703	0.796969	0.032302	Augite
MB97-76C area B	297	0.34971	0.772349	0.790616	0.028766	Augite
MB97-76C area B	298	0.337685	0.745786	0.814255	0.030249	Augite
MB97-76C area B	299	0.340262	0.755063	0.815547	0.029821	Augite
MB97-76C area B	296	0.340338	0.753351	0.811212	0.028985	Augite
MB97-76C orng area A	474	1.16169	1.48568	0.010906	0.000485	Enstatite

Cu constraints

Table 20: Pyroxene Cu constraints

SAMPLE	LINE	Cu WT%	CuO	Cu CDL99	Cu DL (ppm)	Cu %ERR
MB97-15 area A	337	0.00692	0.00866	0.01040	130.15	71.2479
MB97-15 area A	338	-0.00469	-0.00587	0.01046	130.87	-104.73
MB97-15 area A	339	-0.00137	-0.00171	0.01044	130.28	-360
MB97-15 area A	340	-0.00266	-0.00334	0.01033	129.68	-182.27
MB97-15 area B	349	-0.00081	-0.00101	0.01037	129.32	-604.84
MB97-15 area B	350	-0.00256	-0.00320	0.01039	129.86	-191.22
MB97-15 area B	351	0.00104	0.00131	0.01036	129.54	468.141
MB97-15 area B	352	-0.00144	-0.00180	0.01040	130.03	-339.83
MB97-19 area B	193	0.01193	0.01493	0.01434	179.46	57.2878
MB97-19 area B	194	-0.00331	-0.00414	0.01504	188.09	-213.7
MB97-19 area B	195	0.00376	0.00470	0.01472	184.22	185.317
MB97-19 area B multi	793	0.00063	0.00079	0.01460	182.65	1093.64

MB97-19 area B multi	794	-0.00994	-0.01245	0.01479	185.27	-69.527
MB97-19 area B multi	795	-0.00264	-0.00330	0.01446	180.69	-257.88
MB97-37 area A	717	0.02166	0.02711	0.01444	180.76	32.0504
MB97-37 area A	715	0.00861	0.01078	0.01531	191.62	84.3803
MB97-37 area A	716	0.00559	0.00700	0.01452	181.73	122.952
MB97-37 area A	718	-0.01057	-0.01323	0.01573	196.90	-69.625
MB97-37 area A	719	-0.00379	-0.00474	0.01577	197.17	-195.66
MB97-37 area B	691	0.00151	0.00189	0.01556	194.71	485.963
MB97-37 area B	692	-0.00114	-0.00143	0.01572	197.14	-649.24
MB97-38 area A	228	0.01130	0.01415	0.01458	182.45	61.3941
MB97-38 area A	230	0.01160	0.01452	0.01486	185.99	60.981
MB97-38 area A	229	-0.00294	-0.00368	0.01494	187.04	-238.76
MB97-38 area B	222	0.01624	0.02032	0.01468	183.71	43.2187
MB97-38 area B	221	0.00938	0.01175	0.01468	183.79	74.3718
MB97-38 area B	223	-0.00408	-0.00510	0.01486	185.74	-171.24
MB97-39 area A	666	0.01270	0.01589	0.01429	178.91	53.6849
MB97-39 area A	667	0.01277	0.01598	0.01426	178.45	53.265
MB97-39 area A	665	0.00369	0.00462	0.01451	181.65	185.843
MB97-39 area A	668	0.00286	0.00357	0.01454	181.95	240.583
MB97-39 area A	669	0.00018	0.00022	0.01457	182.53	3863.36
MB97-39 area B	677	0.00232	0.00290	0.01462	183.02	298.186
MB97-39 area B	678	-0.00375	-0.00470	0.01470	184.24	-184.07
MB97-39 area B	679	-0.00713	-0.00893	0.01474	184.57	-96.824
MB97-51 area A	380	0.01440	0.01802	0.01017	127.30	33.7438
MB97-51 area A	379	-0.00442	-0.00553	0.01037	129.73	-110.28
MB97-51 area A	381	-0.00469	-0.00587	0.01036	129.63	-103.67
MB97-51 area A	382	-0.00570	-0.00714	0.01042	130.51	-85.72
MB97-51 area B	361	0.00674	0.00843	0.01037	129.81	73.0037
MB97-51 area B	362	0.00461	0.00578	0.01033	129.36	106.02
MB97-51 area B	363	0.00083	0.00103	0.01028	128.66	587.026
MB97-51 area B	364	-0.00460	-0.00576	0.01057	132.30	-107.78
MB97-51 area B	365	0.00483	0.00605	0.01026	128.42	100.511
MB97-51 area B	366	0.00280	0.00351	0.01044	130.64	176.101
MB97-74A area A	131	0.02080	0.02604	0.01459	182.69	33.6818
MB97-74A area A	132	0.00983	0.01230	0.01502	188.02	72.6543
MB97-74A area A	121	0.00457	0.00572	0.01481	185.36	153.509
MB97-74A area A	122	-0.00393	-0.00493	0.01487	186.54	-177.55
MB97-74A area A	123	-0.00088	-0.00111	0.01474	185.91	-784.69
MB97-74A area A	130	-0.00111	-0.00139	0.01489	186.51	-631.3
MB97-74A area A	133	0.00279	0.00349	0.01503	188.10	254.863
MB97-75 area B	191	-0.00184	-0.00230	0.01469	183.63	-376.32

MB97-76A area A	274	0.01008	0.01262	0.01027	128.51	48.4522
MB97-76A area A	277	0.00849	0.01062	0.01029	128.84	57.6106
MB97-76A area A	275	-0.00247	-0.00309	0.01028	128.64	-196.06
MB97-76A area A	276	-0.00334	-0.00418	0.01046	130.94	-147.14
MB97-76A area B	292	0.00072	0.00090	0.01041	130.29	683.675
MB97-76A area B	293	0.00447	0.00560	0.01035	129.62	109.598
MB97-76A area B	294	0.00011	0.00014	0.01030	128.73	4352.55
MB97-76A area B	295	0.00516	0.00646	0.01037	129.80	95.1227
MB97-76B area A	769	0.01147	0.01435	0.01464	183.24	60.8033
MB97-76B area B	760	0.01030	0.01289	0.01476	184.70	68.1481
MB97-76B area B	761	0.00456	0.00570	0.01444	180.79	150.081
MB97-76B area B	763	0.00204	0.00256	0.01474	184.53	340.912
MB97-76C area A	316	0.00827	0.01035	0.01030	128.89	59.1439
MB97-76C area A	317	-0.00285	-0.00357	0.01040	130.27	-171.38
MB97-76C area A	318	-0.00427	-0.00534	0.01034	129.34	-113.78
MB97-76C area B	297	0.01125	0.01408	0.01026	128.43	43.4345
MB97-76C area B	298	0.00675	0.00846	0.01028	128.69	72.1823
MB97-76C area B	299	0.00543	0.00680	0.01032	129.17	89.9878
MB97-76C area B	296	-0.00301	-0.00376	0.01035	129.23	-161.81
MB97-76C orng area A	474	0.01523	0.01906	0.01513	189.36	47.4123

Ilmenite

Oxide concentrations

Table 21: Ilmenite chemical data (oxide concentrations)

Sample	Line	wt% SiO2	wt% TiO2	wt% Al2O3	wt% Cr2O3	wt% FeO	wt% MnO	wt% MgO	wt% CaO	wt% Na2O	wt% K2O	Cu (ppm)	Total
MB97-15	464	0.01	50.73	0.04	0.01	43.89	0.80	2.55	0.04	0.00	0.01	BDL	98.08
MB97-19 area A	820	0.01	49.70	0.08	0.04	44.98	0.49	2.19	0.06	0.00	0.01	BDL	97.58
MB97-19 area A	822	0.01	49.90	0.05	0.05	44.63	0.50	2.42	0.10	0.00	0.00	BDL	97.65
MB97-19 area A	823	0.00	49.08	0.07	0.04	45.94	0.50	1.92	0.02	0.00	0.00	BDL	97.57
MB97-19 area A	825	0.00	49.35	0.09	0.04	45.94	0.51	1.84	0.02	0.00	0.00	BDL	97.78
MB97-19 area B	811	0.04	49.66	0.05	0.08	45.21	0.52	2.10	0.10	0.00	0.01	BDL	97.76
MB97-19 area B	812	0.02	49.66	0.05	0.05	45.10	0.50	2.10	0.10	0.00	0.00	BDL	97.58
MB97-19 area B	813	0.00	49.15	0.10	0.05	46.51	0.54	1.77	0.02	0.00	0.01	BDL	98.13
MB97-19 area B multi	802	0.03	50.76	0.04	0.10	42.57	0.48	3.06	0.14	0.00	0.01	178.30	97.21
MB97-37 area A	720	0.01	49.06	0.08	0.03	45.73	0.47	2.10	0.07	0.00	0.00	BDL	97.54
MB97-37 area A	721	0.01	49.87	0.07	0.04	44.97	0.49	2.11	0.06	0.00	0.00	BDL	97.62

MB97-37 area A	722	0.01	49.21	0.06	0.03	45.55	0.51	2.30	0.07	0.00	0.00	BDL	97.72
MB97-37 area A	723	0.01	49.08	0.07	0.03	46.17	0.51	2.13	0.03	0.00	0.00	BDL	98.03
MB97-37 area A	724	0.01	49.69	0.05	0.03	44.93	0.56	2.55	0.04	0.00	0.00	BDL	97.86
MB97-37 area B	731	0.01	50.14	0.10	0.04	43.75	0.46	2.53	0.08	0.00	0.01	BDL	97.12
MB97-37 area B	733	0.01	49.16	0.07	0.03	45.85	0.51	2.32	0.07	0.00	0.00	BDL	98.01
MB97-37 area B	735	0.00	49.87	0.05	0.03	44.92	0.49	2.37	0.01	0.00	0.00	BDL	97.75
MB97-39 area A	686	0.05	48.06	0.07	0.09	46.02	0.74	1.90	0.11	0.00	0.03	BDL	97.05
MB97-39 area B	658	0.05	48.24	0.05	0.08	46.28	0.50	1.80	0.14	0.00	0.02	BDL	97.18
MB97-75 area D	593	0.00	53.07	0.14	0.06	40.19	1.01	2.67	0.03	0.00	0.00	BDL	97.16
MB97-76A area A	634	0.15	49.79	0.12	0.03	44.79	0.97	1.37	0.04	0.00	0.01	BDL	97.28
MB97-76A area A	637	0.00	51.02	0.05	0.21	42.47	1.14	3.50	0.00	0.00	0.00	BDL	98.39
MB97-76C area A	502	0.00	50.58	0.09	0.03	43.63	0.67	3.42	0.00	0.00	0.00	BDL	98.42
MB97-76C area A	504	-0.01	50.75	0.10	0.04	43.21	0.72	3.60	0.00	0.00	0.00	99.58	98.41
MB97-76C area A	507	0.03	49.40	0.07	0.05	43.60	0.79	3.75	0.06	0.00	0.02	BDL	97.76
MB97-76C area B	493	0.03	51.69	0.06	0.09	41.06	0.54	4.98	0.00	0.00	0.00	BDL	98.47
MB97-76C area B	496	0.00	50.96	0.11	0.04	42.44	0.55	4.33	0.00	0.00	0.00	BDL	98.44
MB97-76C area B	497	0.35	48.39	0.15	0.05	43.58	0.53	5.06	0.02	0.03	0.00	BDL	98.17
MB97-76C area B	498	0.03	51.29	0.08	0.02	41.84	0.54	4.74	0.00	0.00	0.00	BDL	98.54

Formula weights and minerals

Table 22: Ilmenite formula weights and mineral determination

SAMPLE	LINE	Ti FORMULA	Fe FORMULA	O FORMULA	Normalized Ti	Normalized Fe	O	multiplication factor
MB97-15 Ilm (Px setup)	464	2.88	2.77	8.88	3.89	3.74	12	1.35
MB97-19 area A	820	2.84	2.86	8.85	3.86	3.88	12	1.36
MB97-19 area A	822	2.85	2.83	8.85	3.86	3.84	12	1.36
MB97-19 area A	823	2.81	2.93	8.82	3.83	3.98	12	1.36
MB97-19 area A	825	2.82	2.92	8.83	3.84	3.97	12	1.36
MB97-19 area B	811	2.84	2.87	8.84	3.85	3.90	12	1.36
MB97-19 area B	812	2.84	2.87	8.85	3.86	3.89	12	1.36
MB97-19 area B	813	2.80	2.95	8.81	3.82	4.02	12	1.36
MB97-19 area B multi	802	2.90	2.70	8.90	3.90	3.64	12	1.35
MB97-37 area A	720	2.81	2.91	8.81	3.82	3.96	12	1.36
MB97-37 area A	721	2.85	2.86	8.86	3.87	3.88	12	1.35
MB97-37 area A	722	2.81	2.89	8.81	3.82	3.93	12	1.36
MB97-37 area A	723	2.79	2.92	8.80	3.81	3.99	12	1.36

MB97-37 area A	724	2.83	2.84	8.83	3.84	3.86	12	1.36
MB97-37 area B	731	2.87	2.79	8.88	3.88	3.77	12	1.35
MB97-37 area B	733	2.79	2.90	8.80	3.81	3.95	12	1.36
MB97-37 area B	735	2.84	2.85	8.85	3.86	3.86	12	1.36
MB97-39 area A	686	2.77	2.94	8.77	3.78	4.03	12	1.37
MB97-39 area B	658	2.77	2.96	8.78	3.79	4.04	12	1.37
MB97-75 area D	593	3.05	2.57	9.06	4.04	3.40	12	1.33
MB97-76A area A	634	2.87	2.88	8.89	3.88	3.88	12	1.35
MB97-76A area A	637	2.87	2.65	8.88	3.88	3.59	12	1.35
MB97-76C area A	502	2.84	2.73	8.85	3.85	3.70	12	1.36
MB97-76C area A	504	2.85	2.70	8.85	3.86	3.65	12	1.36
MB97-76C area A	507	2.78	2.73	8.79	3.80	3.73	12	1.37
MB97-76C area B	493	2.87	2.54	8.88	3.88	3.43	12	1.35
MB97-76C area B	496	2.84	2.63	8.85	3.85	3.57	12	1.36
MB97-76C area B	497	2.68	2.68	8.71	3.69	3.70	12	1.38
MB97-76C area B	498	2.85	2.58	8.86	3.86	3.50	12	1.36

Cu constraints

Table 23: Ilmenite Cu constraints

SAMPLE	LINE	Cu WT%	CuO	Cu CDL99	Cu DL (ppm)	Cu %ERR
MB97-15 Ilm (Px setup)	464	-0.00581	-0.00728	0.011776	147.55	-86.88
MB97-19 area A	820	0.003791	0.004746	0.011684	146.27	132.89
MB97-19 area A	822	-0.00168	-0.0021	0.011712	146.40	-300.32
MB97-19 area A	823	-0.01131	-0.01416	0.011799	147.72	-44.63
MB97-19 area A	825	0.004572	0.005723	0.011726	146.78	110.62
MB97-19 area B	811	-0.00476	-0.00596	0.011795	147.69	-106.41
MB97-19 area B	812	-0.00042	-0.00052	0.01177	145.72	-1208.30
MB97-19 area B	813	-0.00584	-0.00731	0.011788	147.55	-86.57
MB97-19 area B multi	802	0.014244	0.01783	0.011772	147.36	35.82
MB97-37 area A	720	-0.00192	-0.00241	0.011778	147.84	-263.52
MB97-37 area A	721	-0.00019	-0.00024	0.01167	147.41	-2654.90
MB97-37 area A	722	-0.01273	-0.01593	0.011811	147.80	-39.67
MB97-37 area A	723	-0.00071	-0.00088	0.011788	146.10	-719.03
MB97-37 area A	724	-0.00325	-0.00407	0.011745	147.08	-155.26
MB97-37 area B	731	-0.00674	-0.00844	0.011761	147.27	-74.83
MB97-37 area B	733	-0.00621	-0.00778	0.011738	147.06	-81.05
MB97-37 area B	735	-0.00008	-0.0001	0.011682	146.03	-6002.10
MB97-39 area A	686	-0.00224	-0.0028	0.011789	147.36	-226.58
MB97-39 area B	658	0.006383	0.00799	0.011683	146.24	79.03
MB97-75 area D	593	-0.00116	-0.00145	0.011603	145.04	-431.12

MB97-76A area A	634	-0.00014	-0.00017	0.011726	142.39	-3668.40
MB97-76A area A	637	-0.00057	-0.00072	0.01175	148.42	-882.24
MB97-76C area A	502	0.001079	0.00135	0.011715	146.57	467.60
MB97-76C area A	504	0.007955	0.009958	0.011567	144.79	62.84
MB97-76C area A	507	0.000892	0.001117	0.011652	145.91	562.22
MB97-76C area B	493	0.005925	0.007417	0.011529	144.32	84.00
MB97-76C area B	496	0.00448	0.005608	0.01164	145.71	112.06
MB97-76C area B	497	-0.00691	-0.00865	0.011466	143.53	-71.12
MB97-76C area B	498	-0.00053	-0.00066	0.01167	145.32	-953.01

Weathered Olivine

Oxide concentrations

Table 24: Weathered olivine chemical data (oxide concentrations)

Sample	Line	wt% SiO2	wt% TiO2	wt% Al2O3	wt% Cr2O3	wt% FeO	wt% MnO	wt% MgO	wt% CaO	wt% Na2O	wt% K2O	Cu (ppm)	Total
MB97-15 area A weather	469	35.30	0.03	0.03	0.00	32.67	0.51	29.90	0.32	0.01	0.00	BDL	98.76
MB97-19 area B	806	36.99	0.03	0.03	0.01	23.62	0.31	37.33	0.26	0.01	0.00	113.57	98.60
MB97-19 area B	807	37.06	0.02	0.04	0.01	24.06	0.31	36.99	0.27	0.02	0.00	159.88	98.79
MB97-19 area B	809	36.84	0.03	0.04	0.01	24.98	0.35	36.19	0.30	0.01	0.00	107.45	98.76
MB97-19 area B_multi	792	36.83	0.03	0.03	0.01	23.37	0.30	37.74	0.25	0.01	0.00	BDL	98.55
MB97-19 area B_multi	791	36.74	0.03	0.03	0.01	25.27	0.32	36.31	0.24	0.01	0.00	BDL	98.96
MB97-19 area B_multi	785	36.38	0.03	0.02	0.00	27.31	0.34	34.60	0.24	0.01	0.00	186.97	98.97
MB97-19 area B_multi	787	35.90	0.03	0.04	0.00	29.51	0.39	32.00	0.28	0.01	0.00	233.92	98.20
MB97-19 area B_multi	782	35.66	0.04	0.02	0.00	31.18	0.41	31.20	0.26	0.01	0.00	BDL	98.75
MB97-19 area B_multi	783	35.66	0.03	0.03	0.00	31.31	0.42	31.21	0.27	0.01	0.00	105.04	98.94
MB97-37 area A	729	35.60	0.05	0.02	0.00	33.08	0.47	29.82	0.29	0.02	0.00	147.35	99.35
MB97-37 area A	728	35.06	0.03	0.02	-0.01	35.04	0.48	28.15	0.28	0.01	0.00	151.06	99.09
MB97-37 area A	730	33.41	0.07	0.01	-0.02	43.10	0.64	21.22	0.34	0.01	0.00	BDL	98.78
MB97-75 area A	600	35.31	0.05	0.02	-0.01	33.49	0.52	29.35	0.29	0.01	0.00	BDL	99.01
MB97-75 area A	599	34.66	0.05	0.04	-0.01	36.39	0.64	26.91	0.41	0.02	0.00	BDL	99.10
MB97-75 area B	601	36.25	0.04	0.02	-0.01	29.56	0.44	32.64	0.28	0.01	-0.01	BDL	99.24
MB97-75 area B	602	35.12	0.04	0.02	-0.01	34.79	0.59	28.44	0.27	0.01	0.00	BDL	99.28
MB97-75 area B	606	34.46	0.04	0.02	-0.01	34.40	0.58	28.04	0.32	0.01	0.00	235.81	97.88
MB97-75 area B	610	34.01	0.04	0.02	-0.02	39.13	0.73	24.81	0.31	0.01	0.00	110.84	99.04
MB97-75 area B	607	33.14	0.06	0.00	-0.01	42.87	0.85	20.96	0.36	0.01	0.00	BDL	98.25
MB97-76A area A	556	36.04	0.04	0.05	-0.01	27.91	0.40	33.73	0.27	0.01	0.00	BDL	98.44

MB97-76A area A	558	36.37	0.04	0.04	-0.01	27.89	0.40	33.48	0.27	0.01	0.00	BDL	98.48
MB97-76A area A	557	36.19	0.04	0.04	-0.01	28.05	0.40	33.63	0.27	0.02	0.00	BDL	98.62
MB97-76A area A	555	36.67	0.05	0.06	-0.01	29.02	0.46	33.41	0.27	0.01	0.00	BDL	99.93
MB97-76A area A	554	36.56	0.04	0.06	-0.01	29.30	0.45	33.01	0.26	0.01	0.00	BDL	99.68
MB97-76A area A	553	36.27	0.04	0.05	-0.01	30.19	0.49	32.33	0.27	0.01	0.00	BDL	99.63
MB97-76A area A	552	36.05	0.05	0.06	-0.01	31.32	0.53	31.01	0.29	0.01	0.00	BDL	99.30
MB97-76A area A	551	35.68	0.04	0.05	-0.01	32.99	0.56	29.51	0.30	0.01	0.00	160.07	99.14
MB97-76A area A	550	35.03	0.05	0.05	-0.01	36.13	0.69	26.64	0.35	0.01	0.00	140.33	98.96
MB97-76A area A	549	34.32	0.06	0.03	-0.01	38.42	0.78	24.36	0.37	0.01	0.00	BDL	98.34
MB97-76A area A rim-core	569	36.30	0.04	0.04	-0.01	28.35	0.43	33.71	0.27	0.01	0.00	BDL	99.15
MB97-76A area A rim-core	568	36.54	0.04	0.04	-0.01	28.53	0.41	33.54	0.26	0.02	0.00	242.54	99.39
MB97-76A area A rim-core	567	36.46	0.04	0.03	-0.01	28.85	0.44	33.22	0.26	0.01	0.00	BDL	99.30
MB97-76A area A rim-core	566	36.10	0.04	0.03	-0.01	30.56	0.49	31.91	0.27	0.01	0.00	BDL	99.41
MB97-76A area A rim-core	565	35.85	0.04	0.03	-0.01	31.61	0.53	30.86	0.29	0.01	-0.01	BDL	99.21
MB97-76A area A rim-core	564	35.51	0.04	0.03	-0.01	33.11	0.56	29.50	0.30	0.01	0.00	BDL	99.05
MB97-76A area A rim-core	563	35.15	0.05	0.02	-0.01	34.99	0.64	27.86	0.32	0.01	0.00	BDL	99.02
MB97-76A area A rim-core	562	34.58	0.06	0.02	-0.01	37.24	0.69	25.72	0.34	0.01	0.00	179.23	98.66
MB97-76A area A rim-core	561	33.73	0.07	0.03	-0.01	40.89	0.80	21.76	0.40	0.01	0.01	BDL	97.68
MB97-76A area B	577	35.07	0.07	0.02	-0.01	34.97	0.61	28.15	0.32	0.01	0.00	BDL	99.21
MB97-76A area B	579	35.06	0.16	0.03	-0.01	34.90	0.61	27.76	0.43	0.01	0.00	141.51	98.97
MB97-76A area B	573	35.11	0.05	0.03	-0.01	35.70	0.64	27.70	0.28	0.01	0.00	BDL	99.52
MB97-76A area B	578	34.74	0.09	0.03	-0.01	35.64	0.60	26.81	0.35	0.01	0.00	BDL	98.26
MB97-76A area B	572	34.89	0.05	0.02	-0.01	37.91	0.72	25.64	0.29	0.01	0.00	233.75	99.55
MB97-76A area B	571	34.19	0.06	0.03	-0.01	40.59	0.82	23.30	0.31	0.01	0.00	BDL	99.30
MB97-76A area B	570	33.96	0.09	0.02	-0.01	41.50	0.85	22.26	0.31	0.01	0.00	BDL	99.00
MB97-76C area A	513	35.41	0.04	0.02	-0.01	33.15	0.55	29.68	0.24	0.01	0.00	131.21	99.09
MB97-76C area A	519	35.07	0.04	0.03	-0.02	35.47	0.63	27.84	0.28	0.01	0.00	142.48	99.35
MB97-76C area A	517	34.74	0.07	0.03	-0.02	37.29	0.65	26.30	0.28	0.01	0.00	BDL	99.35
MB97-76C area A	512	34.45	0.03	0.02	-0.02	37.31	0.63	26.09	0.27	0.01	0.00	BDL	98.78
MB97-76C area A	511	34.15	0.04	0.02	-0.01	39.22	0.70	24.88	0.27	0.01	0.00	BDL	99.27
MB97-76C area B	520	36.54	0.04	0.03	-0.01	28.96	0.43	33.16	0.29	0.01	0.00	196.43	99.48
MB97-76C area B	521	36.32	0.04	0.03	-0.01	29.06	0.43	33.11	0.27	0.01	-0.01	BDL	99.25
MB97-76C area B	545	36.31	0.04	0.04	-0.01	29.10	0.42	33.05	0.27	0.01	0.00	BDL	99.22
MB97-76C area B	534	36.03	0.04	0.04	-0.01	29.77	0.45	32.60	0.26	0.01	0.00	BDL	99.18

MB97-76C area B	529	36.01	0.04	0.04	-0.01	29.95	0.44	32.38	0.27	0.01	0.00	BDL	99.11
MB97-76C area B	541	36.07	0.04	0.03	-0.01	29.76	0.44	31.82	0.26	0.01	0.00	BDL	98.44
MB97-76C area B	546	35.98	0.04	0.04	-0.01	30.59	0.48	31.56	0.27	0.01	0.00	BDL	98.95
MB97-76C area B	537	35.93	0.04	0.03	-0.01	30.73	0.50	31.34	0.26	0.01	0.00	BDL	98.84
MB97-76C area B	530	35.77	0.06	0.04	-0.01	30.96	0.50	31.57	0.26	0.01	0.00	BDL	99.18
MB97-76C area B	547	35.48	0.04	0.03	-0.01	33.49	0.56	29.25	0.26	0.01	0.00	BDL	99.10
MB97-76C area B	535	35.27	0.03	0.02	-0.01	34.13	0.59	28.37	0.27	0.01	-0.01	BDL	98.68
MB97-76C area B	526	35.03	0.05	0.02	-0.01	34.59	0.63	28.41	0.34	0.01	0.00	BDL	99.06
MB97-76C area B	542	34.90	0.04	0.02	-0.01	34.79	0.59	27.82	0.26	0.01	0.00	BDL	98.42
MB97-76C area B	531	34.63	0.11	0.03	0.00	36.01	0.60	27.25	0.22	0.01	0.00	BDL	98.86
MB97-76C area B	538	34.62	0.04	0.02	-0.01	35.87	0.59	26.84	0.28	0.01	0.00	BDL	98.26
MB97-76C area B	548	34.74	0.04	0.02	-0.01	36.21	0.64	26.69	0.29	0.01	0.00	BDL	98.62
MB97-76C area B	522	35.00	0.04	0.02	-0.01	36.61	0.62	26.64	0.29	0.01	0.00	BDL	99.23
MB97-76C area B	524	34.75	0.06	0.01	-0.02	37.06	0.66	25.97	0.23	0.01	0.00	BDL	98.74
MB97-76C area B	536	34.70	0.06	0.01	-0.02	37.92	0.70	25.57	0.24	0.01	0.00	286.95	99.22
MB97-76C area B	539	34.42	0.05	0.01	-0.01	38.25	0.68	25.08	0.29	0.01	0.00	BDL	98.78
MB97-76C area B	543	34.13	0.04	0.02	-0.01	39.40	0.71	24.13	0.27	0.01	0.00	BDL	98.69
MB97-76C area B	532	33.98	0.20	0.02	0.01	40.13	0.67	24.17	0.19	0.01	0.00	104.68	99.39
MB97-76C area B	533	33.84	0.08	0.02	-0.01	41.24	0.72	23.11	0.25	0.01	0.00	153.07	99.27
MB97-76C area B	540	33.67	0.05	0.01	-0.01	42.31	0.69	21.83	0.26	0.01	0.00	157.28	98.85
MB97-76C area B	544	33.72	0.05	0.01	-0.02	42.63	0.74	21.52	0.25	0.01	0.00	137.81	98.94

Formula weights and minerals

Table 25: Weathered olivine formula weights and mineral determination

SAMPLE	LINE	Fe FORMULA	Mn FORMULA	Mg FORMULA	Fo	Fa	Tp	Mineral
MB97-15 area A weather	469	1.52	0.02	2.48	61.63	37.77	0.60	Forsterite
MB97-19 area B	806	1.05	0.01	2.95	73.55	26.11	0.35	Forsterite
MB97-19 area B	807	1.07	0.01	2.93	73.00	26.64	0.35	Forsterite
MB97-19 area B	809	1.12	0.02	2.88	71.80	27.81	0.39	Forsterite
MB97-19 area B_multi	792	1.04	0.01	2.98	73.98	25.69	0.33	Forsterite
MB97-19 area B_multi	791	1.13	0.01	2.88	71.66	27.97	0.36	Forsterite
MB97-19 area B_multi	785	1.23	0.02	2.78	69.04	30.57	0.39	Forsterite
MB97-19 area B_multi	787	1.36	0.02	2.63	65.61	33.93	0.46	Forsterite
MB97-19 area B_multi	782	1.44	0.02	2.56	63.77	35.76	0.48	Forsterite

MB97-19 area B_multi	783	1.44	0.02	2.56	63.69	35.83	0.48	Forsterite
MB97-37 area A	729	1.53	0.02	2.46	61.30	38.15	0.54	Forsterite
MB97-37 area A	728	1.64	0.02	2.35	58.55	40.88	0.57	Forsterite
MB97-37 area A	730	2.12	0.03	1.86	46.37	52.84	0.79	Fayalite
MB97-75 area A	600	1.56	0.02	2.43	60.60	38.79	0.61	Forsterite
MB97-75 area A	599	1.72	0.03	2.26	56.43	42.81	0.76	Forsterite
MB97-75 area B	601	1.34	0.02	2.64	65.98	33.52	0.50	Forsterite
MB97-75 area B	602	1.62	0.03	2.37	58.90	40.41	0.70	Forsterite
MB97-75 area B	606	1.63	0.03	2.37	58.82	40.48	0.69	Forsterite
MB97-75 area B	610	1.88	0.04	2.12	52.59	46.54	0.88	Forsterite
MB97-75 area B	607	2.12	0.04	1.85	46.07	52.87	1.07	Fayalite
MB97-76A area A	556	1.27	0.02	2.73	67.98	31.56	0.46	Forsterite
MB97-76A area A	558	1.27	0.02	2.71	67.84	31.70	0.46	Forsterite
MB97-76A area A	557	1.27	0.02	2.72	67.81	31.73	0.46	Forsterite
MB97-76A area A	555	1.31	0.02	2.68	66.89	32.60	0.52	Forsterite
MB97-76A area A	554	1.32	0.02	2.66	66.41	33.07	0.52	Forsterite
MB97-76A area A	553	1.37	0.02	2.62	65.25	34.18	0.57	Forsterite
MB97-76A area A	552	1.44	0.02	2.54	63.44	35.95	0.61	Forsterite
MB97-76A area A	551	1.53	0.03	2.44	61.06	38.29	0.65	Forsterite
MB97-76A area A	550	1.71	0.03	2.25	56.32	42.85	0.83	Forsterite
MB97-76A area A	549	1.86	0.04	2.10	52.55	46.50	0.95	Forsterite
MB97-76A area A rim-core	569	1.28	0.02	2.72	67.62	31.89	0.49	Forsterite
MB97-76A area A rim-core	568	1.29	0.02	2.70	67.38	32.15	0.47	Forsterite
MB97-76A area A rim-core	567	1.31	0.02	2.68	66.90	32.60	0.50	Forsterite
MB97-76A area A rim-core	566	1.39	0.02	2.59	64.68	34.75	0.57	Forsterite
MB97-76A area A rim-core	565	1.45	0.02	2.53	63.12	36.26	0.62	Forsterite
MB97-76A area A rim-core	564	1.54	0.03	2.44	60.96	38.38	0.66	Forsterite
MB97-76A area A rim-core	563	1.64	0.03	2.33	58.22	41.02	0.75	Forsterite
MB97-76A area A rim-core	562	1.78	0.03	2.19	54.72	44.45	0.84	Forsterite
MB97-76A area A rim-core	561	2.02	0.04	1.92	48.20	50.80	1.00	Fayalite
MB97-76A area B	577	1.64	0.03	2.35	58.51	40.77	0.72	Forsterite
MB97-76A area B	579	1.64	0.03	2.33	58.21	41.06	0.73	Forsterite
MB97-76A area B	573	1.67	0.03	2.31	57.60	41.64	0.75	Forsterite
MB97-76A area B	578	1.70	0.03	2.27	56.87	42.41	0.73	Forsterite
MB97-76A area B	572	1.80	0.03	2.17	54.19	44.94	0.87	Forsterite
MB97-76A area B	571	1.96	0.04	2.00	50.06	48.94	1.00	Forsterite
MB97-76A area B	570	2.02	0.04	1.93	48.37	50.58	1.05	Fayalite
MB97-76C area A	513	1.54	0.03	2.45	61.08	38.28	0.64	Forsterite
MB97-76C area A	519	1.66	0.03	2.32	57.88	41.38	0.74	Forsterite
MB97-76C area A	517	1.76	0.03	2.22	55.26	43.96	0.78	Forsterite
MB97-76C area A	512	1.78	0.03	2.21	55.07	44.17	0.76	Forsterite

MB97-76C area A	511	1.87	0.03	2.12	52.62	46.54	0.84	Forsterite
MB97-76C area B	520	1.31	0.02	2.67	66.78	32.72	0.50	Forsterite
MB97-76C area B	521	1.32	0.02	2.67	66.67	32.83	0.50	Forsterite
MB97-76C area B	545	1.32	0.02	2.67	66.61	32.90	0.48	Forsterite
MB97-76C area B	534	1.35	0.02	2.64	65.79	33.70	0.51	Forsterite
MB97-76C area B	529	1.37	0.02	2.63	65.51	33.99	0.50	Forsterite
MB97-76C area B	541	1.37	0.02	2.61	65.25	34.24	0.51	Forsterite
MB97-76C area B	546	1.40	0.02	2.58	64.42	35.02	0.55	Forsterite
MB97-76C area B	537	1.41	0.02	2.57	64.13	35.28	0.58	Forsterite
MB97-76C area B	530	1.42	0.02	2.58	64.13	35.29	0.58	Forsterite
MB97-76C area B	547	1.56	0.03	2.42	60.49	38.85	0.66	Forsterite
MB97-76C area B	535	1.60	0.03	2.37	59.29	40.01	0.70	Forsterite
MB97-76C area B	526	1.62	0.03	2.37	58.97	40.29	0.74	Forsterite
MB97-76C area B	542	1.64	0.03	2.34	58.36	40.94	0.70	Forsterite
MB97-76C area B	531	1.70	0.03	2.29	57.02	42.27	0.71	Forsterite
MB97-76C area B	538	1.71	0.03	2.28	56.75	42.55	0.71	Forsterite
MB97-76C area B	548	1.72	0.03	2.26	56.35	42.88	0.76	Forsterite
MB97-76C area B	522	1.73	0.03	2.24	56.05	43.21	0.74	Forsterite
MB97-76C area B	524	1.77	0.03	2.21	55.10	44.11	0.79	Forsterite
MB97-76C area B	536	1.80	0.03	2.17	54.13	45.03	0.84	Forsterite
MB97-76C area B	539	1.83	0.03	2.14	53.45	45.73	0.82	Forsterite
MB97-76C area B	543	1.90	0.03	2.08	51.74	47.40	0.86	Forsterite
MB97-76C area B	532	1.93	0.03	2.07	51.36	47.83	0.81	Forsterite
MB97-76C area B	533	1.99	0.04	1.99	49.54	49.59	0.88	Forsterite
MB97-76C area B	540	2.07	0.03	1.90	47.50	51.64	0.86	Fayalite
MB97-76C area B	544	2.09	0.04	1.88	46.93	52.15	0.92	Fayalite

Cu constraints

Table 26: Weathered olivine Cu constraints

SAMPLE	LINE	Cu WT%	CuO	Cu CDL99	Cu ppm DL	Cu %ERR
MB97-15 area A weather	469	0.002088	0.002613	0.01502	187.97	339.76
MB97-19 area B	806	0.009072	0.011357	0.014428	180.62	75.59
MB97-19 area B	807	0.012772	0.015988	0.014622	183.04	54.58
MB97-19 area B	809	0.008584	0.010745	0.014564	182.30	80.60
MB97-19 area B_multi	792	-0.01304	-0.01633	0.014721	184.35	-52.60
MB97-19 area B_multi	791	0.003966	0.004965	0.014664	183.58	174.91
MB97-19 area B_multi	785	0.014936	0.018697	0.014601	182.78	46.69
MB97-19 area B_multi	787	0.018687	0.023392	0.014692	183.91	37.66
MB97-19 area B_multi	782	-0.01983	-0.02483	0.015289	191.44	-35.75
MB97-19 area B_multi	783	0.008391	0.010504	0.014991	187.66	84.81

MB97-37 area A	729	0.011772	0.014735	0.015024	188.06	60.75
MB97-37 area A	728	0.012068	0.015106	0.015041	188.27	59.34
MB97-37 area A	730	-0.00229	-0.00286	0.015518	193.81	-319.32
MB97-75 area A	600	-0.00254	-0.00318	0.015204	190.35	-281.68
MB97-75 area A	599	0.0033	0.004131	0.015232	190.68	218.15
MB97-75 area B	601	0.007475	0.009357	0.01485	185.89	94.25
MB97-75 area B	602	-0.003	-0.00376	0.015143	189.79	-237.21
MB97-75 area B	606	0.018837	0.023581	0.01497	187.40	38.05
MB97-75 area B	610	0.008854	0.011084	0.015371	192.42	82.41
MB97-75 area B	607	0.003003	0.00376	0.015556	194.77	244.73
MB97-76A area A	556	0.003376	0.004227	0.014706	184.13	205.93
MB97-76A area A	558	0.000644	0.000806	0.014937	186.94	1093.57
MB97-76A area A	557	0.000842	0.001054	0.0148	185.26	828.89
MB97-76A area A	555	-0.00312	-0.0039	0.014724	184.05	-222.15
MB97-76A area A	554	-0.00034	-0.00043	0.014945	189.01	-2059.60
MB97-76A area A	553	-0.01024	-0.01282	0.015053	188.46	-68.71
MB97-76A area A	552	-0.00057	-0.00072	0.014996	189.42	-1232.40
MB97-76A area A	551	0.012788	0.016007	0.014872	186.16	55.42
MB97-76A area A	550	0.01121	0.014033	0.015222	190.55	64.59
MB97-76A area A	549	0.004281	0.005359	0.015412	192.93	170.29
MB97-76A area A rim-core	569	0.006664	0.008342	0.014828	185.62	105.50
MB97-76A area A rim-core	568	0.019376	0.024254	0.014538	181.98	35.98
MB97-76A area A rim-core	567	0.000495	0.00062	0.015063	188.67	1434.47
MB97-76A area A rim-core	566	-0.0043	-0.00538	0.014933	186.84	-163.13
MB97-76A area A rim-core	565	0.004763	0.005963	0.015021	188.05	149.25
MB97-76A area A rim-core	564	-0.00892	-0.01116	0.015244	190.72	-80.02
MB97-76A area A rim-core	563	-0.00059	-0.00074	0.015306	191.97	-1220.20
MB97-76A area A rim-core	562	0.014318	0.017923	0.015092	188.92	50.27
MB97-76A area A rim-core	561	0.007989	0.01	0.015255	190.95	90.59
MB97-76A area B	577	0.005496	0.00688	0.015173	189.94	130.73
MB97-76A area B	579	0.011304	0.014151	0.015009	187.89	63.18
MB97-76A area B	573	0.006908	0.008647	0.015192	190.16	104.25
MB97-76A area B	578	-0.00401	-0.00503	0.015198	190.64	-177.86
MB97-76A area B	572	0.018674	0.023375	0.015124	189.31	38.76
MB97-76A area B	571	0.003671	0.004595	0.015361	192.27	197.85
MB97-76A area B	570	-0.00071	-0.00089	0.015639	196.04	-1031.70
MB97-76C area A	513	0.010482	0.013121	0.014854	185.94	67.39
MB97-76C area A	519	0.011382	0.014248	0.015002	187.80	62.72
MB97-76C area A	517	-0.00058	-0.00072	0.015381	190.94	-1251.50
MB97-76C area A	512	0.00122	0.001527	0.015398	192.73	595.71
MB97-76C area A	511	0.002318	0.002902	0.01534	192.05	312.49

MB97-76C area B	520	0.015692	0.019643	0.014675	183.70	44.69
MB97-76C area B	521	-0.0011	-0.00137	0.014811	184.46	-635.22
MB97-76C area B	545	0.005298	0.006632	0.01486	186.02	132.82
MB97-76C area B	534	-0.00136	-0.0017	0.014807	185.09	-514.14
MB97-76C area B	529	-0.00639	-0.008	0.014963	187.33	-109.79
MB97-76C area B	541	0.003191	0.003994	0.014794	185.17	219.19
MB97-76C area B	546	0.006583	0.008241	0.014907	186.61	107.33
MB97-76C area B	537	0.007778	0.009736	0.014813	185.42	90.38
MB97-76C area B	530	0.004875	0.006103	0.014948	187.13	145.12
MB97-76C area B	547	0.000522	0.000654	0.015127	189.52	1366.58
MB97-76C area B	535	0.003496	0.004377	0.014913	186.71	201.66
MB97-76C area B	526	-0.00012	-0.00015	0.015115	188.94	-6014.00
MB97-76C area B	542	0.00364	0.004557	0.015125	189.35	196.44
MB97-76C area B	531	0.001027	0.001285	0.015269	191.05	701.66
MB97-76C area B	538	0.00082	0.001027	0.015202	190.40	874.27
MB97-76C area B	548	0.003227	0.00404	0.015213	190.46	222.82
MB97-76C area B	522	0.00655	0.008199	0.015124	189.32	109.44
MB97-76C area B	524	0.007357	0.009209	0.015114	189.19	97.43
MB97-76C area B	536	0.022924	0.028695	0.014979	187.50	31.39
MB97-76C area B	539	0.005402	0.006763	0.015243	190.83	133.59
MB97-76C area B	543	0.00067	0.000839	0.015484	193.90	1089.55
MB97-76C area B	532	0.008362	0.010468	0.015282	191.31	86.72
MB97-76C area B	533	0.012228	0.015307	0.015321	191.79	59.64
MB97-76C area B	540	0.012565	0.015728	0.015459	193.51	58.56
MB97-76C area B	544	0.011009	0.013781	0.015257	190.99	65.91

Copper Sulfides

Table 27: Copper sulfides chemical data

SAMPLE	MB97-76C CuS	MB97-76C CuS	MB97-76C CuS
LINE	488	623	622
SiO2	0.08	0.07	0.05
TiO2	0.74	0.79	0.77
Al2O3	0.01	0.02	0.01
Cr2O3	0.10	0.11	0.11
FeO	4.84	4.97	4.89
CuO	94.76	94.04	93.87
MnO	0.05	0.06	0.05
MgO	0.02	0.01	0.01
CaO	0.03	0.02	0.03
Na2O	0.00	0.00	0.00
K2O	0.01	0.01	0.01
SO3	54.99	55.05	54.19
TOTAL	102.12	101.71	101.13
Cu FORMULA	1.82	1.82	1.83
S FORMULA	1.05	1.06	1.05
Normalized Cu formula	1.73	1.72	1.74
Normalized S formula	1	1	1
Cu WT%	75.70	75.12	74.99
CuO	94.76	94.04	93.87
Cu CDL99	0.03	0.03	0.03
Calc Cu ppm DL	343.44	334.95	334.51
Cu %ERR	0.14	0.14	0.14

Glass

Table 28: Glass chemical data (oxide concentrations)

Sample	MB97-76B glass area B	MB97-76B glass area B	MB97-76B glass area A	MB97-76B glass area A
Line	739	742	765	766
wt% SiO2	70.81	71.50	69.16	68.34
wt% TiO2	0.89	0.84	0.89	1.19
wt% Al2O3	12.60	12.43	13.88	13.13
wt% Cr2O3	0.00	0.01	0.00	0.01
wt% FeO	2.60	2.28	2.60	3.43
wt% MnO	0.22	0.12	0.12	0.28
wt% MgO	0.31	0.16	0.31	0.13
wt% CaO	2.25	2.12	1.66	1.77
wt% Na2O	4.59	3.98	5.95	5.33
wt% K2O	3.12	3.63	3.26	4.87
Cl	0.02	0.01	0.01	0.02
F	0.07	0.00	0.06	0.06
O	-0.03	0.00	-0.03	-0.03
Cu (ppm)	BDL	BDL	BDL	340.36
Total	97.46	97.11	97.87	98.56
Cu WT%	0.006313	0.012255	-0.00287	0.02719
wt% CuO	0.007903	0.01534	-0.00359	0.034036
Cu CDL99	0.030722	0.030547	0.030801	0.03002
Calc Cu ppm DL	384.60	382.37	385.28	375.79
Cu %ERR	199.53	102.62	-437.51	45.94

Amphibole

Table 29: Amphibole chemical data (oxide concentrations)

Sample	MB97-76B amp area B	MB97-76B amp area B	MB97-76B amp area B	MB97-76B amp area B	MB97-76B amp area B	MB97-76B amp area B	MB97-76B amp area B	MB97-76B amp area A
Line	745	746	747	748	749	750	751	768
wt% SiO2	46.53	46.70	45.69	46.05	45.04	45.91	46.03	47.83
wt% TiO2	1.17	1.20	1.25	1.24	1.34	1.12	1.14	1.35
wt% Al2O3	4.84	4.99	5.24	4.86	5.53	5.06	5.07	4.26
wt% Cr2O3	0.00	0.00	0.00	-0.01	-0.01	0.00	-0.01	-0.01
wt% FeO	10.12	10.02	10.69	10.87	11.85	10.93	10.98	8.21
Cu mean ppm	100.75	-50.50	-140.60	62.90	-71.80	-20.70	-38.30	-18.80
wt% MnO	1.00	1.05	1.11	1.03	1.06	1.14	1.10	0.75
wt% MgO	12.08	12.20	11.42	11.77	10.91	11.69	11.57	13.63
wt% CaO	21.82	21.91	21.73	21.84	21.63	21.70	21.64	21.84
wt% Na2O	0.65	0.66	0.72	0.67	0.71	0.69	0.68	0.84
wt% K2O	0.08	0.08	0.08	0.07	0.09	0.05	0.07	0.08
Cl	0.00	0.00	0.00	0.00	0.00	0.00	0.00	0.00
F	0.05	0.02	-0.05	-0.02	0.02	-0.04	-0.05	0.03
O	-0.02	-0.01	0.02	0.01	-0.01	0.02	0.02	-0.01
Total	98.32	98.82	97.89	98.38	98.15	98.25	98.23	98.78
Cu WT%	0.008048	-0.00404	-0.01124	0.005025	-0.00574	-0.00165	-0.00306	-0.0015
wt% CuO	0.010075	-0.00505	-0.01406	0.00629	-0.00718	-0.00207	-0.00383	-0.00188
Cu CDL99	0.026899	0.026904	0.027411	0.027001	0.027579	0.027347	0.027217	0.027218
Calc Cu ppm DL	336.74	336.30	342.88	337.98	344.98	343.08	340.66	341.13
Cu %ERR	137.09	-271.55	-98.96	220.01	-195.54	-676.10	-362.62	-740.79

Iron Sulfides

Table 30: Iron sulfides chemical data (oxide concentrations)

Sample	MB97-19 oxide area B	MB97-19 oxide area B	MB97-19 oxide area B
Line	815	816	817
wt% SiO2	0.21	0.17	0.20
wt% TiO2	0.08	0.12	0.10
wt% Al2O3	0.07	0.06	0.07
wt% Cr2O3	0.02	0.02	0.02
wt% FeO	68.92	72.71	65.19
wt% CuO	5.94	2.08	10.50
wt% MnO	0.02	0.01	0.02
wt% MgO	0.03	0.03	0.03
wt% CaO	0.05	0.05	0.06
wt% Na2O	0.03	0.03	0.03
wt% K2O	0.05	0.05	0.05
Total	75.42	75.32	76.27
CuO CDL99	0.02	0.02	0.02
Cu %ERR	0.26	0.52	0.19

Appendix C - Microprobe Standards

Table 31: Feldspar standards

Si Standard name	Al Standard name	Fe Standard name	Cu Standard name	Mg Standard name	Ca Standard name	Na Standard name	K Standard name
Albite Amelia	Labradorite	Almandine NY	Chalcopyrite	Diopside	Labradorite	Albite Amelia	Orthoclase

Table 32: Olivine standards

Si Standard name	Ti Standard name	Al Standard name	Cr Standard name	Fe Standard name	Cu Standard name	Mn Standard name	Mg Standard name	Ca Standard name
Olivine Fo93	Rutile	Almandine NY	Chromite	Almandine NY	Chalcopyrite	Rhodonite	Olivine Fo93	Diopside

Table 33: Pyroxene standards

Si Standard name	Ti Standard name	Al Standard name	Cr Standard name	Fe Standard name	Cu Standard name	Mn Standard name	Mg Standard name	Ca Standard name	Na Standard name	K Standard name
Diopside	Rutile	Almandine NY	Chromite	Almandine NY	Chalcopyrite	Rhodonite	Diopside	Diopside	Albite Amelia	Orthoclase

Table 34: Oxide standards

Si Standard name	Ti Standard name	Al Standard name	Cr Standard name	Fe Standard name	Cu Standard name	Mn Standard name	Mg Standard name	Ca Standard name	Na Standard name	K Standard name
Diopside	Rutile	Almandine NY	Chromite	Almandine NY	Chalcopyrite	Rhodonite	Diopside	Diopside	Albite Amelia	Orthoclase

Table 35: Weathered olivine standards

Si Standard name	Ti Standard name	Al Standard name	Cr Standard name	Fe Standard name	Cu Standard name	Mn Standard name	Mg Standard name	Ca Standard name	Na Standard name	K Standard name
Diopside	Rutile	Almandine NY	Chromite	Almandine NY	Chalcopyrite	Rhodonite	Diopside	Diopside	Albite Amelia	Orthoclase

Table 36: Copper sulfide standards

Si Standard name	Ti Standard name	Al Standard name	Cr Standard name	Fe Standard name	Cu Standard name	Mn Standard name	Mg Standard name	Ca Standard name	Na Standard name	K Standard name	S Standard name
Diopside	Rutile	Almandine NY	Chromite	Pyrite	Chalcopyrite	Rhodonite	Diopside	Diopside	Albite Amelia	Orthoclase	Pyrite

Table 37: Glass standards

Si Standard name	Ti Standard name	Al Standard name	Cr Standard name	Fe Standard name	Cu Standard name	Mn Standard name	Mg Standard name	Ca Standard name	Na Standard name	K Standard name	Cl Standard name	F Standard name
Albite Amelia	Rutile	Labradorite	Chromite	Almandine NY	Chalcopyrite	Rhodonite	Diopside	Labradorite	Albite Amelia	Orthoclase	Tugtupite	Topaz

Table 38: Amphibole standards

Si Standard name	Ti Standard name	Al Standard name	Cr Standard name	Fe Standard name	Cu Standard name	Mn Standard name	Mg Standard name	Ca Standard name	Na Standard name	K Standard name	Cl Standard name	F Standard name
Albite Amelia	Rutile	Labradorite	Chromite	Almandine NY	Chalcopyrite	Rhodonite	Diopside	Labradorite	Albite Amelia	Orthoclase	Tugtupite	Topaz